Roll Service-life Optimisation using Paper Quality Measurements for Condition Indication

by

James Stewart Newton Meikle

Submitted in partial fulfilment of the requirements for the degree

Master of Engineering
(Mechanical Engineering)

in the

Faculty of Engineering, Built Environment and Information Technology

University of Pretoria

June 2004

Roll Service-life Optimisation using Paper Quality Measurements for Condition Indication

by

James Stewart Newton Meikle

Supervisor : C. J. Stander
Department : Mechanical and Aeronautical Engineering
Degree : M.Eng.

Summary

Paper machine sheet dewatering by roll pressing is critical in the establishment of uniform moisture profiles, as well as other mechanical properties of the paper during manufacture. Roll cover profiles are maintained within specification by removing and regrinding the rolls after fixed periods in service. However, analyses of historical data revealed a high variance in the cover wear rates suggesting the use of a condition-based approach to maintenance. In general excessively uneven wear of the cover profile leads to a reduction in press nip load and an increase in paper moisture content. Papermaking process dynamics, however, result in the moisture content also being influenced by other factors including headbox profile, press felt condition and stock variables such as furnish and consistency. The interrelationships between these variables are highly complex and are thus ideally suited for solution by Artificial Neural Networks. With this work a Neural Network model was used to learn the relationships between these variables based on measurements made in a production environment. The model was shown to successfully model the papermaking process and the influences of press roll wear on paper moisture content. The methodology developed allows the progression of cover wear to be monitored using the moisture profile of the paper produced until quality limits are reached, and the roll is replaced on condition. Comparisons indicate significant benefits of the condition-based approach over conventional methods. Furthermore, the same method can be applied to other nipped rolls, such as roll-coaters and soft-calenders, provided the network is customised for those applications.

Keywords:

Condition-based, Kraft paper, Maintenance, Moisture, Monitor, Neural network, Nip load, Paper quality, Press roll cover, Time based and Wear.

Acknowledgements

The author gratefully acknowledges the support provided by Sappi Kraft (Pty) Ltd for this project. Thanks to the many Sappi participants at the paper mills and at Sappi Management Services. Special thanks to the employees of Tugela Mill for their valued cooperation over the duration of this project.

A particular mention must be made of the support and guidance provided by Phillip Viljoen, the industrial mentor for this project. His insight and inspiration were monumental in ensuring that the objectives were met. Special thanks also to the following individuals who have, in one way or another, provided considerable assistance with this endeavour:

P. Bornman (Sappi Enstra)
A. Carr (Sappi Kraft)
T. Cannon (Rubber Rollers)
H. Dreyer (University of Pretoria)
W. Hoek (Sappi Tugela)
M. Meyiwa (Albany International)
H. Savolainen (Metso Paper)
P. Smith (Sappi Enstra)
M. Truelock (Sappi Management Services)
C. Twigg (H&M Roller Technologies)
M. Uys (Sappi Management Services)
S. Wilcock (Sandusky Africa)
L. Spencer (Dunlop Testing Laboratories)

The success of this project would not have been possible without the assistance of the PM2 and Roll Services teams of Tugela Mill, to whom I am forever grateful. To the many others who have assisted along the way, my sincere gratitude.

Thank you all.

Table of contents

Nomenclature

Roll covers

A	Cross-sectional area of infinitesimal cover element
D	Roll diameter
E	Static modulus of elasticity (Young's modulus)
F	Nip force
G	Equivalent material stiffness
L	Length of spring
L	Nip load Limit
N	Nip width
P	Roll cover hardness
R	Roll radius
$b(y)$	Position of bottom roll at horizontal coordinate y
d	Maximum deflection of the roll covers in the centre of the nip
$e(y)$	Equilibrium position of soft covers at point y
f	Elemental nip force
k	Spring stiffness
$n(y)$	Neutral plane of contact between two soft roll covers
r^2	Correlation coefficient
$t(y)$	Position of top roll at horizontal coordinate y
y	Horizontal coordinate
α	Proportional spring constant
$\delta(y)$	Cover deflection at horizontal coordinate y
γ	Geometric factor
ν	Material Poisson ratio
∂y	Width of infinitesimal cover element
φ	Half the angular nip width of the bottom roll
ρ_m	Empirical material factor
ρ_s	Empirical size factor
ρ_v	Poisson factor
θ	Half the angular nip width of the top roll

Papermaking

P	Nip load
V	Machine speed
f	Permeability factor
h_m	Measured moisture
h_r	Regressed moisture
m	Moisture content after pressing
m_m	Measured mass
m_o	Initial moisture ratio
n	Compressibility factor
∇	Gradient of regression curve

Neural methods

b	Neuron bias
d	Number of network inputs
i	Cross-directional index
tansig	Hyperbolic tangent sigmoid
w_i	Weight factor
x_i	Network input
y	Network output
φ	Activation function
σ	Standard deviation
$[\ ]^T$	Matrix transpose

Abbreviations

ANN	Artificial Neural Network
BS	Back Side of paper machine
C	Centre of paper machine
CD	Cross-machine Direction
CSF	Canadian Standard Freeness

DC	Direct Current
DP	Decreasing Permeability
FEM	Finite Element Model
FFT	Fast Fourier Transform
FS	Front Side of paper machine
MD	Machine Direction
MLP	Multi-Layer Perceptron
NN	Neural Network
P&J	Pusey & Jones hardness
SI	Systeme Internationale
TAPPI	Technical Association of Pulp and Paper Industries

1. Introduction and literature survey

1.1 Introduction

Increasingly stringent customer-driven quality requirements for paper products have resulted in renewed focus on paper machine equipment that directly influences paper quality. Paper machine rolls, together with machine clothing, are the only equipment which make direct contact with the paper web along its path through the paper machine. As a result of this contact paper machine rolls play a substantial part in determining the final product properties. As a group, the rolls also constitute one of the most numerous items of machinery on the paper machine, ranging between 100 and 300 rolls per machine.

To ensure that the rolls are kept in good working order, they are subject to routine maintenance work. For the majority of roll designs the maintenance work focuses primarily on the degradation of two major components of the roll assembly: the bearings and the roll cover. The bearings can suffer from normal wear as well as a host of other conditions which may cause them to fail. It has been shown that vibration monitoring can effectively detect and trend deterioration in bearing condition. Thus most bearing-related roll changes occur on a planned basis. For the roll cover the factors governing an optimal replacement opportunity are not understood well enough. Thus the roll cover profile is maintained by removing the roll and regrinding the cover after fixed periods in service in order to correct excessively uneven abrasive wear of the cover. The duration of this service period is determined by the cover supplier's recommendations or by analysis of historical failure data. In general the roll bearings last longer than the predetermined roll cover service life. Thus the opportunities of roll service-life extension are related to the cover wear.

The rapid technological advancement of the science of vibration monitoring can be ascribed to the widespread use of roller element bearings in nearly every industry. The use of vibration monitoring as a front-line failure prevention method has resulted in significant and indisputable savings in maintenance costs. The fact that roll covers are used in only a handful of industries is perhaps the reason why cover maintenance methodologies are less advanced. On the other hand the advances in design technology and material chemistry in recent decades have drastically increased the performance, and hence the duration that these rolls can be expected to operate in

the machines. The opportunity thus exists to extend the period between grinding intervals, but requires a method whereby the worn state of a roll can be accurately determined. This identification, and the subsequent timely replacement of the roll can directly reduce the maintenance costs.

Many different types of rolls can be found on a single paper machine. Each type is purpose designed and built to perform a specific function. The effectiveness of a single roll is even dependant on the machine in which it is placed, being related to variables such as paper type, rotational speed etc. The result is that not all machines will be able to tolerate the same amount of wear on their rolls, and not all rolls will be able to tolerate the same amount of wear. The service life recommended by the roll cover supplier has to take into account a vast number of unknown conditions and operation probabilities. Consequently the service life is chosen conservatively. Hence a significant amount of the roll service life may not be utilised when replaced at the recommended interval. It may be possible to reconsider the recommended service life using some basic rules of thumb. For example, high speed machines producing lighter, meaning thinner, paper grades under heavy roll loading would be more susceptible to roll wear than slower machines making heavier, meaning thicker sheets under lower loads.

A more precise method would be to determine the exact wear tolerance for each of the rolls on the machine in question. This would require that a reliable technique exists which quantifies the degradation of the roll assembly in terms of both mechanical integrity and the quality of the paper being produced. At present no scientifically conclusive method of this nature is published. In addition to the direct cost savings to maintenance, secondary savings would result, in the form of reduced production losses related to an inferior roll condition.

The dynamics of papermaking on a modern paper machine complicates the establishment of relationships between roll wear and paper properties. For this models of papermaking and the physical behaviour of roll covers are required.

1.2 Literature survey

The objective of the research was to determine if roll maintenance intervals could be extended by considering both the mechanical condition of the roll and the effect of cover wear on paper quality. The literature survey addressed the following topics:

- Current practices of roll maintenance
- Theories of press dewatering
- Neural methods
- Mechanical properties of roll covers

1.2.1 Current practices of roll maintenance

The operation of a roll in a paper machine is such that the effects of roll faults can usually be classified in terms of one of two coordinate axes as shown in Fig. 1-1. The direction of the paper sheet is known as the Machine Direction (MD). Excessive wear at a localised point on the roll cover surface will leave a fingerprint defect on the paper rolled by that point. The defect occurrence on the paper will be at $1x$ the roll rotation frequency. Similarly, wear around the entire circumference of the roll at that point will result in the formation of a streak on the paper. Papermakers refer to this as a streak in the MD. A cross-section of the same paper will identify the streak as a peak relative to other points. This cross-sectional axis is called the Cross-Direction (CD). Thus variations in the CD profile of the paper will be observed as streaks in the MD, which are undesirable.

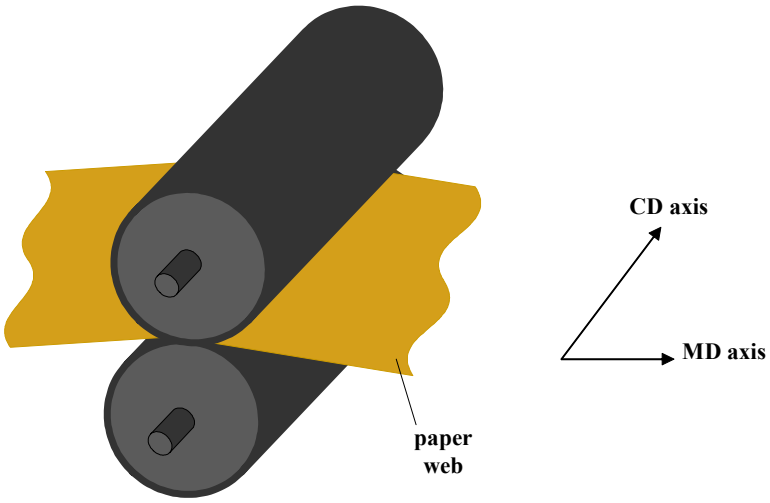

Fig. 1-1 Paper machine MD and CD coordinate axes.

Bearing faults are usually manifested as, but not limited to, vibrations at the bearing housing. For certain rolls the kinetic effects of the vibration can be observed as time-based variations in the MD paper properties. For the majority of the rolls in the paper machine, however, the maximum vibration tolerances are determined by the structural response of the machine frame, roll assembly or the bearing itself. Succi [1] reviewed various prognostic methods for bearing condition monitoring. The concepts of threshold vibration limits are introduced for the purposes of qualifying the severity of bearing damage. Al-Najjar [2] also makes use of threshold limits and provides a method whereby bearings with faults are allowed to run to an optimal change-out point, determined by a number of operational conditions and inspection frequencies. In the practical case this method can be used to establish whether a bearing will continue to function satisfactorily until the next planned maintenance outage.

Vibration technology can also be used to identify and qualify other roll-related faults such as the unbalance of roll shells, as reported by Menon [3] and the barring of press felts, as discussed by Bissessur *et al.* [4]. The low rotational frequencies of the felts in comparison to the rolls warrants the use of more advanced analysis techniques such as acceleration enveloping for fault detection for felts. Most paper mills make use of vibration monitoring systems with widespread reports of successful fault detection. As is the case with most technologies, there are varying degrees of application, as well as degrees of sophistication. One of the more comprehensive systems is the on-line vibration monitoring system as reported by Norrman [5]. In this case the vibration data is monitored continuously and automatically by multi-log stations, without the requirement for human interaction. Bearing faults in this case are reported to the maintenance team by exception.

Other methods of fault detection such as oil analysis and thermography are also used to detect roll-related failures, as discussed by Cutler [6]. With the exception of thermography, however, all of the techniques mentioned above are applicable only to MD faults, or faults that can be observed in the time domain. Roll related faults in the CD direction are becoming more common as modern machines extend the operating envelope to higher speeds and loads, as reported by Beucker [7]. Beucker indicates that the wear of the roll cover is determined by the cover material abrasion resistance and the coefficient of friction. However, this theory correlates only in a general way with measurements on actual paper machines.

Moore *et al.* [8] recommends that regrinding of covered rolls should be undertaken regularly to restore proper roll shape. For this the roll must be removed from service and replaced by a spare roll with identical proportions. The paper recommends cover material removal to approximately 0.8 mm on radius below the deepest surface disparity. This is standard practice in most mills and after a number of regrinds when the cover thickness reaches a minimum value the roll is recovered. The paper further recommends that a nip impression be taken before and after roll changes to determine the uniformity of pressure across the roll face. The nip impression is a test which makes use of pressure sensitive film placed between the non-rotating rolls which are subsequently forced together at nominal loading conditions. The shape of the impression can be used to make various inferences about the loading distribution and state of the roll covers, as discussed in detail by Beucker [9]. Nip impressions are also used when the rolls are suspected of causing uneven CD profiles in paper sheet properties. Paper machines are very sensitive to CD variations in roll conditions, due to the limited capacity of the machinery to compensate for upstream variations. Systems such as steam showers and spray dampeners do provide limited correction for poor CD moisture profiles. Generally, however, in situations where the wear is found to be excessively uneven, the usual response is to halt production, change the roll and in some cases review the maintenance interval to prevent re-occurrence of the failure.

To the author's knowledge a formal study aimed at the quantification of the effect of roll wear on the paper properties has not been undertaken. A revision of the maintenance interval such that excessive CD roll wear does not occur must first establish these limits based on the paper properties. This will undoubtedly become the limiting factor with regard to roll maintenance interval extension. An article by Bloigu *et al.* [10] discusses the extension of the maintenance intervals for suction rolls. The extension is the result of developments in cover material technology and design changes to the mechanical roll structure. However, no specific information about the wear tolerances is provided. The implications of the article are that the practical roll bearing life is not a limiting factor on the maintenance intervals. This is nearly always the case in industrial paper machines, due to the advances in bearing design and vibration monitoring technologies.

1.2.2 Theories of press dewatering

The primary objective of the press section is to remove as much water as possible mechanically before the sheet enters the drying section. In the drying section the dewatering occurs by evaporation which is far more energy and cost intensive. The press section is also responsible for sheet consolidation which ensures good fibre-to-fibre bonding which determines the mechanical strength of the sheet.

In a roll press the wet paper sheet is rolled between two rolls which are forced together. The paper sheet is usually too wet at this stage to support its own weight, and is thus supported by a press felt(s). The felt also acts as a sponge to accept the water which is forced out of the sheet in the nip. The nip is the narrow zone of high pressure which exists along the line of contact between the two rolls. Usually one or both of the rolls are covered in a soft polymer cover which deflects under the load, increasing the width of the nip. The increased nip width is beneficial in increasing the time that the sheet is exposed to the nip pressure, which aids dewatering. In a roll press, water flows in the direction of the shortest exit path, being the plane perpendicular to the paper and felt. The dewatering action is characterised by an increase in pressure for the first half of the nip, during which the paper web and felt are compressed to reach saturation. After mid-nip the felt and paper expand as the gap between the roll covers increases. During this expansion phase the felt absorbs some of the water which first entered the nip as part of the porous paper web. Water removed originates from the voids between wood fibres and also from within the fibre walls.

The fundamental aspects of pressing were first formulated in the late 1950's by Wahlstrom [11]. The model was later revised by Wahlstrom [12] to account for flow out of the fibre cell wall, which is more difficult to remove than water between the wood fibres due to the small pore size. Wahlstrom [13] differentiates between the concepts of pressure controlled and flow controlled pressing. In pressure controlled pressing the resistance to water flow between wood fibres is insignificant. This is normally the case for lightweight sheets. The outgoing dryness is thus predominantly determined by the resistance to flow out of the fibre wall, which is overcome by applying higher loads in the press. By increasing the thickness of the sheet, or basis weight, the flow controlled pressing conditions are reached. Under these conditions the flow of water is resisted by the increased length of the exit path. The amount of water removed thus becomes more dependent on the time available. Dewatering thus becomes a flow phenomenon. Wahlstrom

[12] provides a qualitative press model with eight terms which describes the moisture content of the sheet after the nip. The first three terms are related to the properties of the sheet itself: compressibility, fibre structure and flow resistance out of the cell wall. The five external factors are flow resistance in the felt, uniformity of pressure application and three rewetting terms. Press dryness increases exponentially with nip pressure over most of the pressure range. Temperature affects the exiting moisture content due to differences in the water viscosity, and compressibility and spring-back of the fibre networks which are related to softening of the cellulose, hemi cellulose and lignin at higher temperatures. Wahlstrom [12] indicates that very little quantitative data is available regarding the effect of pressure non-uniformity on water removal. The paper indicates that measurements from one case study showed that in order to operate within 10 ± 1 % moisture at the reel, they required a total press profile variation less than 0.5 %.

Kerekes & McDonald [14] present a second theory of wet pressing, known as the Decreasing Permeability (DP) model. The DP model describes the press as a process of forcing water from a porous medium of decreasing permeability. According to the model, as dewatering proceeds the flow resistance increases because of the smaller pore structure associated with the origin of the water. It also increases because increasing pressure and water removal increase hydraulic resistance by diminishing or closing the flow paths of the water. Based on this picture, the water removal process caused by wet pressing can be modelled as a nonlinear process of liquid flow from a medium of decreasing permeability. The authors indicate that while Wahlstrom's model provides a good conceptual representation of pressing, it also has some shortcomings for mathematical modelling. The DP model begins with the Kozeny-Carman equation and uses variable grouping to represent the effect on outgoing moisture of four major factors: initial moisture content, compressibility, permeability and press impulse. Press impulse describes a time-pressure quantity which represents the average pressure in the nip and the length of time that the sheet was exposed to this pressure. The DP model was shown to provide good agreement with pilot paper machine measurements.

A third pressing theory is presented by Clos *et al.* [15]. Known as the Limiting-Consistency model, the derivation, like the DP model, is also derived from the Kozeny-Carman equation for permeable flow. The model uses physical properties such as density, specific surface area and is based on the tenet that for any dewatering system there is a maximum consistency that can be reached for a given load, regardless of the duration of exposure.

Pressing theories are designed to relate the moisture exiting the nip to that entering the nip. This limits their application on paper machines in the production environment because the samples which are required cause paper breaks and interfere with production. Ideally the post-nip sample should be taken from the final product at the dry-end, but this would require exact knowledge of the drying section performance. If, however, only the CD moisture profile is of interest, then certain deductions can be made under the assumption of consistent, but not necessarily uniform, CD drying capacity. In this case there are a number of conditions which must be considered when performing such a study on a commercial machine.

Felt compression and build up of contaminants in the felt can reduce the felt permeability, as described by Pikulik *et al.* [16], TAPPI Technical Information Paper [17] and the PressManager software marketed by Stowe Woodward [18]. These felt permeability variations, local or complete, affect the ease with which water is absorbed, affecting paper moisture content. Local variations in operating parameters can also cause non-uniformities in the CD permeability profile, leading to bands of high and low moisture on the sheet. Similarly CD moisture variations can be caused by non-uniform felt porosity profiles, as discussed by Young *et al.* [19].

Non-uniform CD loading of the press section will have an obvious effect on CD moisture profiles as well as secondary effects such as felt damage, as described by TAPPI Technical Information Paper [17]. The felt damage can be manifested in uneven wear or compression of the felt and may lead to further non-uniform CD moisture profiles. The PressManager analysis tool [18] also considers a wider scope of factors which can affect the moisture content of the sheet exiting the press including: press configuration, felt structure, percentage recycled pulp, fibre blend and filler quantities.

Kochanik *et al.* [20] discusses a method of evaluating the performance of a press section on a production machine. The method requires that all water streams into and out of the press section be monitored by flow control devices so that a water balance can be established. These flow control devices are not standard on most paper machines. Press section flow analyses of this type show that felt water content entering the nip does have an impact on the sheet dewatering in the nip.

Bottiglieri [21] describes the benefits of the shoe press design in the press section. The shoe press replaces the conventional narrower double-roll nip with a wider hydraulically loaded shoe. By design, a shoe press provides a uniform nip load across the CD width, controlled by individual hydraulic cylinders. A shoe press can replace one or more roll nips in terms of dewatering capacity. As a consequence of the reduction in the number of nips, the press section no longer benefits from the compensating effect of having successive nips. This demands a greater focus on the pressure uniformity from the user, particularly for machines with roll and shoe combinations.

Fekete and Wiebe [22] discuss the effect of varying combinations of nip numbers and nip loads on paper consistency exiting the presses. The results conclude that the higher the nip pressure, the drier the sheet. Interestingly, the dryness is not found to be related to the sum of all the nip loads, but rather by the maximum nip load in any of the presses. This is in contrast the findings of McDonald *et al.* [23], but both authors agree that the final dryness is not related to the sum of the loads in all the presses. This view was confirmed by Pikulik and Hamel [24] who found that the addition of a shoe press in the third nip only increased the sheet solids content by a small amount. The first and second presses, however, which had a combined loading significantly lower than the third press, removed far more water. This indicated that multiple press arrangements are sensitive to the loading in the earlier presses, despite the usual increase in loading in successive nips. McDonald *et al.* [23] also found that the final sheet web solids content was significantly influenced by the first press load of a four press machine, despite increases in loading in the subsequent presses. McDonald & Kerekes [25] discuss the mechanism of rewetting in wet pressing, believed to be the absorption of surface moisture between the felt and the web. Rewet is only considered to be significant for basis weights lower than 100 g/m^2.

1.2.3 Neural Methods

Artificial Neural Networks (ANNs) are mathematical models of reasoning based on the human brain. The brain consists of a densely interconnected arrangement of nerve cells, called neurons. The neurons are basic information-processing units and are linked to other neurons to allow communication. During learning it is the strength of these connections which is either increased or decreased. Similarly ANNs also have basic computing elements, also called neurons, and connections which can be strengthened or weakened. This allows ANNs to learn from experience, learn by example and learn by analogy. Their methods, when combined with modern

day computers, provide a powerful means of learning from measurement data where the relationships between variables are not known exactly.

The programming of a neural network is discussed in the book of Neural Networks for Pattern Recognition, by Bishop [26]. The radial basis function is described along with the consideration of the number of basis functions required for modelling. This number becomes prohibitively large for large databases. In the discussion of the Multi-Layer Perceptron (MLP) the stages of pre-processing, network construction, function definition and post-processing are reviewed. The MLP uses a layered arrangement of neurons whereby outputs from one layer become the inputs to a successive layer. The use of existing theory for feature extraction during the pre-processing steps is highly beneficial. Kolmogorov's theorem can be used as a guide for the ideal number of neurons in the hidden layers, but apparent practical limitations of Kolmogorov's theorem are stated.

There are two common output schemes that can be used, namely classification and regression. Classification schemes can be of the *1-of-c* type where the vector components can only assume the values of 0 or 1, or of the probabilistic type where the sum of vector components must equal 1. The regression type approach makes use of a continuous output function, usually linear to provide a rational output value. The final accuracy of the network model can be improved by choosing an error function which is well suited to the output scheme. The concepts of variance and bias are used to explain why large amounts of data are required for network training, particularly in complex systems. In general the use of complex functions reduces the bias error, but at the same time the variance will increase. Only by increasing the amount of data samples can the variance be minimised. This requirement for adequate amounts of data for training was confirmed experimentally by Edwards *et al.* [27], who studied the curl properties of paper using Neural Networks (NN). In most cases the prediction of the curl properties was acceptable, except for the case of extreme paper curl. The poor accuracy in this case was due to the under-representation of this condition in the data set.

Hussain [28] reviews the development of NNs in chemical process control. The development has advanced due to the increasing requirement for nonlinear process control and the mathematical burden this places on the system designer. Because NNs can learn by example, they offer a cost-effective method of developing useful process models. Most of the networks using the predictive-

type control strategy reviewed by Hussain made use of MLPs. Larkiola *et al.* [29] differentiate between three categories of NNs: (a) signal transfer networks; (b) state transition networks and (c) competitive learning networks. The most widely used signal transfer network in rolling applications is the MLP. State transition networks require dynamic system behaviour, an example of which is the Hopfield network. In competitive learning networks learning occurs through competition between cells which receive the same input data, the winning cell being that which lies closest to the actual solution. An application of an MLP is discussed for the rolling of cold steel. The MLP makes use of a fixed number of inputs and various weight values before each neuron to calculate an output. The error between the MLP output and the actual system output is used in a feedback loop to adjust the values of the weights. This updating of the weight values is repeated a number of times until the network is able to closely approximate the behaviour of the actual system. In their application the MLP was combined with a rolling model and was able to accurately predict the mechanical properties of steel strips.

Gorni [30] describes a number of applications of NNs to the steel rolling industry. In all the applications the network is of the MLP or Rummelhart type due to simplicity and relative stability. In addition to the two mandatory layers i.e. the input and output layers, at least one intermediate or so called 'hidden layer' is used. This increases the complexity of the input interactions which can be modelled. The number of neurons in the hidden layer is calculated using the Hecht-Kolmogorov theorem, which prescribes twice the number of input neurons plus one. Ripley [31] provides a proof which proposes that any continuous function can be described by a feed-forward network with linear output units and logistic units in the hidden layer, and also threshold units or ramp units in the hidden layer.

Applications of MLPs to indicate the state of health of bearings are reported by Liu and Mengel [32], and Randall and Gao [33], in both studies a continuous activation function was used. The latter study also applied a hard limit function post-training for classification. Gearbox fault detection using MLPs were studied by Petrilli *et al.* [34] in which a step function was used to give direct classification of the fault out of the trained network. Paya *et al.* [35, 36] studied gearbox fault classification on drivetrains which had both bearing and gearbox faults. The sigmoidal activation function was used in the MLP for this application. Monsen *et al.* [37] investigated the fault detection and classification in helicopter gearboxes, in which MLPs were able to achieve 100% detection and 0% false alarm rates. Other applications of rotating machinery were

considered by McCormick and Nandi [38] in which the importance of feature extraction methods is demonstrated. The success of MLP training can be significantly improved by presenting measurement data in a format which captures the defect signature. Luo and Wen [39] describe a method of multiple-page mapping of NNs for the constant tension control of paper winding. The method uses six different networks to successfully decouple speed and tension effects. Most commonly, the architecture of the MLP networks are determined experimentally, as was the case in the studies by Liu and Mengel [32], Paya *et al.* [35, 36], McCormick and Nandi [38] and Luo and Wen [39].

1.2.4 Mechanical properties of roll covers

The nip width of a roll press is dependant on a number of parameters, such as roll diameters, cover hardnesses, cover thicknesses and nip loading in the press. Beucker [7] provides an equation to calculate the nip width for a combination of one rock-hard and one soft-covered roll. Beucker [7] investigated many instances of covers that failed inexplicably after relatively long periods of service. The cause is believed to be loading variations in the CD direction imposed by uneven wearing of the covers. In some cases the installation of a new felt or a freshly ground mating roll was the suspected cause of the cover failure. In the paper Beucker postulates that between a roll pair forming a nip, the felt and the paper going through that nip form a small universe. As time goes by, wearing occurs. The wearing of all the universe members occurs in such a fashion that the wearing is actually a form of contour relief. Gradually the higher pressure points are worn down so that the CD pressure becomes more or less uniform. If this process is disrupted by the partial replacement of one of the universe members, it is possible to have localised areas of high overloading which could result in cover failure.

Reese [40, 41] discusses various methods to improve poor moisture profiles. Uniform roll crown is mentioned as a factor, but no quantitative measure of acceptable wear is prescribed. Zwinak [42] reports that the wear of roll covers is considerably diminished when both covers have the same hardness. If the hardnesses are very different then a larger speed differential exists and the softer cover will suffer from excessive wear. Gudehus [43] states that experience has shown that a roll cover with profile can durably withstand the forces incurred only if the maximum pressure per unit area is lower than one tenth of the static modulus of elasticity of the cover material. The

relationship between static modulus of elasticity E_o and the elastomer hardness measured in P&J (Pusey & Jones) is provided, and is reported to be independent of the polymer material type.

Gamsjäger [44] describes the hardness measurements as the most widely used measure for the characterisation of roll cover materials. The hardness tests usually involve the measurement of the penetration depth of a defined conus in the cover surface. Fillers or other inhomogeneities in the cover material can significantly influence this measurement, which means that with equal cover hardness the actual deformation behaviour in the press nip can be different and vice versa. Telama [45] discusses advances in polyurethane cover material technologies. New covers and formulation techniques have increased the resistance to degradation elements such as liquid absorption and chemical attack. This means that two year maintenance intervals are not unrealistic for polyurethane covers, provided the surface wear is not excessive.

Ryder [46] provides an equation which relates total cover deflection to nip width, making use of the geometry of the nip. The formula is not valid for a nip comprising two soft roll covers. Gere and Timoshenko [47] consider the bulk modulus property K of a material. The bulk modulus determines the amount of strain that a material undergoes as a result of equal normal loads in all three planes. It can be observed that for materials where the Poisson ratio ν approaches 0.5, the bulk modulus approaches infinity. This means that while a non-linear spring model may be used to describe the deflection of the polymer cover in a single plane, it must be noted that the cover material is actually being squeezed to other areas.

Moore [48] discusses the cross-machine loading variations which result from incorrect crowning of the press rolls. Crowning refers to the grinding of a profiled diameter along the axis of the roll. The shape of the crown is calculated so that despite the beam-like deflection under load, the nip load along the entire face length of the rolls is the same. The study makes use of a Finite Element Model (FEM) and the beam theory of Timoshenko. The FEM is used to simplify the complex calculations which resulted from the use of non-linear spring elements to model the cover. The spring non-linearity in this case resulted from fact that the contact zone grows as the load increases and non-linearities inherent to the cover materials. The paper considers various permutations of overcrown, undercrown, edge-loading and cover hardness. The non-linearity of the stress-strain behaviour of the cover is highlighted in a case where roll journal loads were moderately increased. The corresponding cover edge load increased significantly and was even

reduced slightly in the centre. The reasons for the non-linear stress-strain behaviour of rubber materials are discussed by Lindley [49]. At high amounts of strain the sections of molecules between adjacent cross-links approach their limiting extension. The situation is intensified in a few rubber types, notably natural rubbers, by the phenomenon of strain-induced crystallization.

Carvalho and Scriven [50] compare the modelling of roll cover deflection using a simple spring model and a plane-strain model. It was found that the computationally cheaper spring model was sufficiently accurate, provided the spring constant was multiplied by a factor of two, i.e. $k = 2*(E/L)$. The factor of two was calculated numerically and may be related to the fact that most roll cover materials are nearly incompressible ($\nu \approx 0.5$). Thus although the cover is modelled as a spring with twice the theoretical stiffness, the understanding is that the cover is actually being displaced to either side of the nip. Use of the spring model in this form is limited to thin covers ($L/R < 0.1$).

1.3 Research objectives

The objectives of this research were to investigate the extension of the period of time that the rolls could be left in operation in the paper machine. The result of this would be a reduction in the frequency of maintenance work that has to be performed. This reduces the maintenance costs of this type of equipment, and the lost production time associated with roll change-outs. The part of the roll assembly which determines the frequency of maintenance work is most often the roll cover. The roll cover wears in operation as a result abrasion and other mechanisms. Thus this research focuses exclusively on the wear behaviour of the roll covers.

Optimisation of the cover service life must be based on two important requirements. The first is that a reliable method must exist which enables the amount of wear that a cover has suffered to be known or estimated at any point in time. The second requirement is that the maximum permissible amount of wear must be known. Considering the first requirement, the amount of wear cannot be feasibly measured directly. This is because of the time constraints related to the fact that the machinery must be stopped for several hours to take these measurements. An indirect method of measurement must thus be found. The possibility of using a predicted wear rate as an indirect measurement will be investigated. This is the current practice, but its repeatability in the case of nipped rolls must be investigated. If this repeatability is found to be

too low to form the basis of an estimated wear calculation, then it will not be fit for use to calculate the expected life calculation. In that case an alternative form of end-life calculation must be developed. The second requirement is that the acceptable limits of cover wear must be known. This should be dependant on two things: the mechanical integrity of the roll cover and the effect of cover wear on the paper being produced. Despite widespread comment of the latter effect, no quantified relationships were found in the literature. The requirements from this dissertation in this regard are that a method be developed which can be used to calculate the limits of wear for a specific roll. This method must then be applied to a roll to demonstrate its application. The consideration of the mechanical integrity of the roll is provided for the sake of completeness.

1.4 Document overview

Chapter 2 provides an overview of the papermaking process on a modern paper machine. The chapter also presents results of a preliminary but conclusive study of the wear behaviour of roll covers on commercial paper machines. The findings of this study provided valuable information required for the development of the solution model developed in chapter 3.

The development of a theoretical maintenance tool for condition-based roll changes is the subject of chapter 3. First a theoretical process model is developed to describe the interactions between paper machine process variables. Then, using the knowledge of these interactions, the model is re-configured as a maintenance tool.

Chapter 4 presents an experimental verification on a commercially active paper machine of both the process model and maintenance tool developed in the previous chapter. Comparisons of the proposed methods with the current practices in industry are provided. The chapter also explains the details of the data handling which are specific for each application of the proposed method.

The research is concluded in chapter 5. Recommendations for further research are provided.

2. The importance of effective roll maintenance

2.1 Overview of the papermaking process

The fundamentals of papermaking have remained unchanged since the Egyptians first used papyrus reeds to make scrolls. In essence all that is required is that a low consistency mixture of fibres and liquid be poured over a screen. The fibres that remain behind on the screen will bond, and when dried, will form a sheet of paper. Nowadays the source of fibre is usually timber, which is chipped and then cooked to release the fibres into a watery solution called pulp. The pulp is then pumped to the headbox which is considered the start of the paper machine, shown schematically in Fig. 2-1.

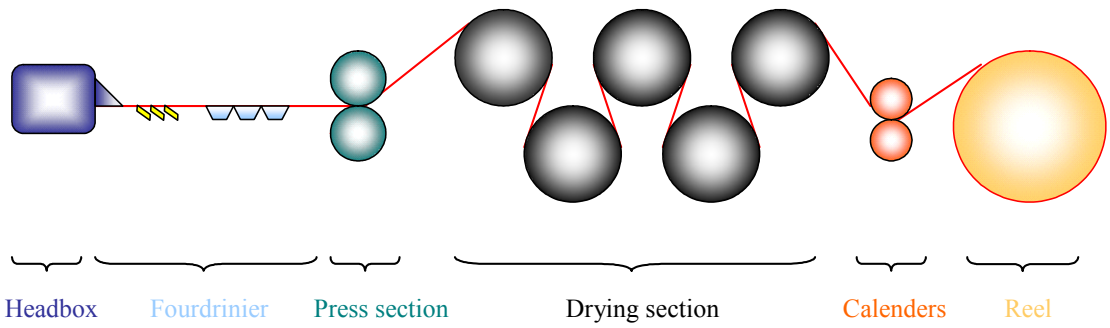

Fig. 2-1 Schematic layout of the paper machine

The pulp arriving at the headbox is a slurry of 0.3% wood fibres in 99.7% water. The purpose of the headbox is to meter a uniformly thick layer of pulp onto the fourdrinier across the width of the machine. The fourdrinier consists of a rotating permeable fabric which supports the fibres and allows the water to drain downwards, first under gravity and later under vacuum. At the end of the fourdrinier the pulp contains approximately 75% moisture, and it now referred to as the paper web. At this point the web is still too weak to support its own weight, and thus is supported by a press fabric as it enters the press section.

In the press section the paper web is carried between the press rolls which are forced together. The force generates nip zone of high pressure along the line of contact between the two rolls.

Usually one or both of the rolls have polymer covers which deflect in the nip, resulting in an increase in nip width. As the paper enters the nip the water is forced out under pressure creating the desired dewatering effect. The press fabric assists dewatering by absorbing the water which is expunged from the web. The high mechanical load in the nip also increases inter-fibre bonds and hence the mechanical strength properties of the paper. There can be more than one press in the press section, usually with less water being removed in each successive press despite increases in nip load. This is due to the fact that water becomes more difficult to remove as the web becomes drier. A practical limit is reached at approximately 55% consistency, where after no more water can be practically removed by mechanical methods.

In the drying section the web is steadily dried as it passes in a figure-of-eight path over steam heated drying cylinders. The cylinders provide a large surface area which can reach temperatures as high as 110^0 Celsius. The drying section uses evaporation as the main dewatering process, which also makes it the most energy intensive and hence expensive method of water removal. At the end of the drying section the moisture content is approximately 7.5%. The sheet is subjected to a final nip in the calender stack which consists of two steel rolls with a surface finish in the order of R_a= 0.1 μm. The calender rolls rotate at dissimilar speeds in order to polish the surface of the sheet. Uniformity of the sheet thickness is also enhanced here. Finally the sheet is rolled up on the reel for further handling.

2.2 Observations of roll wear behaviour

As a rule all roll changes on commercially active paper machines occur on a scheduled basis. This is because the *in situ* measurement of roll wear is a labour intensive exercise and is not feasible given the number of rolls and time available during maintenance outages. Because the roll cannot be measured, its service period is predicted and changes scheduled accordingly. Exceptions to this rule are termed roll failures, because the roll has failed to operate satisfactorily until its planned change-out date. The causes of roll failures are numerous, but can be related to bearing faults or special requests from papermakers who suspect that the roll cover might be the cause of production problems. The previous chapter indicated that in nearly all cases the bearings are in fair condition when removed from the machine. Thus the change-out interval of each roll is determined by the amount of wear of the cover. The success of this scheduled maintenance methodology is dependant on the fact that the roll cover wears by the same amount each time it

is placed in the machine. Stated in engineering terms: the success of the scheduled replacement approach is dependant on the repeatability of the wear rates of the covers. Furthermore if the wear rates are repeatable and can be calculated within a specified accuracy, then this wear rate can be used to calculate new change-out frequencies (given that the maximum upper limits of roll wear have been defined). The objectives would be to decrease the frequency i.e. to extend the period of operation of the rolls. This would not only result in a decrease in the downtime associated with roll changes, but also reduce the maintenance expenditure on labour, new covers and bearings.

The dependence of roll wear on the material abrasion resistance and friction coefficient was indicated by Beucker [7]. However, Beucker concedes in the same paper that measurements of these parameters have only met with general correlation with measurements on actual paper machines. To this author's knowledge no other theories are in existence to estimate/predict the amount of cover wear which will occur for a given set of operating conditions. This despite the fact that in most applications the operating conditions of the rolls are similar if not identical over extended periods of time. In fact changes normally only occur as a result of a design change to the machine. As a result the users of the rolls are in a fortunate position which allows them to study the wear rates by physical measurement alone, without the requirements for any type of underlying theory.

To investigate the repeatability of the cover wear rates a study of the archival records of sixteen nipped rolls was conducted. The records were obtained from four kraft paper machines of vastly differing designs, for five consecutive years of operation. Collectively these machines manufacture a wide range of paper grades from 40 g/m^2 to 400 g/m^2 over a speed range of 150 m/min to 800 m/min. The nipped rolls were selected due to the significance which these types of rolls have on the final product properties.

The wear measurements for one of the rolls are shown in Fig. 2-2. The amount of wear, in mm, is calculated by subtracting the diameters of the roll cover after removal from those taken before the roll went into the machine. For illustrative purposes measurements are shown at only three positions across the roll face and are labelled as Front Side (FS), Centre (C) and Back Side (BS) respectively. The multiple plotted points for each of these positions refer to different sorties in the machine over the five years. The predetermined change-out interval for this roll is six

months, but the practicalities of shut planning necessitated some changes at other intervals. Of concern in this plot is the low repeatability of the amounts of wear given that the roll was placed in the same location of the machine every time. A linear regression was constructed in an attempt to estimate the mean wear amount for each of the positions over the six month period. The gradients of the regression curves thus constitute an aggregate of the wear rates. The value of the correlation coefficients, r^2, represent the accuracy of the linear curve fit, which also indicates the repeatability of the wear amounts. The repeatabilities were very low, with $r^2 < 0$ at all three positions along the roll face. This confirms statements by Beucker [7], but is concerning for maintainers of rolls in paper mills. This is because the repeatability of the wear rates is the underlying theory of the scheduled roll replacements. For this particular roll the repeatability was considered too low to draw any meaningful conclusions from these data. Further discussion regarding the differences in wear rates between the BS, C and FS positions is not of any value given the scatter of the measurement data.

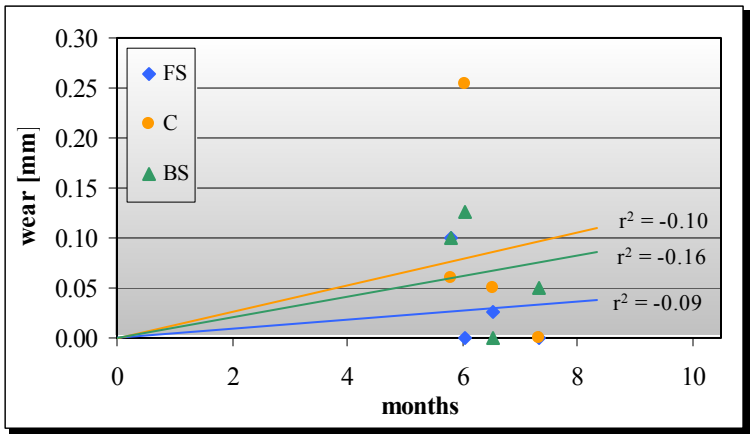

Fig. 2-2 Measurements of wear after removal from machine at predetermined interval

The same analysis was performed on the data from the remaining fifteen rolls. The results are shown in Table 2-A. While there are certain rolls or positions of certain rolls which do wear consistently, these were certainly not in the majority. At the outset of this investigation it was believed that the wear rates would be more consistent. The conclusion that was drawn as a result of these findings was that the wear rates of nipped rolls can not be regarded as consistent enough to form the base of a preventive maintenance plan. The fact that this approach appears to have worked in the past implies that the recommended intervals between maintenance change-outs are probably overly-conservative. This means that a high wear rate is always assumed and the

interval calculated accordingly. This is safe engineering practice, but also means that a significant number or roll changes are probably occurring at a point in service life prior to that which is actually necessary. This leads to high machine down-time, high maintenance costs and more frequent replacement of the roll covers.

Table 2-A Repeatability's of the wear rates for nipped rolls.

Paper machine no.	Roll name	Correlation coefficients (r^2)		
		FS	C	BS
1	1st Press top roll	-0.09	-0.10	-0.16
1	1st Press top roll (spare)	0.39	0.44	0.34
1	2nd Press bottom roll	0.19	-0.09	0.11
1	2nd Press bottom roll (spare)	-0.08	0.32	0.78
1	Lumpbreaker roll	0.20	0.20	-0.32
1	Lumpbreaker roll (spare)	-0.23	-0.13	-0.24
2	1st Press top roll	0.03	-0.05	-0.01
2	1st Press top roll (spare)	0.16	-0.19	-0.24
2	1st Press bottom roll	0.64	0.64	0.29
2	1st Press bottom roll (spare)	-0.02	-0.07	-0.02
3	Suction press top	0.32	0.57	0.28
3	Suction press top (spare)	-1.22	0.72	-1.26
3	Suction press top (spare)	-0.06	-0.30	-0.28
3	Lumpbreaker roll	-0.02	-0.05	-0.02
3	Lumpbreaker roll (spare)	-0.52	-0.68	-0.76
4	Lumpbreaker roll	-0.21	-0.21	-0.21
	Average	-0.03	0.06	-0.11

Beucker [7] describes what the papermaker requires from a roll. The papermaker is the end-user of the roll and hence is the best person to make judgement. The requirement is a roll which has uniformity of the roll surface along the entire roll face. This requirement is best explained by

considering the press-type rolls. These types of rolls were chosen for the pilot study due to intuitive knowledge of their influence on the final properties of the sheet. Any localised wear of either of the soft polymer covers will result in a pressure decrease in the nip and hence less sheet dewatering in that area. This effect is indicated in Fig. 2-3 which shows a magnification of a worn roll cover and the resultant moisture streaks which can be observed in the paper web. The possibility of changing rolls based on the moisture profile of the paper requires that the relationship between the streak severity and the wear amounts must be known exactly, and tolerances defined. Furthermore, if this relationship is known, the wear progression can be monitored using the paper as an indicator. There are other effects which the press rolls have on final sheet properties, but it was decided that the moisture profile would be the most critical and the most obvious effect.

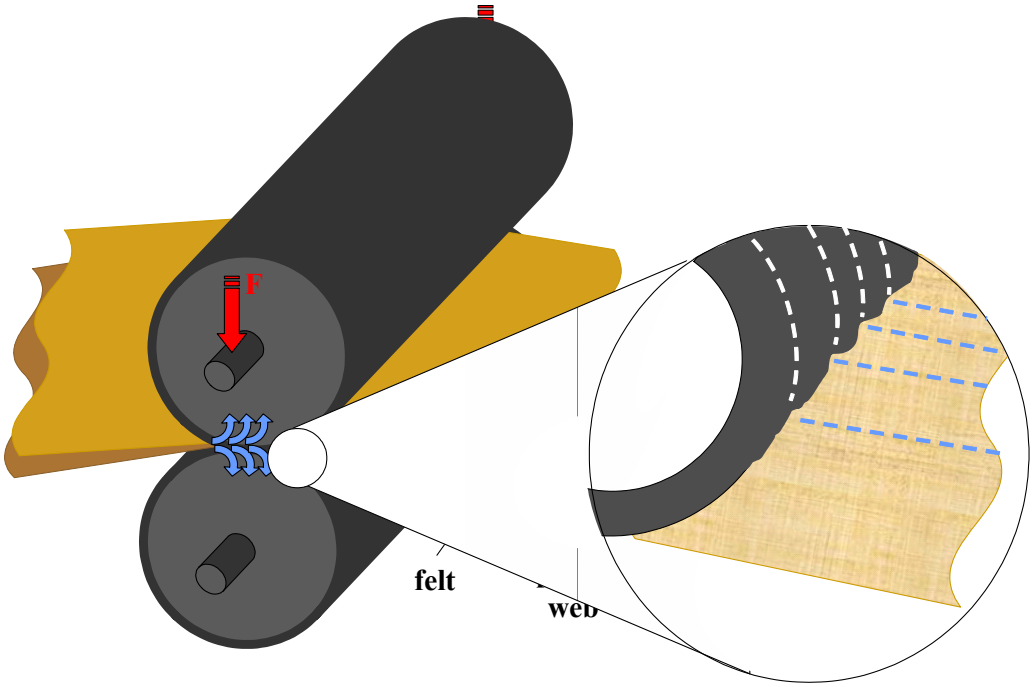

Fig. 2-3 Non-uniform wear along the axis of the roll affects CD moisture profiles

This presents the argument that the nominal wear rate of the roll is unimportant, and that all that is required from the roll cover is that it must wear evenly across its length. This means that from a papermakers point-of-view the roll can wear fast or slow, it doesn't matter, as long as the wear rate is uniform at all points along the cover. If this is the case, then the roll change intervals should be related to the differential wear between different positions along the roll face, and not the nominal wear value. Of course, for the purposes of longevity the nominal wear rate is

important, but this usually related to the inherent properties of the cover material. The proposed argument of replacing rolls based on differential wear and not nominal wear has the best intent, but also presents some practical limitations. One of these is the question of what position should be used as the reference. Or should each position become the reference for its adjacent? Presumably this is why differential wear limits were not used in the calculation of the original maintenance intervals. Some manufacturers do specify a differential wear tolerance per unit length of roll face, but this usually applies to grinding of the cover and not the service life of the roll.

In his review of failures of roll covers, Beucker [7] presents a hypothesis whereby it is believed that rolls wear through a process contour relief. The wear occurs in proportion the pressure at each point, and results in an equilibrium in which roll wear occurs uniformly. No experimental data in support of this theory were presented, however this theory does appear to be intuitively correct. The fact that it is common practice in industry to change press rolls as a set reinforces this type of argument. The underlying basis of this theory is that wear is dominated by pressure effects. If however, wear is more related to the surface effects eluded to earlier in Beucker's paper, then the hypothesis may not be completely accurate.

For the purposes of this study the hypothesis needed to be tested. If it is valid, then only nominal wear rates need to be considered when determining new change-out intervals for the rolls. If not, then an alternative method of determining intervals based on differential cross-directional cover wear must be found. To test the hypothesis a single press roll pair was studied by measuring the diameters of both rolls at a number of points across the roll face. The measurements were taken during maintenance outages over a period of seven months. The long duration of the study was necessitated by the slow progression of cover wear. Measurements were taken after the roll covers were allowed to cool for between three and five hours. This was necessary to isolate the thermal expansion effects from those which were related to the physical wear of the cover. It is conceded that the thermal effects will also contribute to the equilibrium-pressure state, if one exists. However, this contribution will only amplify the observations which can be made from the measurements at a stable temperature. Measured high points, for example, will experience greater contact pressure and hence generate more hysteresis heat. This will result in a greater thermal expansion in those areas than areas with lower pressure. The trended measurements from this study are shown in Figs 2-4a and 2-4b for the top and bottom rolls respectively. The vertical axis has been normalised to indicate only the surface contour effects.

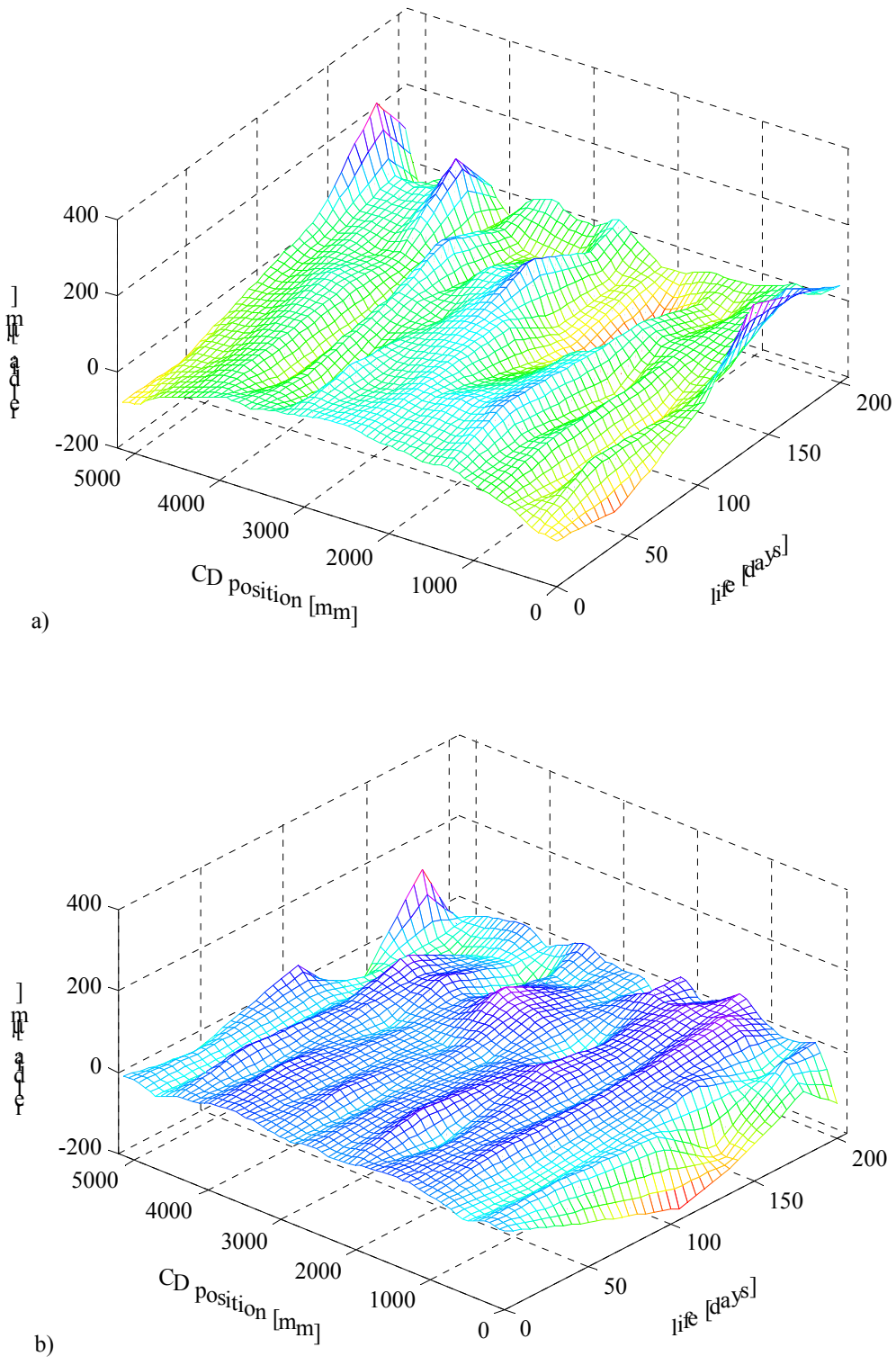

Fig. 2-4 Wear profiles for a) top press roll, and b) bottom press roll

The first observation that can be made is that there is no evidence that any form of contour relief exists. Had this been the case, then peaks would have been observed on one plot which corresponded to valleys in the other plot. To observe this, simply compare values at similar points in the horizontal plane. The second observation that can be made is that no clear pattern of wear progression exists. Had this been the case, peaks and valleys of chronologically increasing magnitude would have been observed. The fact that this was not the case led to the conclusion that the factors which determine roll wear are even more complex than earlier anticipated. This was also reported by Meikle *et al.* [51].

The most important deduction that can be made from this study of roll wear is that nipped cover wear rates are not repeatable. The conclusion reached from this is that a preventive maintenance methodology is not efficient for this equipment. Furthermore, the fact that the mechanisms of wear are not fully understood means that predictive methods will not be possible either. The natural next evolutionary step in maintenance methodologies was to consider a condition-based approach to roll maintenance. This implies a regime whereby rolls are changed based on the condition of the cover. The condition of the cover must be evaluated frequently due to the fact that the wear rates are not consistent. The requirement for such a system is that the acceptable limits of cover wear be known. These limits should be specific to each roll and its location, rather than the generic limits provided by cover suppliers which have already been shown to include overly-conservative safety factors. The physical wear amounts will vary for each roll and location and as such are calculated in a more universal form of nip load reduction as calculated by the models proposed in Appendix B and D.

The important question to be asked at the start of developing a new maintenance methodology is ‘Why are we maintaining the equipment?’ The answer in the case of paper machine rolls has two tiers. Firstly, to preserve the mechanical integrity of the rolls so that they can continue to operate safely. Secondly, to ensure that the design purpose of the rolls are met i.e. their function in the papermaking process. Both these answers are requirements for the new methodology, which is developed in chapter 3.

For the mill manager, the efficiency of this roll maintenance is also an important consideration that must be made. The efficiency in this context refers to the amount of money which is being expended to keep the roll in running condition. One the one hand it is possible to achieve defect-

free operation by changing the roll very frequently. The maintenance costs in this case will be very high. On the other hand operating the rolls to near-fracture will save maintenance costs in the short term. In between there is an optimum change-out point. This occurs at the point where the roll has operated for as long as possible without negatively affecting paper quality. Usually the cost of a roll change includes a new bearing set and the removal of expensive cover material in the process of regrinding. This regrinding can only be performed a few times, typically less than seven, before a new cover must be purchased. The overall cost of a single roll repair is thus more or less fixed. Hence the opportunity for maintenance savings lies in reducing the frequency of these repairs. This is exactly the purpose of chapter 3, which aims at providing a model which will indicate the optimum change-out point of the roll.

3. A model for condition-based roll changes

3.1 Model objectives

The objective of this model was to develop a method whereby rolls can be changed at more optimal intervals. This would avoid roll changes which occur too frequently and also those which do not occur infrequently enough, to the detriment of the paper quality. Unfortunately it is not feasible to measure all of the rolls on each maintenance outage. A method is thus required for calculating an estimate of the amount of wear on a roll at any point in time. Chapter 2 showed a wear rate calculation which predicts the amount of wear after a certain period of time. Chapter 2 also showed, however, that this predictive approach is not accurate for nipped rolls. The lack of success using the predictive-type of approach leads to the next evolutionary step in maintenance methodologies. This is the condition-based method whereby rolls can be changed based on the condition of the cover, and is developed in this chapter.

Ideally a condition based approach could be implemented by physically measuring the rolls at each maintenance outage. The roll would then be changed when the wear had exceeded a certain tolerance. The time constraints prohibit this type of measurement. Thus an indirect roll wear measurement must be used. This indirect measurement should provide an indication of the condition of the roll, without the requirement for physical roll measurements. Ideally this indirect measurement should be able to be evaluated between maintenance outages. This would allow sufficient warning time to plan the maintenance work required to change the roll. The same concept is applied in the vibration monitoring of roller element bearings. The noise level and frequency of vibration are used as indirect measurements of the condition of the bearing. This avoids the necessity of regularly opening up a bearing for inspection, which wastes valuable process time and can damage the bearing. The success of these methods is dependant on whether a relationship between the direct measurement and the indirect measurement can be found. In the case of vibration monitoring, the relationship is provided by the Fast Fourier Transformation (FFT) calculation. The FFT converts vibration readings from the time domain to a frequency domain.

The objectives of this chapter are the establishment of the calculations which relate the direct measurements to the indirect measurements. The integrity of the roll cover is considered in the later stages of the model's development.

3.2 Model methodology

In the development of vibration monitoring methods from vibration measurements, direct measurements of the bearing surface defects were related via the indirect measurements of vibration to the FFT results. The results are very different to the direct measurement, but they allow certain characteristics to be identified. The development path followed in this study is similar in the initial stages, because it also requires direct measurements of the roll wear for a limited period of time, typically a few months. The development paths differ in the latter stages however. For the case of vibration, the known FFT calculation was used to provide a new result which is used for interpretation. In the present study it is the calculation method which is not known, and the result which is known, namely the moisture content, because it can be measured. This is the same thing as being able to read a FFT result in the frequency domain directly from a machine, and being asked to interpret the condition of the bearing. This would only be possible if the relationship between the FFT result and the physical bearing measurement was known.

This approach necessitates the measurement of the moisture content over the same period as the roll wear. A calculation method must then be custom-developed which provides a calculation from the wear measurements to the moisture measurements. This calculation must be accurate. The custom-calculation is thus a simulation of the dewatering behaviour of a paper machine. The importance of this calculation is that even if the wear on the roll cannot be physically measured, it can be back-calculated from the moisture content, which can be measured. The measured moisture content can thus be regarded as an indirect measurement of the roll wear.

The next step is to consider how this calculation can be used as a condition monitoring tool. It is assumed at this point that the custom calculation has been established for the particular paper roll in the machine. To evaluate the cover wear, a measurement of the moisture profile is made. Typically the profile should consist of more than 50 individual measurements. Then, each of the 50 moisture measurements are fed into the reverse of the custom-calculation described above. The result will be the roll wear, because the forward calculation converts roll wear to moisture

content. The calculated amount of roll wear can then be compared to a prescribed tolerance, and a decision made whether or not the roll should be changed. Chapter 2 showed that no consistent chronological trend of localised wear areas on the roll could be found. This may bring into question the purpose of a condition based approach, since no trend can be observed. The purpose of the condition based approach is to evaluate the condition of the roll at a specific point in time, not to trend the wear. If anything, the lack of a trend in the wear behaviour reinforces the need for a type of spot-check on the roll cover. This check can be used for on the run fault-finding exercises when moisture profiles and other roll-affected properties are out of specification.

At the outset of developing the model which is required for this study it may be asked why the forward custom-calculation is required if the condition monitoring tool only requires the reverse-calculation. Why then not develop only the calculation from moisture content to roll wear. The answer is related to complications which are introduced by the papermaking process. These will be described in section 3.3.

The argument that the paper properties are only affected by differential wear has already been made. This simplifies the requirement of the model in that it need only consider the CD variations in moisture. The nominal values given by the models were not considered a requirement of this study. This is a significant simplification, because there are a large number of parameters which can influence the MD or nominal moisture content exiting at the reel. Since only the CD variations in load were considered important, only CD variations in moisture were required from the model. Thus the modelling process would be considered complete if the CD moisture profile was correctly described by the model, irrespective of the mean value of the profile. Such a model is said to exhibit *translation intolerance.*

Because each roll and paper machine behave differently, the custom-calculation must be developed for each application. There are thus two distinct steps for each new application, namely the development and the monitoring steps. In the development step the roll wear must be measured with the moisture content. The physical measurements of the roll are a potentially prohibitive exercise, but are outweighed by the long-term benefits of being able to assess the condition of the roll on the run. In the monitoring step only the moisture profile of the paper sheet needs to be measured. The roll wear measurements are no longer required as they can be reverse-calculated from the moisture profile.

3.3 Other considerations of the model

The objective of this study was to determine if roll change-out intervals could be extended. An extension of the manufacturer-recommended intervals must not be done blindly however. In addition to the paper quality, the mechanical integrity of the roll must also be considered. The constraints regarding mechanical integrity are the cover, the bearings and the steel structure. The bearings can be monitored on-line and the steel structure can be routinely inspected. Thus this study must still concern itself with the integrity of the cover. Uneven wear of the cover material will result in load differences along the length of the nip which may result in cover fracture. For this the permissible load variations must be determined. However, it is very likely that the paper quality will be affected before the cover loading reaches an overstressed state. This follows on to the second objective of this study i.e. the limits of roll wear. There is much to be said regarding the effect of roll maintenance and how it affects the quality of the paper being produced. To the author's knowledge there is no definitive literature on this subject. The model developed in this chapter will address these issues and show that the maximum wear of a press roll is determined by the paper quality.

Early attempts to establish a custom-relationship between the roll wear profile and the moisture profile were unsuccessful. These were mathematically rudimentary, and involved a comparison of the two profiles. Further attempts were made whereby the CD roll wear profiles of the two mating press rolls were superimposed to give a CD nip load profile. The nip load profile indicates a decreased loading in areas where both mating rolls have worn excessively. The roll wear to nip load calculations are described in Appendices B and D. This nip load profile was then compared to the moisture profile to establish the custom relationship. The correlations between the nip load profile and the moisture profile were also unsuccessful. The lack of success of these two approaches was explained by a more extensive literature study. The literature indicated that the moisture profiles are also affected by other factors. In fact the literary material on press dewatering indicates that even within the press a large number of factors can affect the final moisture content, as reported by Meikle *et al.* [51].

As a result of the poor success of the initial overly-simplistic comparisons, a more holistic approach to the problem was conceived. The new methodology suggests that the development of the custom-relationship should begin by considering all the factors which can influence the

moisture profile of the paper sheet. All of these should be included in the calculation so that the intended conversion between roll wear and moisture content can be made. The development of the all-inclusive calculation begins with a review of the papermaking literature study. The intention of the review is firstly to determine which factors, in addition to roll wear, can affect the moisture profile. Secondly, the review should identify any existing calculations which may provide, or assist in providing, a conversion calculation from wear plus other factors to the moisture content.

The dewatering theories of Wahlstrom [12], Kerekes and McDonald [14], Clos *et al.* [15] and Roux and Vincent [54] differ on the *modus operandi* but agree on the basic press parameters responsible for determining the sheet moisture exiting the nip. In general these are related to the initial moisture content, the compressibility and permeability of the sheet, and a time-pressure measure of the conditions in the nip. The scope of application of these models was improved by the consideration of felt flow resistance by Wahlstrom [12], and the lumped compressibility and permeability factors by Kerekes and McDonald [14]. Despite these improvements the application of these models on a commercially producing paper machine is complicated by a wider range of influences such as varying ingoing felt moisture content, calendar load and the fact that grab samples could not be taken directly after the press.

A further difference between a pilot paper machine and a commercially active machine is that on a pilot machine the conditions can be regarded as being constant over the short duration of the experiment. On a commercially active machine there is mechanical wear and tear and also dynamic changes in the process controls which can disturb the results. In fact press section monitoring guidelines published by the TAPPI [17] stipulate a wide range of external factors which can influence the moisture content of the final product. Thus this study required that measurements be made not only of the parameters which were of interest for maintenance purposes, but also all those which were considered to be influencing factors.

Because the proposed method is intended for application in the production environment, particular emphasis had to be placed on its practicality. For this reason the method must make exclusive use of measurement parameters already known to machine operators. The readings must be taken from existing measurement equipment which is used for process control. This is

different from laboratory methods which sometimes make use of tests which would ordinarily cause stoppages if used in the production environment.

In their derivation Kerekes and McDonald [14] indicate that it is not important how specific web properties affect moisture, but how the combined effect of these properties affects moisture. This methodology was extended in the present study to include all measurable parameters which could potentially influence ingoing moisture, compressibility, permeability, time or pressure. For example the softwood-hardwood fibre blend compositions must be measured because softwood fibres are more than double the length of hardwood fibres. Fibres length affects the permeability through differing water exit path tortuousities, and also affects compressibility by differences in fibre arrangement. Using, as a guideline, the various dewatering theories of Wahlstrom [12], Kerekes and McDonald [14], Clos *et al.* [15], Roux and Vincent [54] and a paper on press section monitoring by TAPPI [17], the broadest scope of influencing factors were identified. In total 20 parameters were identified to be relevant on the particular paper machine used in this study. Each of these can be classified into one or more of the four main classes i.e. initial moisture content (IM), compressibility (C), permeability (P) and a time-pressure measure (Pt) of the conditions in the nip. The 20 parameters are listed in Table 3-A, together with their class.

Table 3-A List of influencing parameters.

No.	Parameter	Class
1.	Chemical softwood blend	P, C, IM
2.	Semi-chemical hardwood blend	P, C, IM
3.	Recycled fibre blend	P, C, IM
4.	Re-processed fibre blend	P, C, IM
5.	Top ply load	P, C, IM
6.	Top ply freeness	P, C, IM
7.	Top ply consistency	P, C, IM
8.	Top ply stock temp	IM, P
9.	Base ply freeness	P, C, IM
10.	Base ply consistency	P, C, IM
11.	Base ply stock temp	IM, P
12.	Machine speed	Pt
13.	1st press felt permeability	P, C
14.	1st press felt water content	IM, C
15.	1st press roll wear	Pt
16.	2nd press felt permeability	P, C
17.	2nd press felt water content	IM, C
18.	2nd press load	Pt
19.	Calender load	Pt
20.	Basis mass	IM, P, C

The effect of each of the parameters in Table 3-A on the outgoing moisture of the sheet can be explained by grouping similar effects. Parameters 1 through 4 relate to the proportions of different fibre types, called blending. Different fibre types have different lengths, the influence of fibre length on permeability and compressibility has already been explained. The blend also affects ingoing moisture because the water removed upstream of the press on the fourdrinier is dependant on fibre blend. Parameter 5 describes the proportion of fibre which constitutes the top ply of the sheet. This affect also describes differences in fibre length. Parameters 6 and 9 describe

the amount of mechanical refining or beating of the wood fibres. The purpose of refining is to fibrillate the fibres so that they form mechanical bonds with each other. This process affects the fibre matrix structure and the resistance to water flow. Parameters 7 and 10 describe the ratio of fibre to water in the pulp entering the headbox. This directly influences the ingoing moisture content at the press, and the presence of excess water also affects the compressibility and permeability of the sheet. Parameters 8 and 10 describe the temperature and hence viscosity of the water in the sheet, which naturally affect the rate of water flow. Parameter 12 is the machine speed which has an obvious effect on the time the sheet is exposed to the pressure in the nip. Parameters 13, 14, 16 and 17 all refer to the condition of the press felts which are required to absorb the water expunged from the paper in the nip. Parameter 15 is the main interest in this study, and in particular the influence of wear on the pressure and thus the outgoing moisture content. Parameters 18 and 19 are included to account for the effects of other nips on this particular paper machine. Parameter 18 is the 2nd press load. On this particular machine mechanical dewatering is achieved by two consecutive double-felted presses *viz*. the first and second presses. The second press consists of a shoe press, unlike a roll press, with a maximum nip loading of 1200 kN/m. By design, the shoe press provides a uniform CD nip load, and was thus assumed not to contribute to a study of load variations the CD direction. The 2nd press load was included in the model to allow for any interaction between the two presses. The condition of the felts in the 2nd nip were thus also measured. Parameter 20 is the basis mass, or fibre mass, which describes the mass of fibre in the sheet. This parameter was included to describe differences in mass and the corresponding moisture differences which result from the delivery of pulp in a fixed-consistency slurry form at the headbox.

The requirements of the model are that it is able to explain the behaviour of the dewatering process on the commercial machine used in this study. Only after this behaviour can be explained, can the effect of the roll wear be investigated. A further requirement of the model is that the effect of the worn roll must be able to be isolated from the other dewatering effects. This will require some sort of reverse or iterative calculation in which the load is changed experimentally to determine the effect on moisture. The accuracy required from the model is such that it must be able to predict the wear on the roll as either acceptable or unacceptable. Due to the fact that the paper quality is being used as an indirect indication of roll wear, an advantage of this approach is that the wear limits will be easily defined in terms of paper quality. Thus an additional calculation of the wear tolerances for these rolls will be made from the model.

It may be that the model, when finally developed, is able to describe the dewatering behaviour without considering all 20 measured parameters. This situation may occur due to differences between laboratory or pilot machines versus commercial machines, or because certain of these influencing factors are tightly controlled on the commercial versions. Whatever the reasons, if the relationships can be established using fewer than 20 variables, this would also be considered acceptable.

3.4 Model of the dewatering process

For the purposes of this study the objective was for a model or calculation method which would use the roll wear measurements at any point to calculate the moisture content of the paper rolled by that specific point. If this calculation could be provided, then it would simulate the dewatering process of a paper machine. Furthermore, if the calculation could be reversed, then a measured moisture value could be used to calculate the roll wear. This reverse-calculation could then be repeated at any time with a fresh paper moisture reading to indicate the current amount of wear. An organised program of regular calculations of this nature would thus form a condition monitoring program which would indicate a faulty roll or near-faulty roll. This could result in timely replacement of the roll. However, it was shown in section 3.3 that a number of factors can influence the moisture content of the sheet at the end of the process. These factors would be falsely interpreted as roll wear by the calculation described above. For this reason, each of these parameters must be included in the calculation so that their influence on moisture can be isolated from that of the roll wear.

It is clear that the characterisation of the effect of roll wear on paper moisture content is significantly more complex than a simple analysis of these two measurements in isolation. The previous section discussed the range of factors which were identified as influencing factors. A model is required which is able to incorporate these influencing factors, and still establish the relationship which is required for this study. The fact that model must be applicable to commercial paper machines indicates a requirement that the model be able to adapt by statistical curve fitting, regression or other means to the measured data. It may be possible that a model derived from scratch theoretically is able, in conjunction with a number of empirical constants, to

describe each of the parameters individually. However, the amount of time required in developing and isolating these factors was considered too prohibitive.

Now that the number of influencing factors and the special requirements for the custom-calculation have been described, the need for a reverse calculation can be appreciated. For the forward calculation from roll wear to moisture content there are some models available in the literature. Conversely, there are no calculations in the other direction. Due to the complexity of the problem, it was believed that the forward calculation would provide a firmer base from which to construct the model. Thus the models were evaluated based on the forward calculation, with the concession that additional work would be required to reverse the final model. In the following two sections the two short-listed possible modelling methods are reviewed in terms of their suitability to the objectives of this study.

3.4.1 Decreasing permeability model

The first model that was considered to provide the custom-calculation was the Decreasing Permeability (DP) model proposed by Kerekes and McDonald [14]. This model describes wet pressing as a process of forcing water from a porous medium in which resistance to water flow increases with decreasing water content. According to this model, as dewatering proceeds, the flow resistance increases because of the smaller pore structure associated with the origin of the water. It also increases because increasing pressure and water removal increase hydraulic resistance by diminishing or closing the flow paths of the water. Based on this picture of wet pressing, the water removal process can be modelled as a nonlinear process of flow from a medium of decreasing permeability. This analogy overcomes the mathematical shortcomings of the Wahlstrom [55] model which splits the pressure applied to a wet web into two components – a hydraulic pressure that creates water removal and a network pressure that supports load through the fibrous structure.

The DP model begins with an analysis of the Kozeny-Carman equation [56], and describes each of the variables as a non-linear function of moisture content after pressing, m, and initial moisture ratio, $m_{0,}$ as shown by Kerekes and McDonald [57]. The collective effect of the nonlinear relationships with the moisture ratio, results in the following pressing equation:

$$\frac{m}{m_0} = \left(1 + \frac{nfP}{m_0 V}\right)^{-\frac{1}{n}} \tag{3-1}$$

where:

m = Amount of water remaining in the web after pressing

m_0 = Initial moisture ratio

$\frac{P}{V}$ = Press impulse

f = Permeability factor

n = Compressibility factor

In conceptual terms, f represents the permeability of the web in the initial uncompressed condition, while n reflects the manner in which this permeability is changed with water removal. The derivation of Eq. (3-1) includes the first theoretical proof that the pressure and time effect can be grouped into a press impulse term. The model omits felt non-uniformity as a variable, with the argument that in some cases, such as newsprint grades, that this factor may not be important relative to other factors. The authors concede that the model has two limited objectives. The first objective is to act as a coarse design equation for approximate predictions of wet pressing – in simple paper machine simulations, for example. The second objective is to provide a method of predicting pressing behaviour from one rolling nip to another. McDonald and Kerekes [25] investigated the DP model with rewetting. The paper does not give new insight into the mechanism of rewetting, but does indicate that a special rewetting term is only required for lightweight grades below 100 g/m^2.

The practical application of the DP model is made through the curve fitting of measurement data to calculate experimentally the values of f and n using a nonlinear technique. The correlation coefficient r^2 is used to evaluate the accuracy of the curve fit to the experimental data. The model was tested using laboratory data from the literature over a wide range of incoming moisture ratios, freenesses, and ranges of press impulse. In general the agreement was good, with correlation coefficients in the range of 0.82 to 0.99. In one case the coefficient was measured at 0.60, but this was explained as an outlier data set which would not be practicably encountered on a commercial machine. The model was also tested against data from a pilot paper machine which indicated good agreement between the fitted line and the experimental points, with r^2 = 0.91. In the summary of the model application the authors acknowledge that there may be situations

where a longer form of Eq. (3-1) will be required. Examples provided are shoe presses with linear loads above 1000 kN/m and very long dwell times.

3.4.2 Neural Network model

Artificial Neural Networks (ANNs) were considered as the second modelling tool in this investigation due to their proven application in multi-variabled problems. Unlike the DP model, the ANN is not related to papermaking *per se*. In fact the ANN methods have been applied in many different applications for the precise reason that they do not require foreknowledge of the system they are being used to model. ANNs learn from experience, learn by example and learn by analogy. The similarity between the reasoning methods of the human brain and the ANN were discussed in section 1.2.3.

In the case of this model, it was postulated that the ANN would be able to learn from a database of machine and process measurements. The objective of this learning would be to develop a mathematical description of the dewatering process in a paper machine. This would provide a method of calculating the moisture content from the wear measurements plus a number of process measurements. Then, from the relationships established during the training of the network, estimation of the wear measurements would be possible for given moisture values. Once complete, the methodology would allow the condition of uneven cover wear to be monitored without physical roll measurements, and the roll could be replaced on condition. The use of a neural network does present somewhat of a paradigm shift, and for this reason some background to the method is provided below.

Theory: The neuron

The ANN is a structured arrangement of basic computing elements, called neurons. The functioning of an ANN can be more simply explained by considering a single neuron, depicted in Fig. 3-2a. The inputs x_i, which can be physical or process measurements, are each multiplied by a dedicated weight factor w_i ahead of the neuron. The neuron then uses the sum of the weighted inputs and a bias value b to calculate an output value y according to an ordered activation function φ:

$$y = \varphi\left[\sum_{i=1}^{n}\left(w_i x_i\right) + b\right] \tag{3-2}$$

where:

y = Calculated output value

φ = Activation function

w_i = The i^{th} weight factor

x_i = The i^{th} input, or measurement

b = Bias value

The activation function φ can be described by a wide range of functions including step, linear and nonlinear depending on the application. The neuron output can thus be used to reach decisions based on certain combinations of inputs.

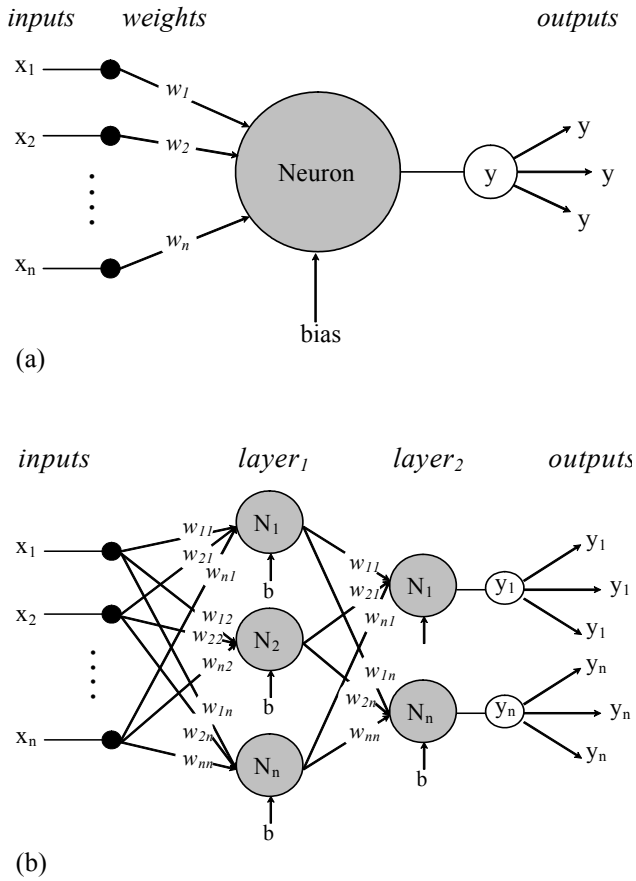

Fig. 3-2 Neural models for, (a) the neuron and (b) the neural network.

The use of the neuron to describe the behaviour of some existing physical system requires that the neuron output assimilate the outputs of that system. This is achieved through a process called neuron training. During training the neuron is presented with a new combination of inputs, called a feature vector, for which the physical output is known. The neuron's output is then calculated and compared with the physical output. The error between the two is used to slightly adjust the values of the weights and bias, such that the neuron output will be closer to the physical output. This process of submitting new feature vectors and adjusting weights and biases is repeated many times. The training process is stopped when the values of the weights and biases do not change significantly with each new iteration. An untrained neuron will initially have large errors at its output. After a number of feature vectors have been presented the neuron 'learns' the relationships between inputs and outputs and hence the errors decline. The neuron model thus learns by example, as opposed to conventional rule-based system models.

Theory: The neural network

Viewed in isolation, the single-neuron model appears to provide little advantage over conventional mathematical models. The real benefits are realised in the collective effect when a number of neurons are combined to form a network, as shown in Fig. 3-2b. A network can have a number of neurons in parallel, called a layer. Layers of neurons can also be arranged in series such that outputs from a single layer become the inputs to a subsequent layer. The number of interconnections between neurons in these networks increases exponentially with the addition of each new layer. Correspondingly the number of weights and biases increase. The result is a significant improvement in the ability to model more complex systems. Benefits of ANNs over conventional models include reduced modelling time and less reliance on expert knowledge of the system being modelled.

Proposed application: The neural network

Fig. 3-3 shows schematically the proposed modelling approach which makes use of a NN. In the first step the measurements of the parameters identified earlier in this chapter are made. In the second step there are basic calculations which extract the most important features from the measurement data, sometimes requiring the amalgamation of two measurements into a single

value. These calculations are shown in section 3.4.5. Ideally step 3 would involve training the NN as a maintenance tool, with 19 measurements and paper moisture as inputs, and the amount of cover wear as the output. However, the complexity of the modelling required prohibits the calculation in this direction. Thus the wear measurements and 19 influencing measurements are supplied as inputs and the desired output is the moisture content measurements. Note that this forms part of the development phase of the model. The construction of the model in this manner is also the most prudent according to our knowledge of NNs. The reason for this is that the moisture content is already a measured result of the inputs to the papermaking process. The training of the NN in the reverse direction would lead to mixing of process inputs and process outputs at the NN input which cannot be tolerated. This would cause a probable likelihood of interaction within the NNs calculations. This could lead to the perception by the NN of false relationships between variable types. A safer method would be to keep the inputs and outputs of the papermaking process on separate sides of the NN. In this arrangement there would be 19 measurements at the input side of the NN and the moisture content at the output. That is to say the NN is trained as process model to describe the dewatering process. This is step 3 in Fig. 3-3.

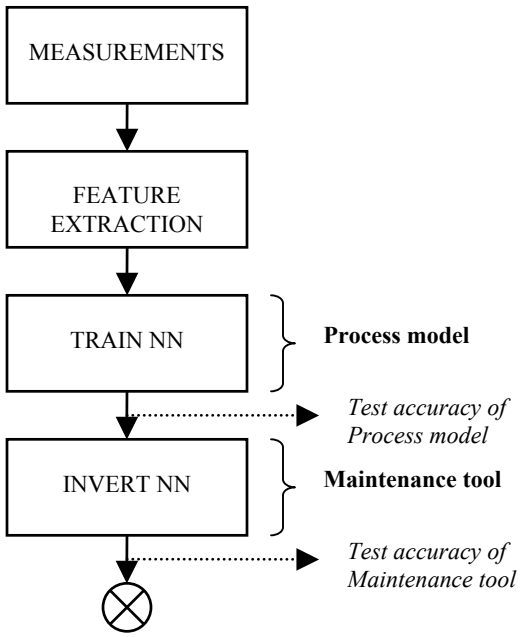

Fig. 3-3 Proposed modelling method, using a NN as a process model.

Of course this approach necessitates a fourth step in which the relationships established by the NN in step 3 are used to construct a maintenance tool. The 4th step can be regarded as the reverse

calculation of the relationships established in step 3, as referred to in section 3.2. In step 4 the cover wear becomes the output of the calculation. The inputs are the on-line on-the-run measurements of the moisture content and the 19 process variables. Note that wear measurements of the roll are not required because they will be the result of the calculation in step 4. Step 4 thus represents the maintenance tool which was the objective of this chapter. In NN terminology the reverse of the NN calculation is referred to as the inverse calculation. This terminology will be adopted from this point forward when referring to the reverse calculation of the trained NN model. The work involved in the inverse calculation of step 4 will be described fully in later sections, and was not considered prohibitive.

One of the considerations when using neural methods is the size of the data set. Neural methods require a large amount of data, particularly in complex systems such as the one proposed here. This is intuitive from neural theory, and was confirmed experimentally by Liu and Mengel [32].

3.4.3 Process model evaluation

In addition to the shortcomings given by the authors of the DP model, there were two further concerns with this model. The first was that there were a number of factors on this particular machine which were known to influence the moisture content, which were not included in the DP model. This is due to the fact that the model is concerned only with pressing. The second concern was that the measurement of the moisture content directly after the 1st press, or even the 2nd press is not possible on a commercial machine without causing production stoppages. Not only was this considered not acceptable in the present study, but it would also render any findings of such a study of little use to industry. The moisture content can usually only be measured at the end of the paper machine, before the reel. It could not be determined *a priori* if the DP model would be able to account for the effects of the drying section.

These concerns were not shared by the ANN-type of model. Rather, the successful application of the ANN methods to rolling in the steel industry where the theory is also limited, promoted its use in this application. The nature of ANN models does unfortunately limit the amount of theoretical deduction that can be made at the end of the study. This was viewed as a calculated risk at the outset of the modelling process, and the ANN model methods were selected as the better of the two options. The calculation of the inverse NN was considered to be more complicated than the

reverse of the DP model, but to a definitive extent. All ANN modelling was performed using the MATLAB® Neural Networks Toolbox distributed by The Math Works Inc.

3.4.4 Detailed process model design

Within ANN methods there are a number of network types that can be used. The most prominent are the Multi-Layer Perceptron (MLP) and the Radial Basis Function (RBF). A complete discussion of the differences between MLPs and RBFs is beyond the scope of this text, and can be found elsewhere in the literature, such as the work by Bishop [58]. It should be sufficient to argue that the MLP was chosen because it forms a distributed representation in the space of the activation values for the hidden units since, for a given input vector, many hidden units will typically contribute to the determination of the output value. By contrast a RBF network with localised basis functions forms a representation in the space of hidden units which is local with respect to the input space because, for a given input vector, typically only a few hidden units will have significant activations.

The general mathematical representation of the MLP was shown in Fig. 3-2b. The exact definition of the number of layers, number of neurons etc. is collectively referred to as the network architecture. This section will describe the network architecture for the MLP used in this study. Later on in the training exercise of chapter 4 the architecture is pruned to remove redundant members and hence simplify the architecture.

The theorem due to Kolmogorov (1957) states that every continuous function of several variables can be represented as the superposition of a small number of functions of one variable. Bishop [59] translates this theorem in neural network terms as: 'the theorem reduces to the fact that any continuous mapping $y(x)$ from d input variables x_i to an output variable y can be represented by a three-layer network having $d(2d+1)$ units in the first hidden layer and $(2d+1)$ units in the second layer'. The recommended size of this network was considered prohibitively large because in this case d = 19, which implies 741 neurons in the first layer. With over 9000 measurements the training time would be impractical. A review of other practical applications by McCormick and Nandi [38] and Paya *et al.* [35, 36] where NNs were used for diagnostic purposes indicated that many were able to successfully learn with a small fraction of the layer size indicated by Kolmogorov. An MLP was set up with 19 inputs, 32 neurons in the first layer, 32 neurons in the second layer and one neuron in the output layer.

The decision to use a single output neuron is not very common in MLPs which are trained for the purposes of fault detection. In most of these cases the requirement of the network is that it must classify the fault into different fault groups or different levels of severity. Representative outputs of this type are shown in Fig. 3-4a and 3-4b. The multiple output 1-of-c type with hard limit function works on a winner-takes-all principle where the output neuron with the highest activation assumes the value 1 and all others are 0. For this study a post-training inverse calculation was required. Hence it was important to retain the highest resolution of the output from the continuous function in the final layer. The multiple output 1-of-c type with continuous output layer shown in Fig. 3-4b was an improvement in this regard. The solution was overly complicated, however, since the values in the solution are actually results of a probability density function which prevents the definition of the exact inverse relationship. The mono-type output using a continuous function, also known as the regression approach, gave exact values of the continuous function. This provided the best resolution and allowed more tangible evaluation methods to be used by the non-academic end-user, such as standard deviations.

a) $\begin{bmatrix} 1 \\ 0 \\ 0 \\ 0 \\ 0 \end{bmatrix}$ b) $\begin{bmatrix} 0.71 \\ 0.20 \\ 0.18 \\ 0.10 \\ 0.07 \end{bmatrix}$ c) $\begin{bmatrix} 0.92 \end{bmatrix}$

Fig. 3-4 Output types (a) 1-of-c with hard-limit, (b) 1-of-c with continuous output layer and (c) mono-type with continuous output.

One of the other options available to the designer is the choice of the activation function in each layer. The activation function is the function which is used to calculate each neuron's output from the sum of the weighted inputs. There are a wide range of functions that can be used, a few of the basic forms are shown in Fig. 3-5. From the previous discussion of output types the requirement is that the output layer must have a continuous output function. The hyperbolic tangent sigmoid (*tansig*) function as shown in Fig. 3-5c was chosen, because it is continuous and does not limit the solution to a linear function. Similarly the *tansig* function was used in all layers due to the fact that it is continuous and non-linear. The increased modelling capacity of non-linear functions such as the logistic and sigmoidal functions is presented by Ripley [31]. The non-linear requirement was also inferred from the derivation of the DP pressing model of Kerekes and

McDonald [57]. The requirement of continuity is intuitive in this application, which would not be the case in a study of shock-wave behaviour at transonic speeds, for example.

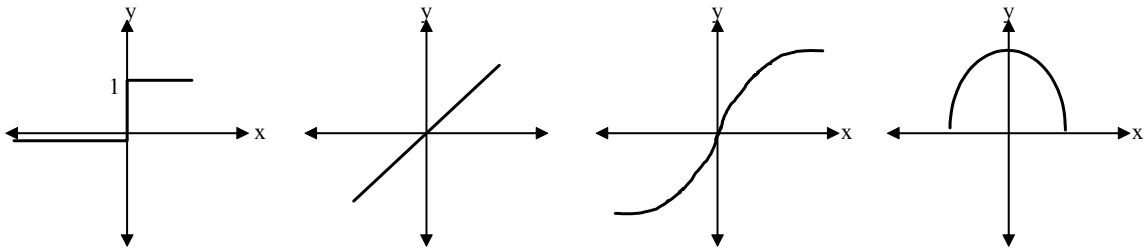

Fig. 3-5 Basic activation function types (a) Hard limit, (b) Positive linear, (c) Hyperbolic tangent sigmoid and (d) Radial basis.

3.4.5 Data requirements of the process model

The accuracy of the NN can be improved by performing a number of basic calculations on the measurement data, as indicated by step 2 in Fig. 3-3. These calculations are collectively called feature extractions, because they combine more than one variable to better describe a certain behaviour or condition. This is analogous to the use of temperature and pressure to describe the mass of gas within a fixed volume. In this study feature extraction calculations were required for two of the measured variables in Table 3-A.

Press impulse

The study of pressing by Kerekes and McDonald [14] indicated that the moisture exiting a press was not related to the press load, but in fact the press impulse. The press impulse is a parameter which describes the combined pressure-time effect in the nip. The nip load and press impulse terms can be used interchangeably to describe the pressure in the nip, but the time-relation of the press impulse quantity makes it a requirement for dewatering calculations. The press impulse is calculated from the nip load data as the quotient of the nip load in [kN/m] and the machine speed in [m/sec]. In the present study the machine speed was known, but the nip load had to be calculated very accurately from the wear measurements of the roll covers. All measurements of wear are reported relative to the ideal camber profile in this study. The camber profile refers to a

convex CD diameter profile which is ground onto the rolls to ensure the uniformity of nip load along the line of contact during loading.

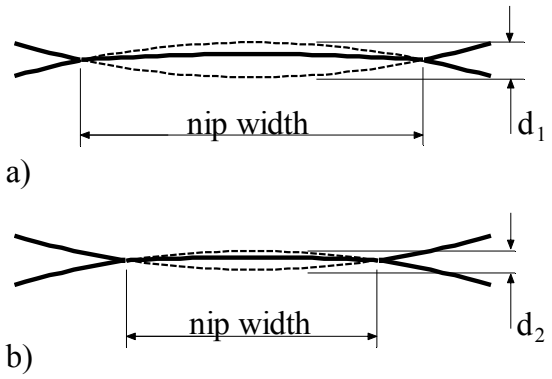

Fig. 3-6 Comparison of nip geometries of a normal and worn roll

.

The effect of localised cover wear on the nip load can be explained by considering the compression of the cover material, as shown in Fig. 3-6. In Fig. 3-6a the nip load causes the roll covers to deflect under compression to an equilibrium boundary position. The deflected distance d_1 is the sum of the deflections of both covers, and is determined by the pressure between the roll covers. In Fig. 3-6b the cover of the bottom roll is worn to a smaller diameter in the plane of the cross-section. Though all other points along the roll face may deflect by d_1, the smaller diameter at this point results in a deflection d_2, so that $d_2 < d_1$. Therefore the pressure in the case of d_2 is less than that of d_1. Usually the magnitude of the differences between these deflections is very small, but the corresponding load differences can be significant, particularly for harder cover materials. Furthermore, loads increase exponentially with deflection, owing to the increased contact area or nip width, indicated in Figs 3-6a and 3-6b, and discussed by Beucker [7] and Ryder [46], and the compressibility limits of the material as shown by Moore [48]. Diameter measurements of the rolls in this study were taken at monthly intervals and indicated that the wear relative to the ideal camber was not uniform across the CD roll face. Thus the calculated nip load profile would also be non-uniform.

The details of how the roll wear measurements along the roll faces were used to calculate the exact nip load at each CD position are given in Appendix B and D. In summary the solution was generated by a 3-dimensional model of cover deflection. The model considers the irregularities along the line of contact which are due to uneven wear. The model also allows for uneven

external loading of the press, and uses the physical properties of the cover materials to calculate the load at each CD position along the roll face. The equation governing the deflection behaviour of the roll covers is similar to that provided by Beucker [7], and is described in Appendix B. However, in this study the covers of both rolls can deflect, which is accounted for in Appendix D. The polymer covers were therefore modelled as a set of radially oriented springs, as proposed by Carvalho and Scriven [50] and Moore [48]. The spring stiffness is calculated from a modulus-hardness relationship reported by Gudehus [43] and confirmed by laboratory tests reported in Appendix A. The web and felts were excluded from the spring model because their stiffnesses had a negligible contribution to the stiffness of the overall system.

The results of the 3-D model show good agreement with the actual nip measurements made by Zwinak [42] over a wide range of diameters, hardnesses and loads. The press impulse in [kPa.sec] was then calculated as the quotient of the nip load in [kN/m] and the machine speed in [m/sec].

Conditioned moisture

The second parameter from Table 3-A which requires feature extraction is the basis mass, due to the effect this has on the moisture content of the sheet. The interest in this study was the CD moisture profiles determined by the press section. However, moisture profiles are also affected by headbox profiling. As this effect was undesired in this study, this profiling effect was quantified and deducted from the measured moisture profiles. Headbox profiling describes the capability to control the flow of stock from a discrete number of points individually across the CD width of the machine. Since the stock is a slurry with fixed proportions of fibre and water, headbox profiling actually controls the water flows and fibre flows in tandem. The result is that a sample, taken after the headbox which has a higher fibre mass, would also have a correspondingly higher moisture content. By contrast, the press section affects the moisture content only, while the fibre mass remains constant. These relationships were used for separating the effects of the headbox from those of the press section.

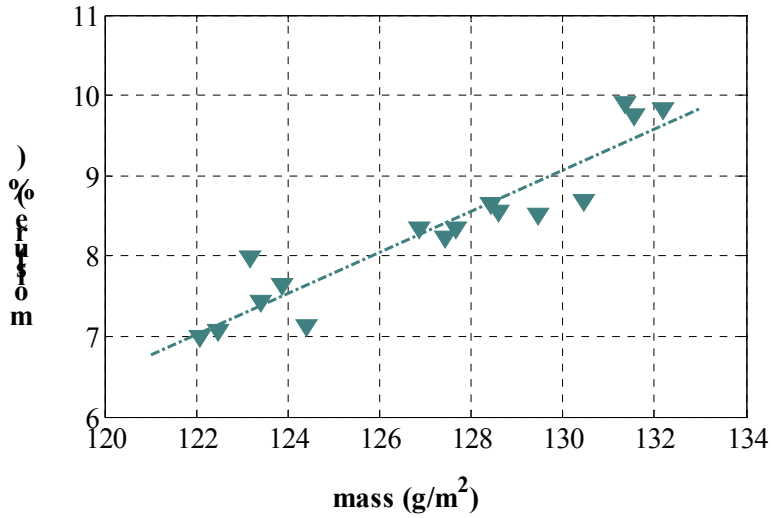

Fig. 3-7 Sample regression curve for the calculation of regressed moisture h_r.

In order to quantify the effect of headbox profiling, both mass and moisture were measured at 136 CD points at the exit of the papermaking process. Sample measurements for a single CD position, taken at 40-minute intervals, are indicated by the plotted points in Fig. 3-7. The plotted data shows scatter in both the x and y coordinates. The scatter in the x coordinate indicates variations in fibre mass, which variations are headbox related. The scatter in the y coordinate indicates variations in moisture, which may relate to the headbox and to the press section. By considering only the variations in the x axis it is possible mathematically to exclude the contributions that the headbox makes to the overall moisture content. What remains will be the variations in moisture caused by the press section, called the regressed moisture h_r. The linear regression curve which is fitted to all the data for this specific CD point is also indicated in Fig. 3-7. The gradient of this curve will determine the moisture content at 125.0 g/m^2. In simple terms, the mass variations are used to calculate an equivalent moisture content at 125.0 g/m^2. In mathematical terms, the regressed moisture h_r is calculated by using Eq. (3-3):

$$h_r = \nabla(125.0 - m_m) + h_m \tag{3-3}$$

where:

h_r = regressed moisture

∇ = gradient of regression curve

m_m = measured mass

h_m = measured moisture

The regression calculation of Eq. (3-3) must be performed for each CD position, so that specific regression gradients can be used to describe each position. The difference in the gradients of each of the 136 CD positions is the key to describing the different dewatering behaviours across the width of the machine.

The measured moisture profiles for a single grade-run are shown in Fig. 3-8(a). As mentioned earlier a single grade run consists of many profile measurements taken at 40 minute intervals. Each profile is in turn generated by 136 individual measurements across the 5000 mm width of the machine. The general shape of the profiles in Fig. 3-8(a) indicates that the moisture content is low at the immediate edges of the sheet, climbing rapidly towards the 400 mm mark just inside of the edges. Between the 400 mm and 4600 mm marks there is a general tendency to a lower moisture content, a drier sheet, in the centre. This could indicate, among other things, poorer dewatering on the outer 600 mm edge regions of the machine. There is, however, a prevalence of high-frequency noise in the measurement data, visible as small fluctuations around the mean profile. In the context of this study, noise refers to unwanted variations in moisture with respect to distance, not time. Noise frequency is thus measured here in cycles per millimetre or simply mm^{-1}, and not cycles per second, *Hertz*. This noise was attributed to the natural fluctuations in the process and in the control systems' responses. The amplitude of the noise was reduced by the calculation of Eq. (3-3) but only to a limited extent. A digital Fast Fourier Transform (FFT) filter was used for removing the fluctuations which were not of interest in a long-term study of roll wear. The FFT low-pass filter was set to remove all frequencies above 0.001 mm^{-1}. This frequency was determined to give optimum noise filtering without loss of valuable moisture profiling information. Fig. 3-8 indicates the progression through measured, regressed and FFT-filtered CD moisture profiles for a sample set of moisture data. The variation between the profiles in Figs. 3-8(a) to 3-8(c) reduces with each calculation step, indicating that the resultant trends were indicative of long-term effects, such as felt condition and roll wear. The final calculation step for feature extraction involved the normalization of the profiles, in a method similar to the DC offset removal in a study of alternating current. The reference moisture profile employed in this step was measured using a newly installed pair of rolls and fresh felts.

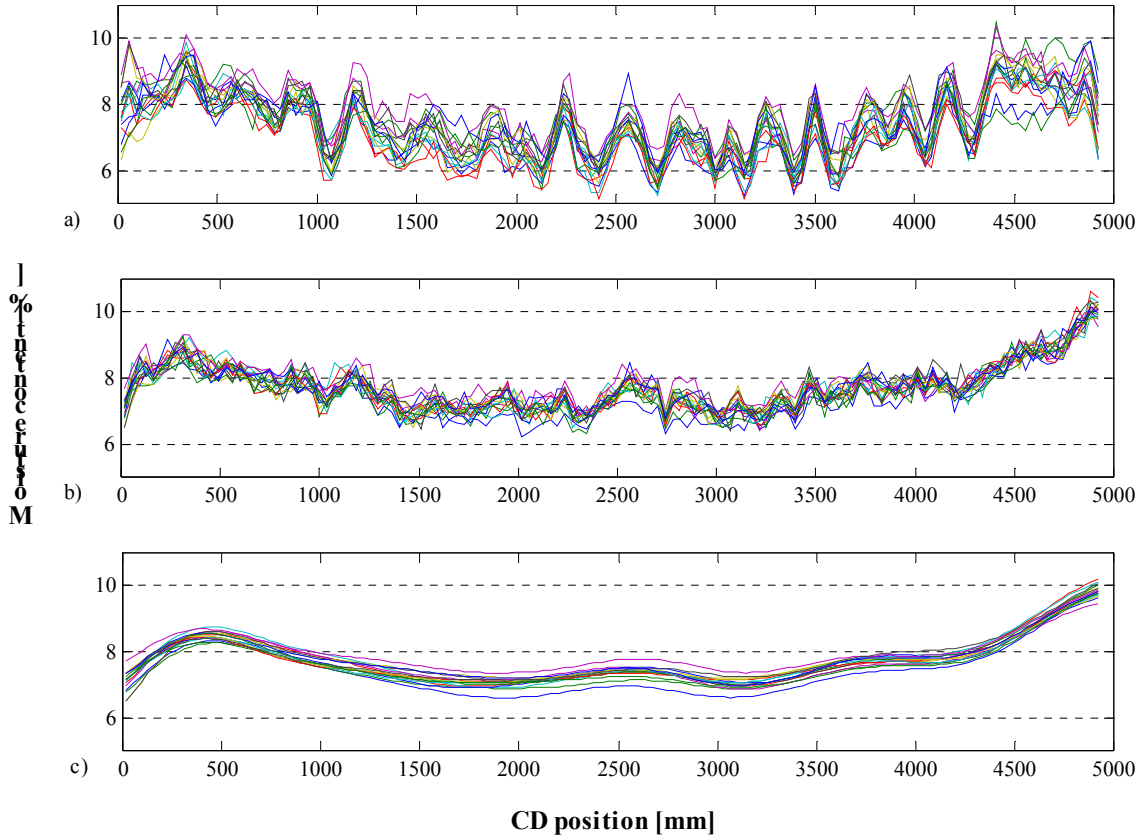

Fig. 3-8 Moisture profiles, (a) as measured, (b) regressed, and (c) FFT filtered.

Normalisation of measured parameters and extracted features

One of the requirements of the NN calculation methods is that all inputs and outputs lie within the range [-1 : 1]. This required a basic calculation whereby each parameter in Table 3-A, and the two extracted features described previously were normalised according to their own maxima and minima. As a safety measure to avoid so-called 'bottoming-out' of the range, this study made use of the smaller range [-0.9 : 0.9]. This was simply done by setting the maximum value of each input to 0.9, likewise the minimum to -0.9 and the values in between were calculated proportionally. Each input type was normalised relative to its own maxima and minima, and not the global maximum and minimum, since this would cause unwanted weighting problems during training. Thus all of the 9656 feature vectors were reduced to vectors with a maximum of 0.9 and a minimum of -0.9.

3.5 Development of the maintenance tool

According to the modelling methodology depicted in Fig. 3-3 the final step is the construction of a maintenance tool. The maintenance tool is the calculation that will be used to evaluate the current condition of the roll. Recall that the NN was trained as a process model from limited measurements of roll wear and other process measurements to calculate the moisture content. By training the NN, it forms a mathematical simulation of the process. However, it is not feasible to directly measure the wear on every roll on an ongoing basis. Once the training is complete, the relationships between inputs and outputs of the NN become fixed. If the mathematical simulation, or NN, were to be inverted, then the reverse calculation would be possible. This implies that if the moisture content and the 19 process measurements were measured at a specific point on the paper, and submitted to the inverted NN, the result of the calculation would be the roll wear. This means that the condition of the roll can be known by taking indirect measurements. In actual fact the solution of the inverse calculation is the nip impulse in [kPa.sec], not the roll wear in [mm]. However, these units can be interchanged by using the calculations provided in Appendices B and D. This section describes how step 4 of Fig. 3-3 is achieved. That is to say, this section describes the inverse calculation so that the NN can be used as a maintenance tool.

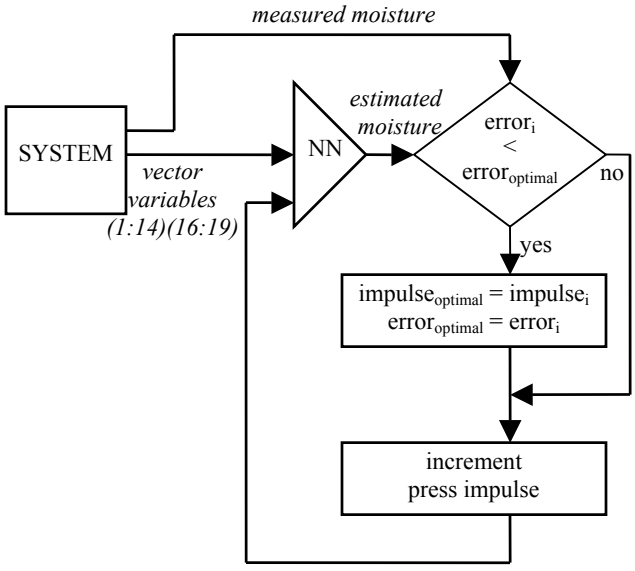

Fig. 3-9 Neural network in inverse model calculation.

We know from Fig. 3-2(b) that the output of an MLP is nothing more than an ordered summation of a number of inputs. The values of the weights and bias will be fixed after training. It may be possible to determine the values of each of the weights and biases and try to construct a mathematical inverse-NN model. However, a simpler approach would be to invert the model in a manner similar to that described by Hussain [28]. Using this approach the NN is regarded as a 'black box' which can only perform the forward calculation. The black box is then incorporated in a bigger calculation process, indicated in Fig. 3-9. At the start of the process the measured values 1:14 and 16:19 are submitted together with a random starting value for press impulse (variable 15), called $impulse_i$, to the NN. The trained NN then calculates the estimated moisture content. In the next step the estimated and measured moisture values are compared. The error between these two is temporarily saved as $error_{optimal}$ i.e. in the first iteration the calculation in the diamond is not performed. Irrespective of the next immediate step, the press impulse value is incremented. The direction of incrementation (increase or decrease) is dependent on whether the estimated moisture was higher or lower than the measured moisture value. The entire loop of Fig. 3-9 is then repeated a second time with the new incremented press impulse value, $impulse_i$. The NN will calculate a new estimated moisture value. If this new value has a smaller error with respect to the measured moisture than the previous iteration, then the incremental values are stored into the optimal variable fields i.e. $error_{optimal} = error_i$ and $impulse_{optimal} = impulse_i$. The iterations will continue until the entire measurement range has been explored.

When complete, the value of $impulse_{optimal}$ will be returned. This value is thus the press impulse value which according to the NN would have resulted in a moisture value closest to that measured on the paper machine. Furthermore, because the NN is a process model of the paper machine, this statement is the same as saying 'for the given moisture content, and under the conditions prevailing on the machine, the press impulse is $impulse_{optimal}$'. The inverse model can be used to calculate the press impulse at any combination of process inputs and moisture values. The linear nip load is then simply calculated as the product of $impulse_{optimal}$ and machine speed. The spring model is then used to calculate the roll wear from the linear nip load. Note that physical measurements of the roll wear are only required for the training of the NN. Once successfully trained, these measurements can be ceased because the NN would have established the required relationships between process inputs. Thereafter, the inverse model will be able to calculate the wear on the roll.

This concludes the objectives laid out at the beginning of this chapter. These were that a model be developed which could describe the dewatering process in a paper machine, and secondly that the effect of a worn roll on paper quality can be isolated. In chapter 4 the method will be tested using measurement data from a commercial paper machine. This will require training of the NN and then inverse calculations to test the maintenance tool developed in this section.

4. Experimental verification of the method

4.1 Measurement protocol

The paper machine used in this study was an 820 ton/day kraft liner machine, producing paper grades used predominantly for packaging. The machine has a maximum production speed of 800 m/min and a CD width of five meters. The machine has two presses. The first press is a roll press, with a nominal nip load of 75 kN/m, and is the subject of this study. The first press top and bottom rolls are approximately 830 mm in diameter, with 12 P&J hardness nitrile rubber and 14 P&J hardness polyurethane covers respectively. The second press is a shoe press, which by design provides a uniform CD nip load profile.

From the methodology proposed in chapter 3 a total of 20 parameters were identified as possible factors influencing the moisture profile of the sheet. Two of these also required feature extraction calculations which converted roll wear to nip impulse and measured moisture to normalised moisture respectively. The basis mass measurements can be discarded after their use in the calculation of the normalised moisture. Simultaneous measurements of all of these variables were required to effectively model the behaviour of the process.

Paper grades are differentiated primarily by their grammage, or grams per square meter g/m^2. In this study the 125 g/m^2 paper grade was chosen due to its known sensitivity to moisture profiling problems on this machine. Measurements were taken over nine months to track the progression of the cover wear. Over this period seven individual measurement windows, called ‘grade runs’ existed. On the odd occasion when dryer-screen oil-contamination, or similar CD moisture affecting situation was extreme, a reliable measurement could not be made. Each grade run consisted of simultaneous measurements of all the variables listed in Table 4-A, repeated a number of times at 40 minute intervals. Table 4-A also indicates the range of the measurement values that were made and the class of each parameter. These being abbreviated as follows: Ingoing Moisture (IM), Compressibility (C), Permeability (P) and Pressure-time (Pt) respectively.

Table 4-A List of measured variables.

No.	Variable	Range	Class
1.	Chemical softwood blend	34.4 - 50.9 %	P, C, IM
2.	Semi-chemical hardwood blend	21.9 - 50.3 %	P, C, IM
3.	Recycled fibre blend	0 - 34.1 %	P, C, IM
4.	Re-processed fibre blend	27.4 - 47.1 %	P, C, IM
5.	Top ply load	18.5 - 30.0 %	P, C, IM
6.	Top ply freeness (CSF)	100 - 440 ml	P, C, IM
7.	Top ply consistency	0.13 - 0.30 %	P, C, IM
8.	Top ply stock temp	48.3 - 57.6 ºC	IM, P
9.	Base ply freeness (CSF)	90 - 300 ml	P, C, IM
10.	Base ply consistency	0.28 - 0.52 %	P, C, IM
11.	Base ply stock temp	48.1 - 54.5 ºC	IM, P
12.	Machine speed	653 - 700 m/min	Pt
13.	1st press felt permeability[a]	1082 - 1456 ml/min	P, C
14.	1st press felt water content[a]	800 - 1231g/m^2	IM, C
15.	1st press roll wear[a]	43 - 234 µm	Pt
16.	2nd press felt permeability[a]	591 - 945 ml/min	P, C
17.	2nd press felt water content[a]	773 - 930 g/m^2	IM, C
18.	2nd press load	850 - 1000 kN/m	Pt
19.	Calender load[a]	14.8 - 24.2 kN/m	Pt
20.	Basis mass[a]	109.9 - 142.0 g/m^2	…
21.	Moisture content (wet basis)[a]	3.4 - 11.6 %	…

[a)] Parameters which required measurements across the CD width

Some of the measurement parameters can exhibit variation in the CD direction at any instant in time, and required that measurements be taken at a number of points across the width of the machine (indicated by [(a)] in Table 4-A). Others, such as machine speed, are uniform across the machine, but can still influence the CD moisture profile. For the variables which exhibited CD variation the measurements were either made at 136 CD positions, or interpolated to 136

positions. These positions were calculated in exact CD alignment with the 136 measurement points of mass and moisture made by the scanner at the end of the drying section. The scanner which was used on this machine was of the Smart Platform 1200 type, manufactured by ABB (Asea Brown Boveri). The roll wear and felt conditions can be regarded as constant over the duration of a single grade run, and as such the values were obtained by interpolation from measurements taken before and after the grade run in question. In total 71 measurements were made, and since each measurement has 136 CD positions, this equated to 71 x 136 = 9656 readings of all the values in Table 4-A. The requirement for such a large number of measurements arose from the fact that measurements of moisture which were out of specification were rather rare, thus necessitating a lengthy study. The large data base requirement also stems from the NN methods which were described in the previous chapter.

The steam shower and spray dampener systems, normally used for moisture profile correction were deactivated during all measurements. The existence of these systems may bring into question the purpose of this study. This is answered by considering that these systems address symptoms, and that while they may be effective in their purpose, the interest here is the quantification of the root cause of poor moisture profiles.

4.2 Pre-processing of data set

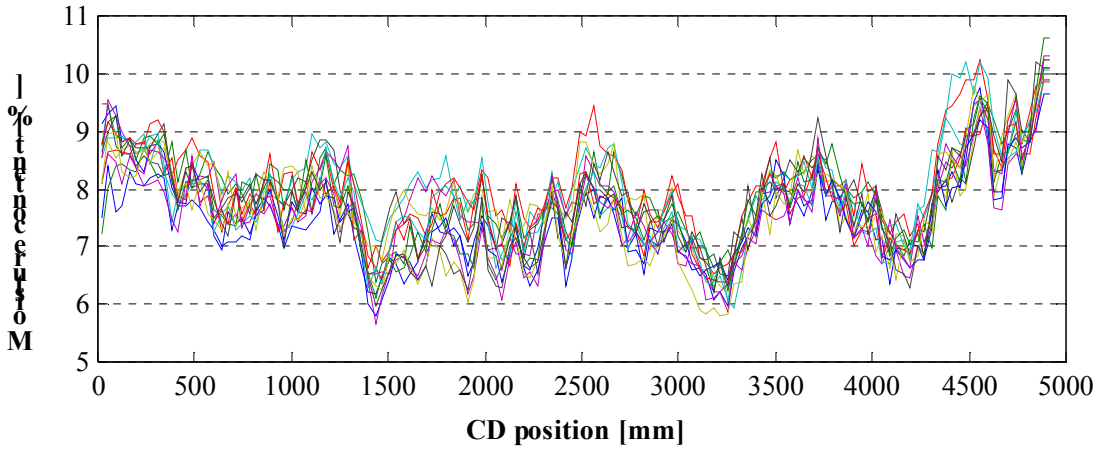

Fig. 4-1 Sample moisture profiles from grade run 5

One of the patterns that emerged from the measurements of moisture data was that the distribution of data was not uniform across the range of measurement. Fig. 4-1 shows the moisture profiles plots from grade run 5, where each profile is generated from 136 individual CD measurement points. The figure clearly indicates that there is a higher concentration of data in the range between 7% and 9% moisture. Similar patterns were observed for all other grade runs and are largely due to the moisture controls on this particular paper machine, which use 7.5% as a mean moisture control setpoint.

From a Neural Network point of view the higher density of measurements in the 7-9% moisture range was undesirable. The reason being that during learning the NN adjusts the weights and biases with the objective being to minimise the mean error over the total data set. If, however, the data set is biased with more data in a certain region of vector space, then the network will tend to bias the learning toward this region of higher vector density. That is to say that the NN will focus on minimising the error of the data in the more populous areas. It is true that data in less populous regions will then have a higher error, but because they are fewer in number, the sum of their errors will be less. This phenomenon is particularly detrimental to this study because it is exactly the data from less populous regions which is of highest importance. High and low nip loads cause low and high moisture values respectively.

To eliminate this effect some of the input feature vectors from the more populous regions of measurement were discarded. This was carefully done by classifying the feature vectors into five classes according to moisture content, as shown in Table 4-B. The composition of the vectors in each of the classes was then made equal using a vector handle which differentiated by moisture class and CD index, *i*. The first five rows of the vector handle identified the moisture, while the CD index indicated the original CD position of the measurement data. The discarding of the data from more populated classes was then handled according to the following programming methodology: Remove vectors from classes where vector composition is greater than 20%, but ensure that removed vectors are evenly distributed across the range of values of *i* from 1 to 136. By adding the second of these two instructions the diversity of the remaining input feature vectors was ensured.

Table 4-B Classification of feature vectors according to moisture content.

Class name	Moisture range	Data composition	Vector handle
Class 1	3.4 – 5.2 %	20 %	$[0\ 0\ 0\ 0\ 1\ i]^T$
Class 2	5.2 – 6.6 %	20 %	$[0\ 0\ 0\ 1\ 0\ i]^T$
Class 3	6.6 – 7.3 %	20 %	$[0\ 0\ 1\ 0\ 0\ i]^T$
Class 4	7.3 – 8.3 %	20 %	$[0\ 1\ 0\ 0\ 0\ i]^T$
Class 5	8.3 – 11.6 %	20 %	$[1\ 0\ 0\ 0\ 0\ i]^T$

i = CD index [1:136]

The same routine was employed for each of the grade runs individually, since the distribution of the input feature vectors for each of these was not the same. It may be argued that allowance for the non-uniformity of the data set may have been possible within the NN using backpropagation with an increased momentum term. It is true that this would cause the larger errors in the less populous regions of vector space to play a more important role in the calculation of the new weights and biases. However, this approach was not followed due to the fact that there was no assurance that the momentum term would be addressing these regions specifically.

4.3 Process model learning

4.3.1 Learning limits

One of the risks involved with NN methods is the possibility of overtraining the network. This occurs when the network output errors are minimised to such an extent that the network can no longer generalise for unseen data. In the human context this is the same as memorising the facts instead of understanding the concepts. If all of the measured data is used for training the NN then the phenomenon of overtraining will not be detected, and the reported accuracy of the network will be optimistic. This fact was reported in a review of various methods of evaluating the application of NN models for engineering problems by Reich and Barai [60]. A more commonly used method, known as hold-out, exists whereby the data set is randomly divided into disjoint

training and testing sets. Only training data is used for training, and the test data set is used to evaluate the results of the network and estimate the generalisation error.

According to Reich and Barai it is common to select $^2/_3$ of the set for training and the remaining $^1/_3$ for testing. If anything, results reported using this method will be conservative. The relative sizes of the data sets proposed by Reich and Barai are commensurate with many practical applications of NNs in the literature. Therefore this study made use of the same ratios. The test set was then further divided into two equal $^1/_6$ portions to allow the use of an Early Stopping (ES) routine. The ES routine is a function which ensures that the training is stopped after the optimum number of epochs i.e. at the start of overtraining. In ES the training set is used to compute the updated values of the network weights and biases. The error on the first $^1/_6$ of the data, called the validation set, is monitored during the training process. The validation error will normally decrease with that of the training set during the initial phase of training. However when the network begins to over-fit the data, the error on the validation set will typically begin to rise. This is because of the subtle differences between the train and validation data sets. When the validation error increases for a specified number of iterations, the training will be terminated by the ES routine. The weights and biases that will be returned will be those which existed at the point where the validation error had its minimum. The remaining unused $^1/_6$ of the data is called the test set and is used to report the final accuracy of the model. Note that the test set is not used during the training process. However, it is useful to plot the test error alongside the validation error during training, because the similarity of these two curves indicates that the division of the data sets was good.

The division of the feature vectors in this study was done using the vector handles discussed in section 4.2. The result was three sets of train, validation and test feature vectors of proportional size ($^2/_3$, $^1/_6$, $^1/_6$) which each had equal amounts of data in the five moisture classes. The same procedure was repeated for each grade run. The uniqueness of the data across the three sets was ensured by using a further criterion whereby data from the same *CD index, i* could not be shared by two sets, e.g. test and validation.

4.3.2 Learning routines and regularisation

There are a number of options which must be specified by the designer to determine the final behaviour and accuracy of the NN. Some of these can be determined *a priori*, and these were discussed in chapter 3. In other cases the best option must be found by trial and error. In the latter case, good judgement will often narrow the range of possibilities which must be explored experimentally. This always depends on the requirements of the particular application. This section describes completely the final details of the NN used in this study.

Network learning can be supervised or unsupervised. In this case supervised learning was chosen because the target output of the network i.e. the moisture content was known. In unsupervised learning this is not the case. Furthermore, batch training was used whereby weights and biases are only updated after each epoch. An epoch, in NN terminology, refers to a cycle during which all feature vectors in the training set are presented to the network once. The alternative approach to batch training, whereby weights and biases are updated after every feature vector submission was considered too volatile for this application, particularly because of the size and number of feature vectors being used.

In this MLP network the feature vectors were fed forward through network to the output, and the error with respect to the measured output was back-propagated from the back of the network towards the front. This type of network, called a Feed-Forward Back-Propagative Neural Network (FFBPNN, or just simply BPNN) was selected based on the successes reported by Larkiola *et al.* [29] and Gorni [30] in modelling steel rolling, and the review of applications of NN in the chemical process industry by Hussain [28].

The method by which the contributions to network error-of-estimates are associated to specific neurons in the network and the manner in which the weights and biases are updated are determined by the training algorithm. There are a large number of algorithms available, each with a different mathematical optimisation routine. The selection of the most suitable training algorithm is usually done experimentally, based on the speed of convergence and the final accuracy that is reported. These can differ significantly between different algorithms because of the differences in underlying mathematical theory and the performance functions they use. In this

particular study the speed of the training was not a constraining factor, because of the slow progression of roll cover wear. The algorithm which gave the highest accuracy was the Bayesian Regularisation learning algorithm of MacKay [61]. This algorithm uses the Mean Squares of the Errors (MSE) as its performance function, meaning that it is the MSE of all the training data that is minimised during training. A complete discussion of the Bayesian Regularisation mathematics is beyond the scope of this study, and can be found in the work of MacKay [61]. This algorithm also has the added benefit that it updates the weights and biases such that the mean squares of these values are also reduced. This effectively reduces the network into the simplest structure that can still model the dewatering process accurately.

At the beginning of the training all weights and biases were assigned values according to the initialisation function of Nguyen and Widrow [62]. This function allocates starting values such that the active regions of the layers neuron's will be roughly evenly distributed over the input space, which in the case of the *tansig* function is sigmoidal.

4.3.3 Results of model learning

The model learning was conducted on a Pentium IV desktop computer with a 1.6 GHz microprocessor and 40 Gigabyte hard drive. The Random Access Memory (RAM) was upgraded from 512 kB to 1 GB to provide faster training while different algorithms were being investigated. The additional RAM was not required by the final algorithm which was more efficient.

The first observation that was made during the model learning was that the curves of the training and validation data were always close to each other. This observation was tested by re-executing the data subdivision subroutines which were the topics of sections 4.2 and 4.3.1. Despite changes in the domination of the *CD index* each time, the curves remained practically similar over several repetitions. This implies that the handle used in Table 4-B was effective in providing uniformly distributed and hence representative data for the train, validation and test sets. Even though the handle uses moisture and *CD index* as its criteria for classification.

The second observation that was made was related to the plot of the number of active parameters as training progressed. This was a bonus of the Bayesian Regularisation which was discussed in

the previous section. It was observed that this figure decreased significantly whenever the NN was trained, indicating that there were redundant weights and biases in the architecture. In order to remove the redundancy, not only to speed up the network, but also to determine which of the 19 inputs were significant, a pruning exercise was undertaken. This involved a laborious process of unplugging individual inputs, or combinations of inputs, to determine the effect on the NN result. The NN had to be retrained a number of times to ensure repeatability of the behaviour with each permutation. Thereafter, the number of neurons in each layer were reduced, likewise the number of layers. After several hundred iterations the NN was reduced from a 19-input network with neuron architecture 19:32:32:1 to a 14-input 14:24:1 arrangement. The final feature vectors included the parameters 1 through 14 of Table 4-C. Parameter 15 was the target value of the training. The best combination of activation functions was hyperbolic tangent sigmoid in all layers. After final optimisation the network could be trained within an average of 47 epochs or 64 seconds.

Table 4-C Feature vectors used for Neural Network training.

No.	Variable	Range
1.	Chemical softwood blend	34.4 - 50.9 %
2.	Semi-chemical hardwood blend	21.9 - 50.3 %
3.	Recycled fibre blend	0 - 34.1 %
4.	Top ply load	18.5 - 30.0 %
5.	Top ply freeness (CSF)	100 - 440 ml
6.	Base ply freeness (CSF)	90 - 300 ml
7.	Machine speed	653 - 700 m/min
8.	1st press felt permeability[a]	1082 - 1456 ml/min
9.	1st press felt water content[a]	800 - 1231g/m^2
10.	1st press impulse[a]	2.85 – 9.4 kPa.sec
11.	2nd press felt permeability[a]	591 - 945 ml/min
12.	2nd press felt water content[a]	773 - 930 g/m^2
13.	2nd press impulse	77.2 – 88.9 kPa.sec
14.	Calender press impulse[a]	1.29 – 1.98 kPa.sec
15.	Regressed moisture content (wet basis)[a]	3.4 - 11.6 %

[a)] Parameters which included data at various points across the CD width

The accuracy of the network was evaluated by comparing the measured moisture values of the test data set with those estimated by the trained NN. The NN used the measured nip impulse and 13 other measured values for its calculation. Recall that the test data set had never been seen by the NN, and thus results obtained from this comparison can be regarded as conservative, as reported by Reich and Barai [60]. Furthermore, the fact that the data is new to the NN implies that the results obtained will be representative of the results which will be received from the commercial condition monitoring program.

Fig. 4-2 Comparison of the measured and NN-modelled moisture.

Fig. 4-2 provides the graphical comparison of the measured and NN-calculated moisture for the test data set. There were 334 individual feature vectors, implying 334 separate NN calculations. The 334 measured moisture values were measured at the same time as the feature vectors. The data subdivision routines of sections 4.2 and 4.3.1 ensured that the 334 points are representative of any point across the CD width of the machine, and any period over the duration of this study. Note that the plotted points are not averaged CD values, but rather the individual CD points. The y-axis indicates the normalised moisture values.

Given that the 334 points represent semi-randomly distributed vectors across the global data set, there is no expected particular pattern of Fig. 4-2. This curve should be regarded as a comparison of two sets of 334 points each, where similarity is desired. The correlation in the shape of the two data sets in Fig. 4-2 indicates that the NN has been able to learn the concept of paper moisture and how each influencing parameter affects it. A detailed analysis of the error in any particular

region of the moisture range can be made by comparing the vertical deviation between the two sets of data. The mean error was calculated as –0.06% moisture and standard deviation as 0.25% moisture. These values are small in comparison with the operational tolerance of 5.1% on the machine. The neural network is thus able to successfully model the CD variations in moisture, given specific information about the process conditions at the time.

As a second check of the results the errors in each of the five classes were calculated individually. The objective being to determine whether the feature vector set divisions of section 4.2 and 4.3.1 had been successful in achieving uniform distribution of the error over the vector space. The histogram in Fig. 4-3 shows that in general the deviations are not disproportionately higher for the less populous classes (classes 1 and 5). Overall, the error distribution appears to be relatively flat, with only $\sigma = 0.11$ difference between the maximum and minimum values. Once again this difference is small in relation to the operational tolerance of the machine. This concluded the modelling and evaluation of the NN as a tool for characterising the dewatering process of a paper machine. The results indicate that the desired calculation from measured nip impulse to moisture content has been achieved. That is to say that a calculation-simulation of the paper machine dewatering process has been successfully developed. This despite the 13 external influencing factors which had to be taken into account. In the next section the final step in the methodology proposed in chapter 3 is presented. This is the inclusion of the trained NN in the inverse calculation so that new measurements of moisture and 13 factors can be used to calculate the nip impulse. This will provide an indirect measurement of roll wear.

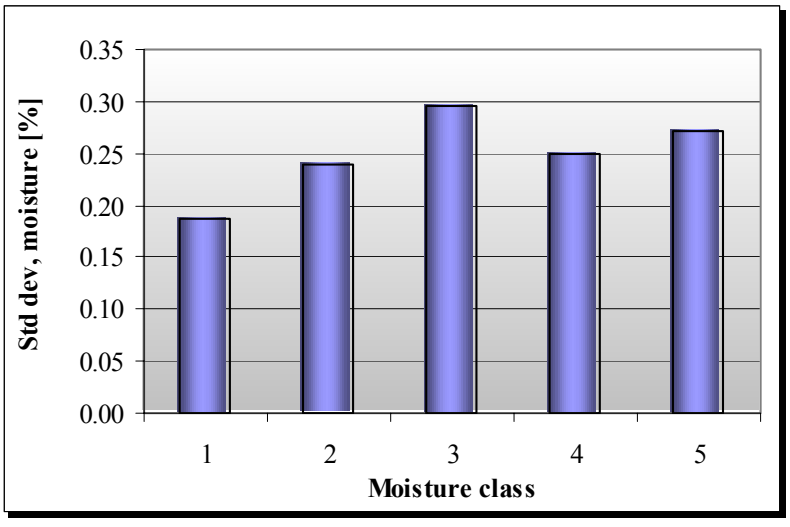

Fig. 4-3 Comparison of error distributions over the vector space.

4.4 Experimental results of the maintenance tool

The accuracy of the NN when trained as a process model was indicated in the previous section. The final step is the evaluation of the inverse model as a maintenance tool. This is important because some of the accuracy of the NN process model may be lost when incorporated in the inverse calculation. If the accuracy is acceptable, then the inverse model can be used, without further training of the NN, to indicate the press impulse of the nip. This will require a single measurement of the sheet moisture and corresponding to this the 13 process measurements (1 to 9 and 11 to 14 of Table 4-C. Alternatively an entire profile of these measurements can be made, and a press impulse value obtained for each point along the profile. The combined wear of the two mating rolls in [mm] can be calculated from the press impulse in [kPa.sec] using the calculations provided in Appendices B and D.

Before this, however, the quality-based wear tolerances must be calculated for the rolls in this press. For this calculation the moisture value as well as the operating conditions of the machine must be specified, since this combination will influence the magnitude of the effect which the roll has. This was shown in the logic diagram of Fig 3-9. The moisture value to be used for the tolerance calculation is easily determined, since this is the maximum moisture specification of the paper, defined by the Quality Control (QC) limits at the paper mill. However, the values which must be assumed by the other 13 model inputs while calculating the wear tolerances must be determined heuristically. This is because the operational conditions which will exist on the machine when the roll is worn cannot be foretold, yet they have been shown to influence the machines' susceptibility to roll wear. Operational conditions on a commercial paper machine change all the time, and will act to either amplify or dampen the effect of a worn roll to a certain degree. Thus a representative set of values must be drafted for the special feature vector which will be used to calculate the wear tolerances, rather than having a varying tolerance which is a logistical impracticality for a paper mill. The choice was made in this study to use the lower-quartile values of the measured range, which can be regarded as conservative dewatering conditions. Thus the feature vector used to calculate the wear tolerances had lower quartile values for inputs 1:9, input 10 was the incremented press impulse, and inputs 11 to 14 were also lower quartile values. The output of the NN was the uppermost limit defined by QC. Thus roll wear tolerances were calculated using a known moisture value, and lower quartile process conditions.

The first nip load tolerance value of interest was that which corresponded to the maximum allowable moisture value, according to paper quality limits. The allowable MODA (MOisture Difference Average) range is (-2.55:2.55) centred on the mean CD moisture value. Consideration of the natural process fluctuations, which were observed during the FFT filtering, reduces this tolerance by 0.65% moisture to (-1.9:1.9). Furthermore, only the upper limit which is related to the wear of the covers is of interest in this study. Using the inverse model methodology of Fig. 3-9 the minimum load tolerance is calculated iteratively as L_{alarm}= 48 kN/m (132 μm wear from the model of cover deflection). Recall that the nominal load for this press is 75 kN/m. It is preferable to report the tolerance in kN/m, rather than μm. This is because it is possible for the loading arms of a press to descend unevenly, and thus compensate for large areas of wear. The equivalent value in μm is intended for use with localised wear only. Note also that the value indicated in μm is the combined wear value for both rolls, since it is the total summed wear which results in nip load reduction.

A second wear tolerance is defined which takes into account the ability to control moisture profiles using headbox profiling. This control is achieved by adjusting the CD profile of the fibre-slurry flow during formation, but its effect is limited by the basis mass quality specification of 121.3 to 128.8 g/m^2 for this grade. Nonetheless, it provides a means of moisture profile correction, and as such the rolls can be operated to lower nip loads. Using the relationships established by regression of the moisture profiles in section 3.2.5, the magnitude of correction using the entire basis mass range is 1.6% moisture. Since it is overoptimistic to assume that the entire range of headbox basis mass profiling will be available for roll cover wear compensation, a more realistic figure of 1% was used for calculations. Headbox profiling also affects the mechanical strength profile of the sheet and as such is used to compensate for a wide variety of operating conditions. Using the inverse model in the same manner that was used to calculate L_{alarm}, the wear tolerance is expectedly lower at $L_{critical}$ = 34 kN/m (211 μm from the model of cover deflection).

It is important to note that although the roll wear may cause a reduction in the nip load in some areas, the load will increase correspondingly in other areas of the nip in order to maintain a force equilibrium with the hydraulic loading. This is important because when changing rolls on the basis of their condition consideration has to be given to the allowable stress in the felts and roll cover, as well as the effect on the paper properties. For the duration of this study, the highest

recorded load was below the allowable limits prescribed for roll cover materials by Gudehus [43], and those for maximum felt loading. Hence for these rolls the factor limiting the amount of roll wear was confirmed as the effect on paper quality.

The steam shower and spray dampener systems on this particular paper machine are designed to provide moisture profile correction. This does not detract from the justification for this study, since the present objectives are to establish the degree to which rolls can affect the moisture profile. Both systems were turned off during the measurement intervals of this study, to allow the isolation and quantification of the effect of roll cover wear. A separate study was conducted to determine, as with headbox profiling, the extent of profile correction that could be fulfilled by the spray dampener system. The details of the experiment are shown in Appendix E. The conclusions being that the spray dampener system on this particular machine has no effect, being undersized for the present production volumes. These findings were confirmed by the original supplier of the equipment, and an upgrade was underway at the time of writing this report. The effect of the steam shower was not investigated because the papermakers indicated that at 125 g/m^2 they usually turned the system off as it had no effect. The system only has a measurable effect on heavier grades from 175 to 400 g/m^2.

The accuracy of the inverse model method was evaluated by comparing the nip load calculated from wear measurements with the nip load estimated by the inverse model, for a given moisture value and process conditions. The results are shown in Table 4-D as conditional probabilities to better explain the distribution of the data into the four categories. The four categories describe the ability of the inverse model to correctly distinguish between a nip load which is below tolerance (a worn roll), and a nip load above the tolerance (acceptable roll). The value in each case can be interpreted as “the probability of ‘Estimated’ statement being true, given that ‘Actual’ statement is true”. The probability value indicates the percentile of data, where 1 = 100%. L_M, L_T and L_E represent the Measured, Tolerance and Estimated loads respectively. The results are given for each of the measurement windows, or grade runs.

Table 4-D Probabilistic results table: worn roll classification.

Actual	$L_M < L_T$		$L_M > L_T$		
Estimated	$L_E < L_T$	$L_E > L_T$	$L_E < L_T$	$L_E > L_T$	
Target probability	1	0	0	1	Percentile data below L_T
Grade run 1	0.93	0.07	0.06	0.94	0.184
Grade run 2	0.42[a]	0.58	0.21	0.79	0.103
Grade run 3	0.81	0.19	0.43	0.57	0.213
Grade run 4	0.97	0.03	0.30	0.70	0.213
Grade run 5	0.54[a]	0.46	0.09	0.91	0.140
Grade run 6	0.96	0.04	0.25	0.75	0.316
Grade run 7	0.61	0.39	0.55	0.45	0.199
Average	0.75[a] (0.86)	0.25	0.27	0.73	0.195

[a)] Lowest probabilities.

In summary the results show that on average a worn roll was correctly classified with a probability of 0.75, and an acceptable-condition roll with 0.73. It is important to note that the lowest probabilities occurred in grade runs 2 and 5 (indicated by [a]). Investigation of these results indicated that these two grade runs also had the lowest percentile of data below the load tolerance L_T. Essentially what this indicates is that the volume of measurement data related to positions of severe wear became the limiting factor to the accuracy of the method. This is intuitive from NN theory, the requirements of which for sufficient training data have been discussed. Were it not for these two values, the prediction accuracy would have increased to 0.86 in the case of the correct classification of a worn roll. This highlights the reliance of this method on an appreciable amount of data below the load tolerance. For this study, the figure required appears to be in the region of 18%. The same fault-data shortage problem was noted by Edwards *et al.* [27] in their study of neural methods for the prediction of paper curl properties. The importance of the size of the training data set on final network accuracy was determined experimentally by Liu and Mengel [32]. From a manufacturers perspective this requires a marriage between the need to produce quality paper in the immediate period and the need to obtain good data variety for the model to be effective in the long term.

The figures reported in Table 4-D are not only a reflection of the inverse modelling process, but are actually representative of the culmination of all the methods used in this study. The roll wear measurements were used to calculate the nip load profile using the model of cover deflection. The nip load values were used in conjunction with other process measurements to train the neural network to estimate the moisture content. The trained neural network was then used in the inverse model calculation to calculate the nip load from a given moisture value. Thus Table 4-D can be regarded as a report of the final accuracy of the proposed condition-based methodology.

The worn-state prediction accuracy of 75% is a suitable achievement for the application of this method in industry. Particularly when one considers the very inconsistent wear rates of the covers which were discussed in chapter 2. The preventive approach, whereby rolls are removed after fixed service periods, is traditional and to the author's knowledge the only practised method in this industry. These methods are based on the repeatability of the wear rates. To support this argument, a final comparison which can be made is that between the current preventive methods of roll maintenance and the proposed condition-based method. The comparison of the two methods is made in Fig. 4-4. The rolls used for the comparison were the same rolls used for the experimental verification in this chapter. The figure indicates in red the nip load tolerances which were established in this study. The proposed method would be able to determine with a reliability of 75% that the roll had reached these tolerances by looking only at the paper quality and process conditions. Also indicated in blue are the historical records of when the rolls were changed in the past. The nip load value indicated is the lowest nip load that would have occurred over an appreciable length of the nip (260mm).

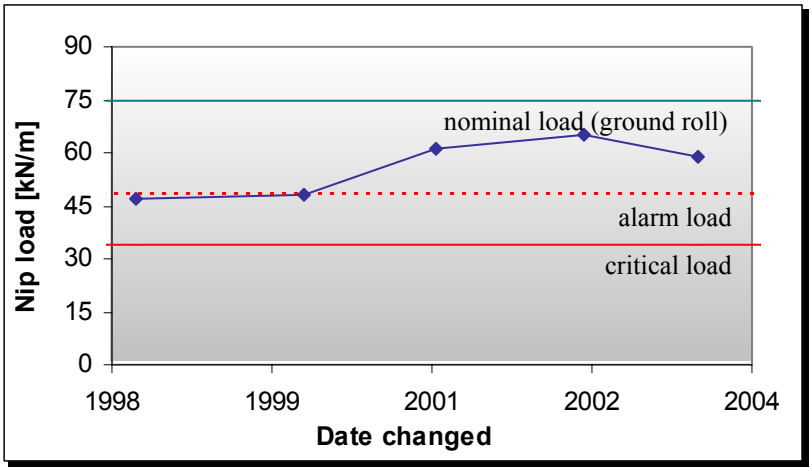

Fig. 4-4 Comparison of historical roll changes with tolerances.

The roll changes which occurred in the years 1998 and 1999 occurred at exactly the point where the proposed method would have recommended them to be changed. However, the last three roll changes occurred at points in time when the rolls were still fit for further use. The opportunity to run the rolls for longer periods between grinds using the proposed method is thus evident, as three out of five roll changes were premature. The proposed condition-based method takes advantage of these opportunities. The fact that this life extension considers both the condition of the roll and the effect on the paper quality makes this method even more beneficial in a second scenario. This scenario would occur when, for whatever reason, the wear is excessive over a shorter period of time than the regular replacement frequency. This excessive wear would lead to excessive moisture streaks in the paper. Under existing maintenance methods, this would initiate a troubleshooting exercise to identify the cause of excessive moisture. The roll would not be able to be measured because of the danger involved with its rotation in the machine. Conversely the condition based method would be able to identify on the run whether the roll cover is the root cause of the poor moisture profiles in the paper.

5. Conclusions and recommendations for further research

5.1 Conclusions

5.1.1 Analysis procedure

The purpose of this study was to determine if the roll maintenance program could be optimised to give longer intervals between maintenance services without negatively affecting the quality of the paper being produced. The current best practices of roll maintenance in the industry are of the preventative methodology. According to this approach the rolls are removed after fixed predetermined time intervals, irrespective of their condition. One of the requirements for the success of this approach is that the cover wear rates must be repeatable. In the present study the repeatability of the wear rates of nipped rolls was investigated using historical wear records from four kraft paper machines in Southern Africa. It was found that the repeatability of the wear rates was so low that meaningful conclusions could not be drawn from the data. It may be that the wear rates of un-nipped rolls are more repeatable. However, the interest in this study was the paper quality, which is affected more by the nipped rolls than those which are un-nipped.

In a subsequent study the mechanisms of wear were studied by measuring the wear on a press roll pair *in situ* over a period of months. It was found that the wear patterns were not exclusively related to time effects. As a progression of the maintenance methodology, roll changes based on the condition of the roll covers were considered. A press roll pair was selected for this study due to the importance of mechanical pressing in determining final sheet characteristics. From a papermaking point of view the wear on a roll cover must be uniform along the roll's axis. Non-uniformities will lead to, among other effects, poor moisture profiles in the paper sheet. The roll cover wear and moisture content were measured over a period of months. Due to the influences of other process conditions on the moisture content, a number of other variables were also measured. A Neural Network model was used to establish the relationship between roll wear and moisture content. The methodology developed allows the progression of cover wear to be monitored using the moisture profile of the paper produced until quality limits are reached, and the roll is replaced on condition. Wear tolerance limits for the rolls were also established using the relationships derived by the model. It was shown by comparison that the proposed approach indicates

significant benefits of the condition-based approach over conventional methods. The benefits to the paper manufacturers will be realised not only through the direct maintenance cost savings, but more significantly through reduced production losses related to inferior roll conditions.

5.1.2 Model of cover deflection

A calculation method was required in this study which allowed radial wear measurements to be converted to an equivalent nip load in the press. Accurate calculation models exist in the literature for nips with one rock-hard and one soft covered roll. A reliable model for the case of two soft covered rolls could not be found, and hence was developed as part of the present work. This model was developed in stages, beginning with the case of one rock-hard and one soft cover, derived in Appendix B. The second model for the case of two soft covers is derived in Appendix D. These derivations were not included in the chapters of this report because they were regarded as calculation tools. However, their existence is significant enough in the field of this study to warrant inclusion and discussion here.

The model is based on the principle that the soft cover can be modelled as a series of radially orientated springs. This approach has been used by other researchers with success, and is simpler than the finite element approach. Through considerations of the geometry and material properties, the model was derived mathematically. The accuracy of the mathematical model was improved by empirical methods. The agreement between the pseudo-mathematical model and the results reported by other researchers indicates that the model provides a good representation of stress-strain behaviour in the nip.

The two-dimensional model is then extrapolated in a third dimension along the roll axis. The force at each point along the roll axis is calculated through the application of a force equilibrium condition between the forces in the nip and the external loading applied to the press. Misalignment of the rolls is taken into account through the requirement for a moment equilibrium condition in the model. This is an important consideration because the rolls generally have spherical roller type bearings loaded by independent arms, and are tolerant of small amounts of misalignment.

5.1.3 Process measurements

In addition to the cover wear a number of other process conditions were perceived to influence the moisture profile of the paper sheet. From existing pressing theories and literature of papermaking these parameters were identified and measured on the paper machine used in this study. Measurements of these parameters and the moisture content were conducted on numerous occasions over a period of months. On each occasion a few thousand measurements were taken, at a number of points across the width of the machine.

The characterisation of the impact of some of these parameters on the moisture of the paper was further enhanced by post-measurement calculations, known as feature extractions. The extracted features and remaining measurement data was then used to construct a model of the dewatering process of the paper machine. A post-modelling analysis of the dewatering process indicated that not all of the measured parameters were required to fully describe the paper machine behaviour. It is conceded that the redundant parameters may well play a part in sheet dewatering, but that tight control of their variance by the process control software lead to their effect remaining undetected in this study.

5.1.4 Neural methods

A Neural Network (NN) model was used to describe the dewatering process of a commercially active paper machine. This model was chosen over wet pressing models in the literature due to the fact that it was able to consider a wider scope of variables which potentially affected the moisture profile. Unlike existing pressing theories, the NN did not require that measurements be taken directly after the press. This is a critical requirement for commercial machines. The NN was trained off-line due to the fact that some of the inputs required manual measurements. A multi-layered perceptron (MLP) network was trained in a supervised manner from measurement data. This negated the requirement for an expert papermaker to construct the model, and also reduces the errors which result from differences between theoretical models and practical situations.

Comparisons between the measured moisture content with that estimated by the MLP indicated that the MLP is able to model the dewatering process to a high degree of accuracy. Then, using the relationships established by the MLP, an inverse model was developed to describe the condition of the roll based on a given set of process conditions and sheet moisture content. The inverse model was able to correctly identify worn and acceptable-condition rolls with an accuracy which is acceptable for its application in industry. It was further shown by comparison that the condition based method is superior to that of conventional methods. The comparisons made use of historical roll wear data and showed that the rolls could have operated for longer periods of time.

One of the limitations of the method at present is the excessive number of man-hours required to measure and train the network. Further applications of this method in industry will require a higher degree of automation to reduce these hours. A second limitation is that the proposed approach requires the existence of a relationship between the cover wear and the paper quality. For many un-nipped roll types, such as wire rolls and felt rolls this relationship does not exist, and hence it is not advisable to use this method. This approach will only work on more critical rolls, which do have an influence on paper quality, and hence will allow the justification of the expense of these methods. Typical applications other than the press section would be soft calenders, roll coaters and size presses.

5.2 Recommendations for further research

5.2.1 Model of cover deflection

The derivation of the cover deflection model for a nip with two-soft roll covers was based on the assumption that the cover can be modelled as a set of radially orientated springs. This approach was also used by Carvalho and Scriven [50], in which a factor α was determined experimentally to give the most accurate solution. In the present study two more empirical factors were required to complete the model, believed to be related to the Poisson ratio of the material. A more thorough investigation into the material behaviour could well result in a mathematical term to replace the empirical factors. One of the suggested areas of investigation is the relationship between the Poisson ratio and the Bulk Modulus κ of the material, and how these properties affect the spring model.

5.2.2 Paper quality indices

For the purposes of this study the one particular type of roll was chosen, the press roll. Furthermore, because of the complexity of the papermaking process, only one feature of the paper was chosen as a wear indicator: the moisture content. There are other features which are worth investigating, such as the *Burst Index* (BI) property of the paper. The BI provides an indication of the mechanical strength of the paper, which is determined by the inter-fibre bonds in the sheet. The fact that the sheet fibres are compressed together in the press nip indicates that BI could also be a good indicator of the uniformity of the nip load profile of press rolls.

In addition to the press rolls, there are a number of other rolls which could also benefit from condition-based roll changes. Examples are soft-calenders, roll coaters and size-presses. For the latter two the required relationships are likely to be more easily defined than in this study because there are fewer non-roll related influences. Be aware that the measurements of roll wear will have to be taken over a period of months to gather a sufficient and diverse amount of wear data.

5.2.3 Neural methods

In this study the Multi-Layer Perceptron (MLP) with back-propagation was used due to its widespread use in industry and in similar applications in the steel rolling industry. The field of mathematics called Artificial Intelligence (AI), of which neural networks is a part, is vast and the methods have increased dramatically since the 1980's. The MLP proved to be successful in this application, however, the authors do not assume to know all of the AI techniques. It may be that another research group with more experience of AI methods might suggest an alternative to the MLP, resulting in even better results.

One of the burdens of neural methods is the high amount of data which is required to train a network to a respectable accuracy. This requirement results in lengthily measurement periods, particularly for more complex systems. Randall and Gao [33] studied the possibility of using simulated feature vectors in addition to measured feature vectors to diagnose faults on roller element bearings. A suggestion for further research would be to determine if simulated vectors could be constructed for this application. This would alleviate the requirement for the paper

machine owners to operate the rolls in near worn-out conditions to provide training data for the neural network.

5.2.4 On-line implementation

The opportunities which have been realised in this study are significant. Unfortunately there are a number of practicality issues which must be addressed before such a method can become economically viable. The first is that the measurements which are required as inputs and outputs to the Neural Network must be either automated from DCS (Distributed Control Systems) or migrated automatically from other databases so that the data can be received in electronic format. The large amount of data which is required by this method can not be submitted manually in industrial applications, as the cost in man-hours will be extremely prohibitive. If software could be developed which allowed the data to be submitted automatically to the NN, then the system would be able to learn on-line which will have significant man-hour saving benefits.

One of the more time-consuming measurements which will be required for all applications of this method in roll maintenance is the initial measurements of the roll wear during the training phase. This phase will generally last more than six months, during which a number of measurements must be taken. In the present investigation these measurements were made manually, which was difficult because these must occur during a maintenance outage of the machine. The demands of this task might be significantly alleviated if a more efficient measurement method existed. This function could be served by a device which, mounted to a beam or the existing machine frame, could traverse the length of the roll and measure the roll profile. Similar systems exist for roll measurement on the grinding machines, as developed by Hilden & Jaakkola [63]. Their measurement system uses a floating measuring device which is mounted to the tool carriage of the grinding machine. It measures the diameter in the same way that a conventional micrometer does. Unfortunately this system is not portable, which would be a requirement for its use in the proposed application.

References

[1] G. P. Succi, "Prognostic Methods for Bearing Condition Monitoring," Proceedings of the 3rd International Machinery Monitoring and Diagnosis Conference, Las Vegas, Nevada, pp. 335-342 (1991).

[2] B. Al-Najjar, "Prediction of the Vibration Level when Monitoring Rolling Element Bearings in Paper Mill Machines," International J. of COMADEM 4 (2), pp. 19-26 (2001).

[3] A. Menon, "Watching for the Wobbles," Pulp & Paper International (2001).

[4] Y. Bissessur, E. B. Martin and A. J. Morris, "Monitoring the Performance of the Paper Making Process," Control Engineering Practice 7, pp. 1357-1368 (1999).

[5] H. Norrman, "Paper Mills Gain from Condition Monitoring," Evolution: Publication of SKF International (4), pp. 21-23 (1999).

[6] M. J. Cutler, "Paper Machine Bearing Failure," Tappi J. 79 (2), pp. 157-167 (1996).

[7] A. W. Beucker, "The Roll Cover in Modern Paper Machines," Tappi J. 69 (9) pp. 66-71 (1986).

[8] R. Moore *et al.*, "Maintenance of Covered Rolls," TAPPI Technical Information Paper TIP 0420-02 (2001).

[9] A. W. Beucker, "The Nip Width Impression; A Powerful Tool for Better Machine Operation," Beloit Company Publication, Beloit Corporation Wisconsin, pp. 1-24 (1990).

[10] A. Bloigu, A. Rantanen and A. Telama, "Two-year Maintenance Intervals for Suction Rolls," PaperNews 11 (2), pp. 22-23 (1995).

[11] P. B. Wahlstrom, Pulp & Paper Mag. Canada 61 (8, 9), pp. 379, 419 (1960).

[12] B. Wahlstrom, "Opportunities in Pressing," Paper Technology, pp. 119-129 (1980).

[13] B. Wahlstrom, "Pressing – the State of the Art and Future Possibilities," Paper Technology 32 (2), pp. 18-27 (1991).

[14] R. J. Kerekes and J. D. McDonald, "A Decreasing Permeability Model of Wet Pressing: Theory," Tappi J. 74 (12), pp. 150-156 (1991).

[15] R. J. Clos, L. L. Edwards and I. Gunawan, "A Limiting-consistency Model for Pulp Dewatering and Wet Pressing," Tappi J. 77 (6), pp. 179-187 (1994).

[16] I. Pikulik *et al.*, "Water Permeability of Press Felts," TAPPI Technical Information Paper TIP 0404-43 (1995).

[17] Water Removal Committee of the Engineering Division TAPPI, "Press Section Monitoring," TAPPI Technical Information Paper TIP 0404-19 (1997), P.O. Box 105113, Technology Park/Atlanta, Georgia 30348, USA.

[18] Stowe Woodward, "Stowe Woodward's Advanced Computer Aided Roll Service Support for Analysis of Dewatering Processes in the Paper Machine," Stowe Woodward company release of the PressManager product.

[19] E. Young *et al.*, "Porosity Measurement of Press Felts on the Paper Machine (HSPT)," TAPPI Technical Information Paper TIP 0404-29 (1997).

[20] W. Kochanik *et al.*, "Press Section Water Balance using Portable Sensors," TAPPI Technical Information Paper TIP 0502-18 (2001).

[21] J. Bottiglieri, "Shoe Presses: Dressing for Success," Solutions for People, Processes and Paper (11), pp. 34-38 (2001).

[22] E. Z. Fekete and K. M. Wiebe, "The Limits of Pressing," Tappi J. 82 (11), pp. 81-87 (1999).

[23] J. D. McDonald, I. I. Pikulik, C. J. Mentele and D. V. Lange, "A Pilot Paper Machine Evaluation of the Effects of Pressing on Newsprint Quality," Tappi J. 81 (6), pp. 131-137 (1998).

[24] I. Pikulik and J. Hamel, "The Effects of Shoe Pressing on the Properties of Wood-containing Papers", Tappi J. 83 (8), p. 88 (2000).

[25] J. D. McDonald and R. J. Kerekes, "A Decreasing-permeability Model of Wet Pressing with Rewetting," Tappi J. 78 (11), pp. 107-111 (1995).

[26] C. M. Bishop, Neural Networks for Pattern Recognition, (Oxford, Oxford University Press, 1995), pp. 137-138

[27] P. J. Edwards, A. F. Murray, G. Papadopoulos, A. R. Wallace and J. Barnard, "The application of neural networks to the paper-making industry," Proceedings of the European Symposium on Artificial Neural Networks, Bruges (Belgium) pp. 69-74 (1999).

[28] M. A. Hussain, "Review of the Applications of Neural Networks in Chemical Process Control – Simulation and Online Implementation", Artificial Intelligence in Eng. 13 (1), pp. 55-68 (1999).

[29] J. Larkiola, P. Myllykoski, A. S. Korhonen and L. Cser, "The Role of Neural Networks in the Optimisation of Rolling Processes," J. of Materials Processing Tech. 80-81, pp. 16-23 (1998).

[30] A. A. Gorni, "The Application of Neural Networks in the Modelling of Plate Rolling Processes," JOM-E (formerly Journal of Materials) 49 (4), (1997).

[31] B. D. Ripley, Pattern Recognition and Neural Networks, (Cambridge University Press, New York, 1996), pp. 173-175.

[32] T. I. Liu and J. M. Mengel, "Intelligent Monitoring of Ball Bearing Conditions," Mechanical Systems and Signal Processing 6 (5), pp. 419-431 (1992).

[33] R. B. Randall and Y. Gao, "A Simulation Model for Training Neural Networks to Recognise Bearing Faults," presented at the University of New South Wales International conference on noise and vibration engineering, (September 2000).

[34] O. Petrilli, B. Paya, I. I. Esat and M. N. M. Badi, "Neural Network Based Fault Detection using Different Signal Processing Techniques as Pre-processor," Structural Dynamics and Vibration 70, pp. 97-101 (1995).

[35] B. A. Paya, I. I. Esat and M. N. M. Badi, "Artificial Neural Network Based Fault Diagnostics of Rotating Machinery using Wavelet Transforms as a Preprocessor," Mechanical Systems and Signal Processing 11 (5), pp. 751-765 (1997).

[36] B. A. Paya, I. I. Esat and M. N. M. Badi, "Fault Classification in Gearboxes using Neural Networks," ASME International (1996).

[37] P. T. Monsen, E. S. Manolakos and M. Dzwonczyk, "Helicopter Gearbox Fault Detection and Diagnosis using Analog Neural Networks," Proceedings of the 27th Assilomar Conference on Signals, Systems and Computers, pp. 381-385 (1993).

[38] A. C. McCormick and A. K. Nandi, "Classification of the Rotating Machine Condition using Artificial Neural Networks," J. of Mechanical Engineering Science 211 (C6), pp. 439-450 (1997).

[39] F. L. Luo and C. Wen, "Multiple-Page Mapping Artificial Neural Network Algorithm Used for Constant Tension Control," Expert Systems With Applications 13 (4), pp. 307-315 (1997).

[40] J. Reese *et al.*, "Troubleshooting Cross-machine Direction Moisture Profile Problems," TAPPI Technical Information Paper TIP 0404-57 (2001).

[41] R. A. Reese *et al.*, "Press Section Optimization," TAPPI Technical Information Paper TIP 0404-52 (1997).

[42] J. A. Zwinak, "Specially Designed Roll Covers are required in Modern Press Sections," Pulp & Paper (5) pp. 84-86 (1984).

[43] T. Gudehus, "Draining Profiles for Press Rolls", published in a company release (Felix Böttcher, Köln), pp. 15-16 (1988).

[44] N. Gamsjäger, "Elastic Calender Covers Based on Advanced Composites," Company Publication, M-G Cylindres.

[45] A. Telama, "Roll Covers and Coatings for Every Application," Valmet Paper News, Company Publication by Valmet Paper Machinery, Inc., Helsinki, Finland 12 (1-2), 28-29 (1996).

[46] L. Ryder, "Rubber Covered Roll Nip Calculations Made with a Computer," Paper Trade J. 14 (12), (1970).

[47] J. M. Gere and S. P. Timoshenko, Mechanics of Materials, 3rd ed. (Chapman & Hall, 1991), pp. 428-429.

[48] R. H. Moore, "Crowns and Cross-machine Loading Variations", Tappi J. 80 (4), pp. 219-229 (1997).

[49] P. B. Lindley, "Engineering Design with Natural Rubber," The Natural Rubber Producers Research Association, Technical bulletin no. 8, p. 8 (1963).

[50] M. S. Carvalho and L.E. Scriven, "Flows in Forward Deformable Roll Coating Gaps: Comparison between Spring and Plane-Strain Models of Roll Cover," J. of Computational Phys. 138 (2), pp. 449-479 (1997).

[51] J. S. N. Meikle, C. J. Stander and P. Viljoen, "Determining Roll Service-life from Paper Quality Measurements with Neural Networks," Proceedings of the 90th Annual Meeting of Pulp and Paper Technical Association of Canada, Montreal, January 2004, pp. B63-66.

[52] Beloit Walmsley Limited, "Crowning and Dubbing Information," Company Publication, Beloit Walmsley Limited, Atlas Works, Lancashire, England, pp. 1-5 (1979).

[53] J. M. Gere and S. P. Timoshenko, Mechanics of Materials, 3rd ed. (Chapman & Hall, 1991), pp. 59-73.

[54] J. C. Roux and J. P. Vincent, "A Proposed Model in the Analysis of Wet Pressing," Tappi J. 74 (2), pp. 189-195 (1991).

[55] P.B. Wahlstrom, Pulp & Paper Mag. Canada 61 (8), p. 379 (1960).

[56] P. C. Carman, Flow of Gases Through Porous Media (Academic Press, New York, 1954).

[57] R. J. Kerekes and J. D. McDonald, "A Decreasing Permeability Model of Wet Pressing," Preprints of the 76th Annual Meeting, Technical Section, Canadian and Paper Association, Montreal, Canada, pp. 173-179 (1990).

[58] C. M. Bishop, Neural Networks for Pattern Recognition, pp. 182-183.

[59] C. M. Bishop, Neural Networks for Pattern Recognition, pp. 137-140.

[60] Y. Reich and S. V. Barai, "Evaluating Machine Learning Models for Engineering Problems," Artificial Intelligence in Engineering 13, pp. 257-272 (1999).

[61] D. J. C. MacKay, "Bayesian Interpolation," Neural Computation 4 (3), pp. 415-447 (1992).

[62] D. Nguyen and B. Widrow, "Improving the Learning Speed of 2-layer Neural networks by Choosing Initial Values of the Adaptive Weights," Proceedings of the International Joint Conference on Neural Networks 3, pp. 21-26 (1990).

[63] K. K. Hilden and T. Jaakkola, "New Roll Measurement and Control Technology Result in Better Paper Machine Performance," Pulp & Paper Canada 98 (3), pp. 91-95 (1997).

Appendix A

Modulus testing of polymer materials

One of the requirements of the model developed in chapter 3 was that wear measurements of the rolls be converted to an equivalent nip load. This conversion is provided for two different cases of roll hardnesses in Appendix B and Appendix D. Both of these require that the modulus of the cover materials be known. This appendix describes laboratory tests which were conducted on various roll cover materials to confirm the relationship between hardness and elastic modulus as reported by Gudehus [43] and a supplier to the industry who requested not to be named. The tests were performed on polyurethane and rubber materials which closely approximated those of the roll covers used in the present study. The exact polymer materials could not be reproduced due to the proprietary nature of the compositions of these materials. The testing machine was an Instron 4465 materials testing machine, shown in Fig. A-1.

Fig. A-1 Instron 4465 materials testing machine.

The control software for the Instron was the INSTRON Series IX Automated Materials Tester, version 8.06.00. The tests were conducted according to the International Standard for Rubber, Vulcanized and Thermoplastic Determination of Tensile Stress-Strain Properties, ISO 37 (1994). The only modifications to the method were a reduction of the recommended rate of elongation from 500 mm/min. This was necessary to allow a larger amount of sample data to be recorded

over the small amounts of strain which were of interest in this study. Strain measurements were made using the built in electronic extensometer of the Instron device. The modulii of the samples were calculated automatically by the software. Dumbbell-shaped samples were cut from a material blank according to the Standard Test Methods for Vulcanized Rubber and Thermoplastic Elastomers – Tension: ASTM D412-98a. A photograph of one of the blanks is shown in Fig. A-2a.

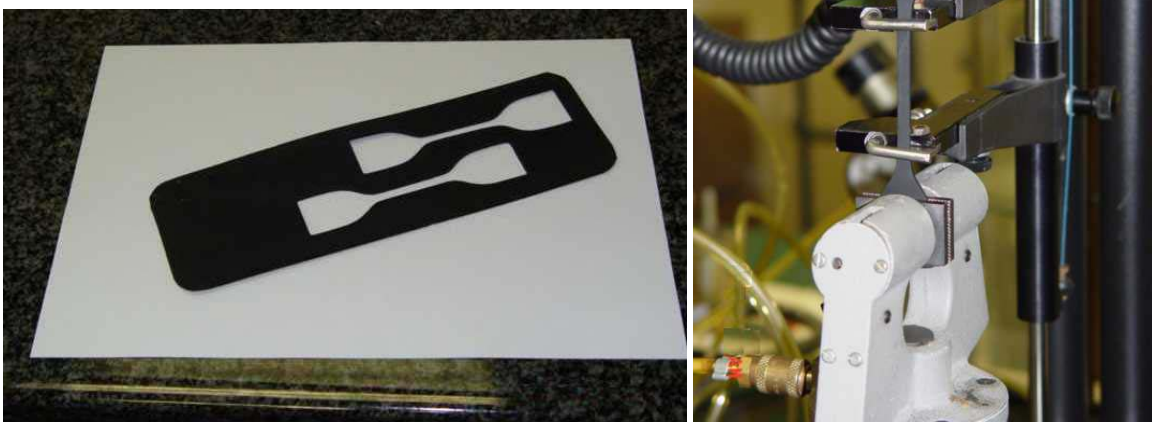

a) b)

Fig. A-2 a) Material blank with dumbbells removed and b) tensile test in progress.

In practice the polymer covers are loaded in compression, however the test device was only able to perform tests in tension, shown in Fig. A-2b. However, Lindley [49] indicates that the load-deflection curves for rubber in tension and compression are approximately linear for strains of the order of a few percent, and values of elastic modulus E can be obtained from these linear regions. As the curves are continuous through the origin the values of E in tension and compression are approximately equal. The use of the tensile test was justified in this study, and the results are shown in Table A-A.

Table A-A Results of modulus-hardness tests.

Material type	No. of samples	Hardness [P&J]	Mean *E* [MPa]	Std dev. [MPa]
Natural rubber	6	10	211.0	40.5
Nitrile rubber	6	12	80.4	16.1
Polyurethane	6	14	68.0	6.9
Polyurethane	6	27	35.3	3.1

The higher standard deviations at lower values of P&J (corresponds to increased hardness) are due to the nonlinear relationship of the hardness-modulus relationship. The gradient increases significantly at lower hardness values. The results of the tests were used to confirm if the relationships given by Gudehus [43] and a supplier were valid for the types of cover materials used in this study. The comparisons between these relationships and the present results are given in Fig. A-3.

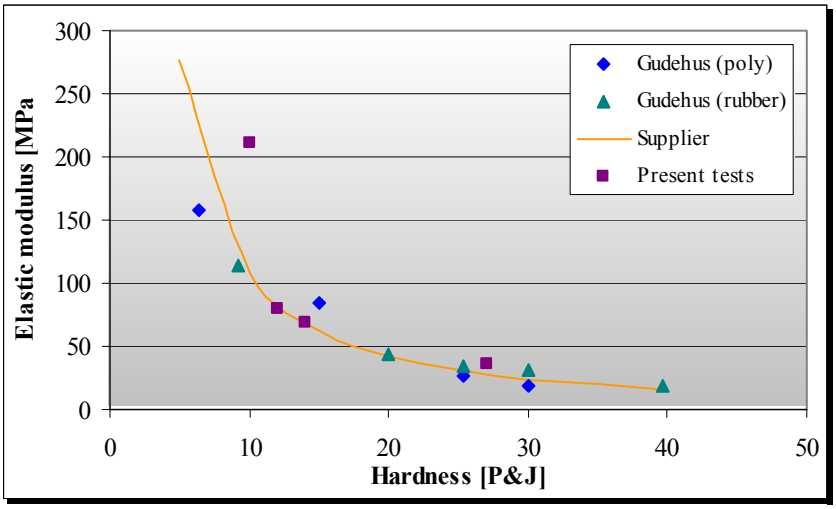

Fig. A-3 Comparison of experimental results with previous relationships.

In general there is good correlation between the three sources. The present results correlated better ($r^2 = 0.86$) with the relationship given by the Supplier. Deviations are more prominent at hardness values below 10 P&J. The results of the 10 P&J tests conducted in this study were higher than expected when compared with previous results. This may be due to inaccuracies in

the measurement of the hardness, as the test normally has a ±3 P&J tolerance. As can be seen, a 3 P&J error in the sub-10 P&J area of Fig. A-3 could result in significant differences in modulus. A possible second reason is that the 10 P&J sample was of the natural rubber type compound. This compound is hardened through the addition of sulphur to promote cross-linking of the polymer chains. It may be that with the high degree of cross-linking at 10 P&J the mechanisms which allow movement between the polymer chains were altered, which would not have occurred in the case of polyurethane. The higher level of confidence in the supplier curve and the fact that this provided better agreement between the mathematical model derived in Appendix B and measurements by other researchers resulted in this curve being used for the remainder of this investigation. The equation describing the curve was provided by the Supplier as follows:

$$E = 359607P^{-1.36208}$$

where:

E = Elastic modulus, in PSI

P = Roll cover hardness, in P&J

or the SI equivalent:

$$E = (6894.757)(359607)P^{-1.36208} \qquad \text{(A-1)}$$

where:

E = Elastic modulus, in Pa

P = Roll cover hardness, in P&J

Appendix B

Mathematical model: One rock-hard and one soft cover

The model developed in chapter 3 requires a method whereby the decrease in nip load can be calculated from known amounts of cover wear. In principle this concept is a simple one: if the rolls wear in a certain area then the nip load will be supported by other areas along the length of the cover. In the worn area there will be less compression of the cover material, and thus less force in the material in that area. In practice this concept is complicated by two factors: the nip geometry and the non-linear stress-strain behaviour of polymer materials.

To explain the nip geometry consideration must be given to what is happening to the roll covers in the press. The wet paper sheet is fed between two rolls which are forced together. In this study the rolls had polymer covers which deflected in the nip, resulting in an increase in nip width. For simplicity of notation, the combined effect of the re-arrangement of the polymer materials is simply referred to as 'cover deflection'. The model developed for this calculation should also take into account the physical parameters of the system such as roll diameters, cover hardnesses and the thickness of the cover material. A related equation is provided by Beucker [7] which calculates the nip width from the nip load, as shown in Eq. (B-1). Eq. (B-1) is only valid for the case of a nip with one rock-hard cover and one soft cover.

$$N = \left[\frac{5.8 \times 10^{-6} L T_1 D_1 D_2 P_1^{1.35}}{D_1 + D_2} \right]^{0.81 D_1^{-0.232}} \tag{B-1}$$

where:

N = Nip width, in in.

L = Press load, in PLI

T_1 = Working cover thickness of the soft roll, in in.

D_1 = Diameter of the soft roll, in in.

D_2 = Diameter of the hard roll, in in.

P_1 = Hardness of the soft roll, in P&J

The maximum cover deflection (d) will occur at the centre of the nip width, on the line intersects the centres of the two rolls. The relationship between nip width and the magnitude of d is given by Ryder [46] in Eq. (B-2).

$$d = \frac{N^2\left(D_1 + D_2\right)}{4D_1D_2} \tag{B-2}$$

By combining Eqs (B-1) and (B-2) the cover deflections in the plane of the roll axes can be readily calculated for a given load. The shortcomings of this approach are that Eq. (B-1) is only valid for nips which have one rock-hard and one soft covered roll. The press for which this study was intended had two soft nips, as do many commercial paper machines. The difference between the two is significant because the deflected shapes are not the same. In the case of the nip with one rock-hard roll the soft roll will assume a concave shape over the area of contact. In the case of a nip with two soft rolls the deflected shapes can vary depending on the relative hardnesses. One extreme will exist where the rolls have identical hardness and the contact area assumes a straight line. The other extreme occurs at large differences in hardness, in which case the deflected shape geometry will tend to the approximation of a rock-hard and soft roll combination.

A model for the two soft cover scenario was provided by a supplier to the industry who has asked not to be named. This is unfortunate because the model could not be found elsewhere in the literature to evaluate its origin. The model calculates the nip width from the nip load and geometry, as shown below:

$$a_0 = \sqrt[3]{\frac{6dP}{E_{eff}}\left(\frac{D_1D_2}{D_1 + D_2}\right)}$$

where:

a_0 = Nip width

P = Linear load

d = Average thickness of the polymer covers

D_1, D_2 = Diameters of the top and bottom rolls

and:

$$E_{eff} \approx 2.6E_0$$

and:

$$E_0 = \left(\frac{d_{B1}}{E_{B1}\left(d_{B1} + d_{B2}\right)} + \frac{d_{B2}}{E_{B2}\left(d_{B1} + d_{B2}\right)} \right)^{-1}$$

This model was not used for modelling purposes in the remainder of this study due to the lack of information regarding its origin. It was, however, used for comparative purposes to evaluate the accuracy of the two soft roll model developed in this chapter. In the absence of any other model in the literature for the two soft roll nip case, a mathematical model was derived from first principles using the geometry of the nip and the stress-strain behaviour of the cover materials. The model is based on the principle that the soft cover material can be modelled as an elastic spring. This approach was used successfully by Carvalho and Scriven [50] in a study of roll coating gaps. The model was first derived in this Appendix for the case of one rock-hard roll and one soft roll to evaluate the accuracy of the methods. The model is verified against the Beucker [7] model of Eq. (B-1). Based on the success of this model, the solution was extended along the same mathematical methods to consider the case of a two soft roll nip, described in Appendix D.

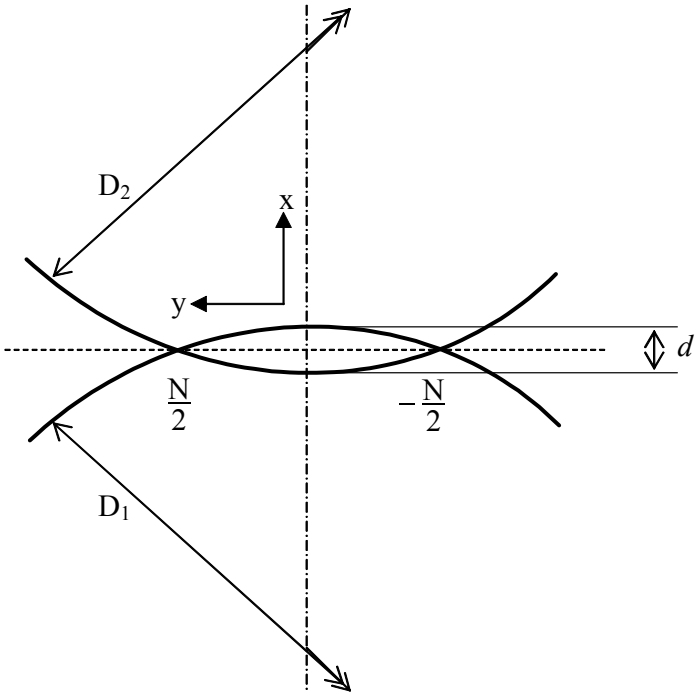

Fig. B-1 Geometry of rolls and interference

When the rolls are forced together in the nip, the soft roll deflects to assume a concave shape at the contact surface, as shown in Fig. B-1. The shape of the concave is determined by the diameter and degree of interference of the rock-hard roll. This shape is described geometrically using the positions of the circumferences. Choosing the origin of the co-ordinate system arbitrarily at the geometric centre of the nip, the bottom roll circumference is described in rectangular co-ordinates by:

$$(x+u)^2 + y^2 = \left(\frac{D_1}{2}\right)^2 \tag{B-3}$$

where:

x = Dependent vertical co-ordinate, in m

u = x Coordinate of the centre of the bottom roll, in m

y = Independent horizontal co-ordinate, in m

D_1 = Diameter of the bottom roll, in m

Substitute the co-ordinates of the known point on the circumference $\left(0;\frac{N}{2}\right)$, where N is the nip width, in meters.

$$(0+u)^2 + \frac{N^2}{4} = \frac{D_1^2}{4}$$

$$u = \pm\frac{1}{2}\sqrt{D_1^2 - N^2} \tag{B-4}$$

Considering only the solution where the roll centre is below the origin, and substituting for u from Eq. (B-4) into Eq. (B-3):

$$\left(x + \frac{1}{2}\sqrt{D_1^2 - N^2}\right)^2 + y^2 = \frac{D_1^2}{4}$$

Solving for the dependent variable x, and choosing the solution which describes only the upper hemisphere of the bottom roll:

$$b(y) = \sqrt{\frac{D_1^2}{4} - y^2} - \frac{1}{2}\sqrt{D_1^2 - N^2} \tag{B-5}$$

Similarly for the top roll:

$$(x+v)^2 + y^2 = \left(\frac{D_2}{2}\right)^2 \tag{B-6}$$

where:

v = x Coordinate of the centre of the top roll

D_2 = Diameter of the top roll, in m

Substitute $\left(0; \frac{N}{2}\right)$:

$$(0+v)^2 + \frac{N^2}{4} = \frac{D_2^2}{4}$$

$$v = \pm\frac{1}{2}\sqrt{D_2^2 - N^2} \tag{B-7}$$

Considering only the solution where the roll centre is above the origin, and substituting for *v* from Eq. (B-7) into Eq. (B-6):

$$\left(x - \frac{1}{2}\sqrt{D_2^2 - N^2}\right)^2 + y^2 = \frac{D_2^2}{4}$$

Solving for the dependent variable *x,* and choosing the solution which describes only the lower hemisphere of the top roll:

$$t(y) = -\sqrt{\frac{D_2^2}{4} - y^2} + \frac{1}{2}\sqrt{D_2^2 - N^2} \tag{B-8}$$

Since the magnitude of compression of the soft cover at any point can be described by the geometric union of the undeflected roll surfaces, the vertical overlapping or interference, $\delta(y)$, can be calculated as:

$$\delta(y) = b(y) - t(y)$$

$$\delta(y) = \sqrt{\frac{D_1^2}{4} - y^2} - \sqrt{\frac{D_1^2}{4} - \frac{N^2}{4}} + \sqrt{\frac{D_2^2}{4} - y^2} - \sqrt{\frac{D_2^2}{4} - \frac{N^2}{4}}$$

$$\underline{\delta(y) = \frac{1}{2}\left(\sqrt{D_1^2 - 4y^2} - \sqrt{D_1^2 - N^2} + \sqrt{D_2^2 - 4y^2} - \sqrt{D_2^2 - N^2}\right)} \qquad \text{(B-9)}$$

which is valid over the range of y from $\left[-\frac{N}{2} : \frac{N}{2}\right]$

Now that the amount of deflection of the roll cover in terms of the roll's geometries has been described, the radial force at any point in the nip zone can be calculated using the simple linear spring theory:

$$f = k\delta(y) \qquad \text{(B-10)}$$

where:

f = Force in the spring, in N

$\delta(y)$ = Displacement of the spring, in m

And k is the equivalent spring stiffness of the cover material. The spring stiffness of the press fabric is not included in the calculation because its magnitude is negligible in relation to that of the roll cover materials. This fact is confirmed by the existence of the Nip test. In this test a sheet of pressure-sensitive film is placed between the press rolls which are then loaded against each other to check the uniformity of the nip. The fact that the test can be performed while the press fabrics are in position is testament to the insignificance of the press felts in load determination. So from the cover material properties and Hooke's law:

$$k = \frac{EA}{L} \qquad \text{(B-11)}$$

where:

E = Elastic modulus for the material

A = Area of the material under load

L = Thickness of the cover

While Eq. (B-10) is useful in calculating the force at a specific point in the nip, a more practical quantity is required, i.e. the resultant of the all the forces at all points in the nip. This is done by considering the cover in the area of the nip as an arrangement of infinitesimally small rectangular segments. Each segment then constitutes an axially loaded member, which can be modelled as an individual spring elements. The sum of all the forces in all of the elements will be the resultant of the nip load. A geometrical simplification can be made in which the soft cover can be conceptually considered to be flattened out over the length of the nip, and the radial spring elements become vertically aligned. This translation simplifies the calculation of the vertical force f but introduces problems related to the fact that not all springs have the same length (i.e. not all springs are as long as the cover is thick due to the curvature of the cover inner radius). This is compensated for by using a volumetric factor γ which uses the geometry of the rolls to calculate an equivalent stiffness. The volume factor is derived in Appendix C.

The infinitesimally small rectangular sections are shown in Fig. B-2 as having a width ∂y and original length of L. Assuming that L<<D for the soft roll, which is true in all industrially sized applications, then the width ∂y of each infinitesimal element will not change significantly between the inner- and outer- radii of the element. The symbol ∂ in this text does not imply a partial derivative. It is used instead to represent a singular derivative, and to avoid confusion with the symbol d which is the industry-norm for the symbol representing deflection of the cover at the centre of the nip.

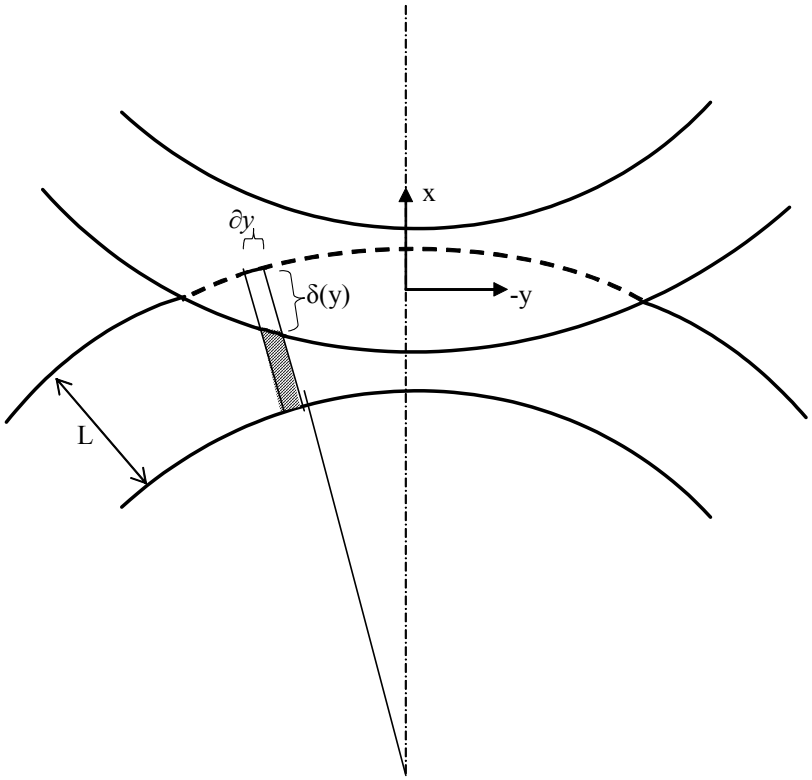

Fig. B-2 Infinitesimally small angular elements of the roll cover.

Combining Eq. (B-10) and Eq. (B-11) the vertical spring force for the i^{th} element, f_i, can be calculated:

$$f_i = \frac{A_i E}{L}\delta(y)_i$$

Given that only the nip load is of interest, which has units force per unit length, the A_i term reduces to a length term ∂y :

$$f_i = \frac{E}{L}\delta(y)_i \partial y$$

So for the total resultant force:

$$F_{res} = \sum_{i=0}^{n} \frac{E}{L} \delta(y)_i \partial y$$

Which can be calculated by integrating for ∂ y over the width of the nip:

$$F_{res} = \int_{-\frac{N}{2}}^{\frac{N}{2}} \frac{E}{L} \delta(y)_i \partial y$$

From symmetry about the x-axis:

$$F_{res} = \frac{2E}{L} \int_{0}^{\frac{N}{2}} \delta(y)_i \partial y$$

Substituting for δ(y) from Eq. (B-9):

$$F_{res} = \frac{2E}{L} \int_{0}^{\frac{N}{2}} \left(\frac{1}{2} \left(\sqrt{D_1^2 - 4y^2} - \sqrt{D_1^2 - N^2} + \sqrt{D_2^2 - 4y^2} - \sqrt{D_2^2 - N^2} \right) \right) \partial y$$

$$= \frac{E}{L} \left[\frac{y}{2} \sqrt{D_1^2 - 4y^2} + \frac{D_1^2}{4} \sin^{-1}\left(\frac{2y}{D_1} \right) - y\sqrt{D_1^2 - N^2} + \frac{y}{2} \sqrt{D_2^2 - 4y^2} + \frac{D_2^2}{4} \sin^{-1}\left(\frac{2y}{D_2} \right) - y\sqrt{D_2^2 - N^2} \right]_0^{\frac{N}{2}}$$

$$= \frac{E}{2L} \left[\frac{N}{2} \sqrt{D_1^2 - N^2} + \frac{D_1^2}{2} \sin^{-1}\left(\frac{N}{D_1} \right) - N\sqrt{D_1^2 - N^2} + \frac{N}{2} \sqrt{D_2^2 - N^2} + \frac{D_2^2}{4} \sin^{-1}\left(\frac{N}{D_2} \right) - N\sqrt{D_2^2 - N^2} \right]$$

$$F_{res} = \frac{E}{4L} \left[-N\sqrt{D_1^2 - N^2} + D_1^2 \sin^{-1}\left(\frac{N}{D_1} \right) - N\sqrt{D_2^2 - N^2} + D_2^2 \sin^{-1}\left(\frac{N}{D_2} \right) \right] \qquad \text{(B-12)}$$

In their solution of the complete Navier-Stokes system coupled with Hookean spring elements, Carvalho and Scriven [50] found the model to be most accurate when the stiffness equation Eq. (B-11) was multiplied by a proportionality factor α, and in particular when α = 2. Furthermore to

account for the differences in the deflected volume which is less than the product of *Nd*, a volume ratio γ is derived in Appendix C from the geometry, as shown in Eq. (B-13):

$$\gamma = \frac{8Nd}{D_1^2(2\varphi - \sin 2\varphi) + D_2^2(2\theta - \sin 2\theta)} \tag{B-13}$$

where:

d = Maximum deflection at the centre of the nip, calculated from Eq. (B-9), with y = 0, in m

φ = Half the nip width, in radians of the bottom roll

θ = Half the nip width, in radians of the top roll

The modulus term E in Eq. (B-12) can be represented by the cover hardness P from Eq. (A-1) which is repeated here as Eq. (B-14):

$$E = (6894.757)(359607)P^{-1.36208} \tag{B-14}$$

where:

E = Material elastic modulus, in Pa

P = Roll cover hardness, in P&J

Introducing γ from Eq. (B-13) and α, and substituting for E from Eq. (B-14) the final useable form of Eq. (B-12) is obtained:

$$F_{nip} = \frac{\alpha\gamma(6894.757)(359607)P^{-1.36208}}{4L}\left[-N\sqrt{D_1^2 - N^2} + D_1^2 \sin^{-1}\left(\frac{N}{D_1}\right) - N\sqrt{D_2^2 - N^2} + D_2^2 \sin^{-1}\left(\frac{N}{D_2}\right)\right]$$

….(B-15)

The model developed in this appendix was verified using all the results that could be found in the literature which specified all the required quantities. Unfortunately very few results related to nip load or nip width are published which fully specify all of the relevant information about the measurement set-up. Fig. B-3 has been divided into two distinct regions to explain the verification of the model. Published results by Beucker [7] are compared with the results of the

presently developed model in samples 1 through 8. There is fair agreement between the two models. The samples 9 through 15 show the measurement results by Beliot [52], against which the Beucker and presently developed models are evaluated. Likewise samples 16 through 22 show comparisons of calculated data from Zwinak [42] with both model results.

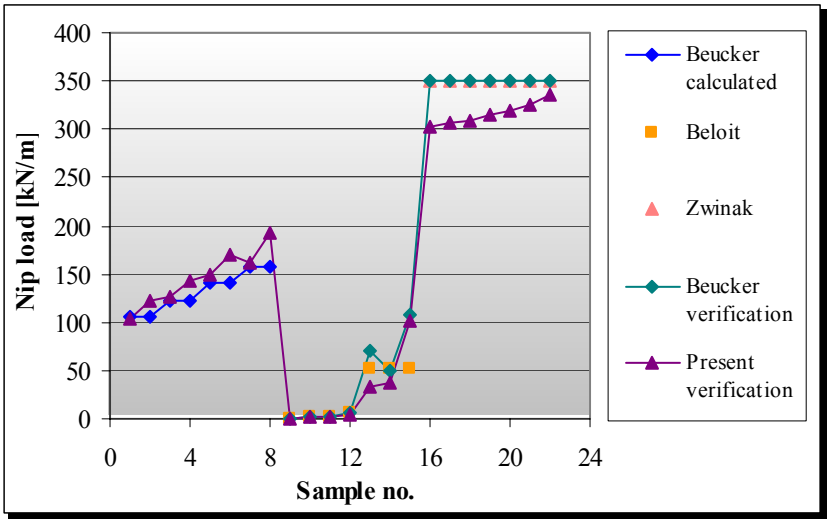

Fig. B-3 Verification of the present and Beucker models

In all cases but one the Beucker [7] model was found to be more accurate than the presently developed model. In fact, the agreement between the Zwinak data and that of the Beucker model is exact. Zwinak's calculation method is not specified, but it is highly likely that the Beucker model was used because the model also forms part of a paper making guideline published by Moore [8] for TAPPI (Technical Association of Pulp and Paper Industries). Any further verification of the models with other data was limited by the shortage of properly defined measurement conditions.

The conclusions which were reached from the verification process were that the accurate agreement between the results of the presently developed model and that of other researchers could not be confirmed due to lack of sufficient and independent data. However, the proposed model does have the ability to model differences in geometrical and material conditions in a general way. This was confirmed by the similarity of the trends of the presently developed model with that of Beucker, which is widely used. Since the objective of this exercise was to confirm the general modelling capabilities of the spring-type model, this approach was considered to be valid. Since more measurement data was available for the case of the two soft cover nip, it was believed

that the use of the model in conjunction with some empirical results would yield a higher accuracy in that application than was observed here.

Appendix C

Derivation of the volumetric factor γ

The roll covers can be considered as axially loaded members, with the axis being perpendicular to the roll shell. In this case the stress-strain behaviour of the cover in compression can be described using a simple linear spring element as shown in Eq (C-1).

$$f = kx \tag{C-1}$$

where:

f = Force in the spring, in N

k = Spring constant, in N/m

x = Displacement of the spring, in m

The equivalent spring constant for the cover material can be calculated from the material properties and Hooke's law using Eq. (C-2).

$$k = \frac{AE}{L} \tag{C-2}$$

where:

A = Area over which the load is exerted

E = Elastic modulus of the cover material

L = Length of the spring (in this case the thickness of the cover)

However, the geometry of the nip is such that not all points in the nip will experience the same amount of deflection. The maximum deflection will occur in the geometrical centre of the nip and taper off towards the edges. It would be incorrect to use the total area of the nip for A in Eq. (C-2) in conjunction with the maximum deflection for x in Eq (C-1). Therefore the deflected volume must be considered more closely, as indicated by Fig. C-1.

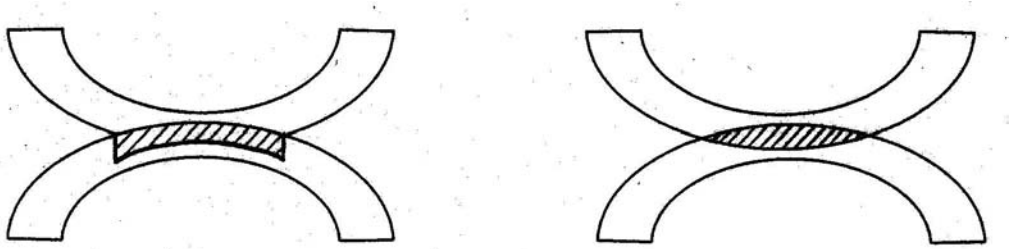

a) b)

Fig. C-1 Deflected volumes of cover material.

Fig. C-1a indicates the deflected volume as being the maximum deflection over the entire nip width. While this representation may be geometrically incorrect, it does provide a much simpler solution to the calculation of the Hooke's forces using Eq. (C-1) and Eq. (C-2). The error in misrepresentation of the deflected volume can then be taken into account using a second term, called the volumetric factor γ. The volumetric factor is multiplied by the solution of Eq. (C-2) and results in a new modified stiffness factor $k_{intrinsic}$. The use of the $k_{intrinsic}$ term simplifies the calculation of the resultant nip load in the mathematical models of Appendix B and D. The calculation of the volume factor is requires only rudimentary geometry of the rolls in the nipped state.

To calculate the volumetric factor, the deflected volumes indicated in Figs C-1a and C-1b are calculated first. Because a single plane along the roll axis is being considered, the volumes actually reduce to areas in two dimensions. First the macroscopic deflected area A_m is calculated from Fig. C-1a.

$$A_m = Nd \tag{C-3}$$

where:

N = Nip width, in m

d = Maximum cover deflection in the centre of the nip

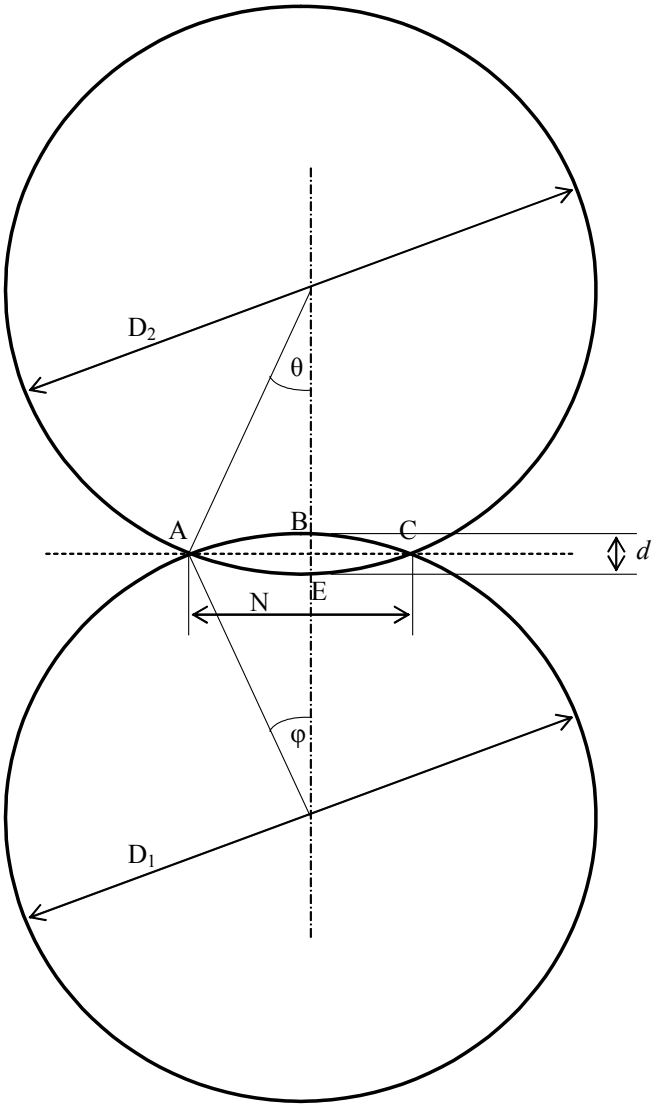

Fig. C-2 Geometry of the rolls and nip.

The area of the actual, or intrinsic area A_i, shaded in Fig. C-1b is calculated using the geometrical references shown in Fig. C-2.

A_i = area enclosed by the two arcs $\overline{ABC}$ and $\overline{AEC}$

= (area of circular segment $\overline{ABC}$) + (area of circular segment $\overline{AEC}$)

$$= \left(\frac{D_1}{2}\right)^2 (\varphi - \cos\varphi \sin\varphi) + \left(\frac{D_2}{2}\right)^2 (\theta - \cos\theta \sin\theta)$$

$$= \frac{D_1^2}{4}\left(\varphi - \frac{1}{2}\sin 2\varphi\right) + \frac{D_2^2}{4}\left(\theta - \frac{1}{2}\sin 2\theta\right)$$

$$= \frac{1}{8}\left[D_1^2\left(2\varphi - \sin 2\varphi\right) + D_2^2\left(2\theta - \sin 2\theta\right)\right] \qquad \text{(C-4)}$$

where:

D_1, D_2 = Diameters of the bottom and top rolls respectively, in m

φ = Half the nip width of the bottom roll, in rad

θ = Half the nip width of the top roll, in rad

The volumetric ratio γ is then calculated using Eqs (C-3) and (C-4):

$$\gamma = \frac{A_m}{A_i}$$

$$\gamma = \frac{8Nd}{D_1^2\left(2\varphi - \sin 2\varphi\right) + D_2^2\left(2\theta - \sin 2\theta\right)} \qquad \text{(C-5)}$$

Appendix D

Mathematical model: Two soft covers

D. 1. Derivation of the model

The difference between the 'one-rock hard and one soft roll model' and the 'two soft covers' models is due to the fact that in the latter model the force is determined by the stiffnesses of two different materials. For the former case all deflection occurred in one of the covers. In the latter case there is a special case where both soft covers have the same stiffness and the contact boundary will be a flat surface between the two nip edges, indicated by *n(y)* in Fig. D-1. For the more general case however, the contact boundary will follow a curve *e(y)* which lies between the original top cover surface *t(y)* and the original bottom cover surface *b(y)*. The position of this curve is determined by the relative hardnesses and diameters of the two covers.

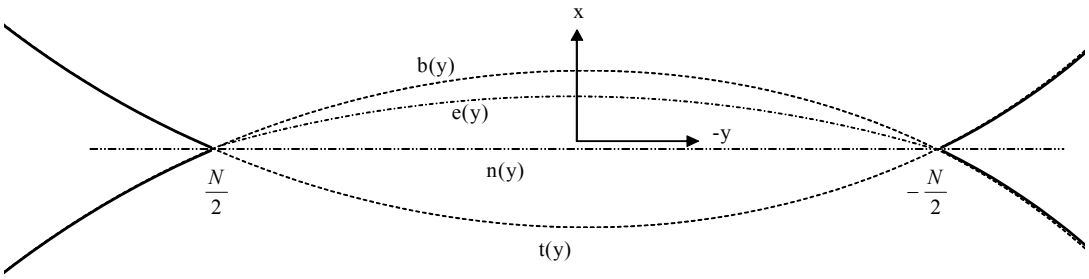

Fig. D-1 Geometry of the two-soft roll nip.

The exact position of the curve *e(y)* cannot be described explicitly using the geometry alone. In fact, since neither the forces nor the displacements of each of the covers are known, the system is statically indeterminate. In this study the stiffness method described by Gere and Timoshenko [53] was used to solve the problem. First, however, the geometry of the problem must be fully described in terms of the rectangular co-ordinate system. The equations describing the undeflected cover surfaces for the bottom roll *t(y)* and top roll *b(y)* were derived in Eqs (B-3) and (B-6) of Appendix B as:

$$b(y) = \sqrt{\frac{D_1^2}{4} - y^2} - \frac{1}{2}\sqrt{D_1^2 - N^2} \tag{D-1}$$

where:

D_1 = Diameter of the bottom roll, in m

N = Nip width, in m

and

$$t(y) = -\sqrt{\frac{D_2^2}{4} - y^2} + \frac{1}{2}\sqrt{D_2^2 - N^2} \tag{D-2}$$

where:

D_2 = Diameter of the top roll, in m

As in Eq. (B-9) of Appendix B, the total interference δ of both covers is calculated at any point (x, y) from:

$$\delta(y) = b(y) - t(y)$$

or

$$\delta(y) = \frac{1}{2}\left(\sqrt{D_1^2 - 4y^2} - \sqrt{D_1^2 - N^2} + \sqrt{D_2^2 - 4y^2} - \sqrt{D_2^2 - N^2}\right) \tag{D-3}$$

which is valid over the range of y from $\left[-\frac{N}{2} : \frac{N}{2}\right]$

If the covers are considered as axially loaded members, where the axis is perpendicular to the roll shell, then the linear spring equation applies:

$$f = kx \tag{D-4}$$

where:

f = Spring force, in N

x = Displacement of the spring, in m

Where k is the equivalent spring stiffness of the material, calculated from the cover material properties and Hooke's law. For an element of homogeneous composition:

$$k = \frac{EA}{L} \tag{D-5}$$

where:

E = Elastic modulus for the material, in Pa

A = Area of the cover under load, in m^2

L = Uncompressed thickness of the cover, in m

While Eqs (D-4) and (D-5) are useful in calculating the force at a specific point in the nip, a more practical quantity is of more interest, i.e. the resultant of the all the forces at all points in the nip. This is done by considering infinitesimally small rectangular sections of the covers as individual spring elements, and calculating the sum of the springs' forces. Thus the soft covers can be conceptually considered to be flattened out over the length of the nip, and the radial spring elements become vertically aligned. This translation simplifies the calculation of the vertical force f but introduces problems related to the fact that not all springs have the same length (i.e. not all springs are as long as the combined cover thicknesses due to the curvature of the cover inner radii). This is compensated for by using a volumetric factor γ which uses the geometry of the rolls to calculate an equivalent stiffness. The volumetric factor is derived in Appendix C.

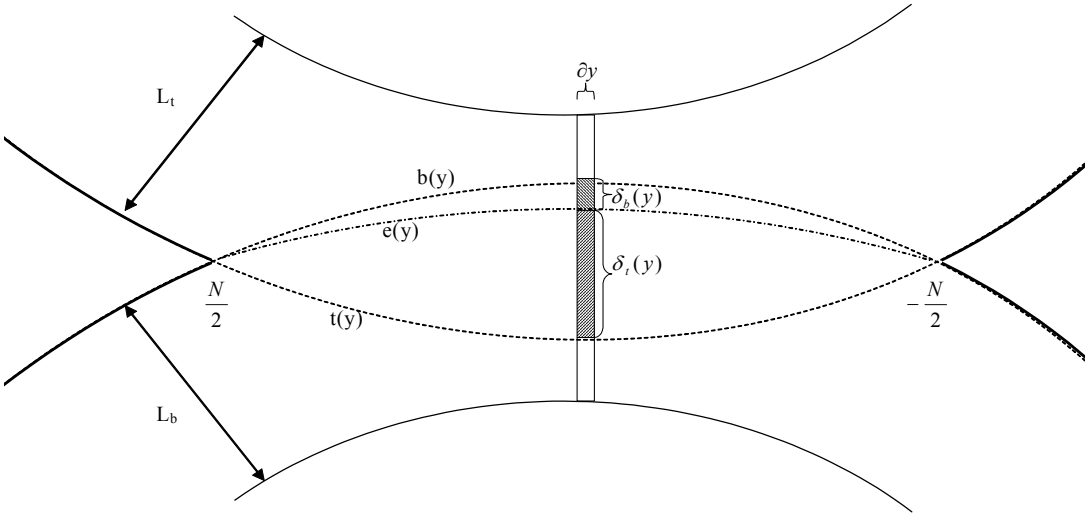

Fig. D-2 Infinitesimal elements of top and bottom roll covers.

The infinitesimally small rectangular sections have equal width ∂y. The length of the sections differ for the top and bottom rolls due to the differences in original cover thicknesses, represented

by L_t and L_b respectively in Fig. D-2. The vertical deflection of the top cover in Fig. D-2 is represented by $\delta_t(y)$, and likewise the bottom cover has deflection $\delta_b(y)$. It is assumed that $L<<D$ for both rolls, which is true in all industrially sized applications. Thus the width ∂y of each infinitesimal element will not change significantly between the inner- and outer- radii of the element. The symbol ∂ in this text does not imply a partial derivative. It is intended in this case to represent a singular derivative, and to avoid confusion with the symbol d which is the industry-norm for the symbol representing the maximum deflection of the cover.

Returning to the vertical elements shown in Fig. D-2, it can be seen that the top cover elements deflect by δ_t and the bottom by δ_b. Since neither of these are known, and the forces in the elements are also unknown, the problem is statically indeterminate. Using the stiffness method of Gere and Timoshenko [53] an expression can be obtained for the total force in both elements by considering an equivalent stiffness and the total deflection. Choosing the two elements, one from each cover, along the same vertical line, the reference system for both becomes synchronised, so that both may be referred to as the i^{th} element from each cover. Consider first the element from the bottom cover, which has original length L_b, and has been compressed by $\delta_b(y_i)$. From Eqs (D-4) and (D-5) an expression for the force in the i^{th} element is obtained:

$$f_{bi} = \frac{A_{bi} E_b}{L_b} \delta_b(y_i)$$

where:

E_b = Elastic modulus of the bottom cover material, in Pa

A_{bi} = Area of the bottom roll cover under compression, in m^2

Since nip loads have units of force per unit length, the area term can be reduced to a length term:

$$f_{bi} = \frac{\partial y E_b}{L_b} \delta_b(y_i) \qquad \text{(D-6)}$$

Similarly the i^{th} top element has a force per unit length of:

$$f_{ti} = \frac{\partial y E_t}{L_t} \delta_t(y_i) \qquad \text{(D-7)}$$

where:

E_t = Elastic modulus of the top roll cover material, in Pa

And since there is no acceleration of the roll centre, it is deduced from basic Newtonian physics that the action and reaction forces are equal. Therefore equating Eqs (D-6) and (D-7):

$$f_{bi} = f_{ti}$$

$$\frac{\partial y E_b}{L_b}\delta_b(y_i) = \frac{\partial y E_t}{L_t}\delta_t(y_i)$$

$$\delta_t(y_i) = \left(\frac{L_t E_b}{L_b E_t}\right)\delta_b(y_i) \qquad \text{(D-8)}$$

Since the total deflection of both elements is nothing other than the sum of the deflections of each of the elements:

$$\delta_{itotal}(y_i) = \delta_b(y_i) + \delta_t(y_i)$$

Into which $\delta_t(y_i)$ is substituted from Eq. (D-8):

$$\delta_{itotal}(y_i) = \delta_b(y_i) + \left(\frac{L_t E_b}{L_b E_t}\right)\delta_b(y_i)$$

$$\delta_{itotal}(y_i) = \delta_b(y_i)\left(1 + \frac{L_t E_b}{L_b E_t}\right)$$

But the total deflection of both covers was calculated from the geometrical union in Eq. (D-3). Thus substituting $\delta(y)$ of Eq. (D-3) into $\delta_{itotal}(y_i)$ gives:

$$\frac{1}{2}\left(\sqrt{D_1^2 - 4y^2} - \sqrt{D_1^2 - N^2} + \sqrt{D_2^2 - 4y^2} - \sqrt{D_2^2 - N^2}\right) = \delta_b(y_i)\left(1 + \frac{L_t E_b}{L_b E_t}\right)$$

Substituting for $\delta_b(y_i)$ from Eq. (D-6):

$$\frac{1}{2}\left(\sqrt{D_1^2-4y^2}-\sqrt{D_1^2-N^2}+\sqrt{D_2^2-4y^2}-\sqrt{D_2^2-N^2}\right)=\frac{f_{bi}L_b}{\partial y E_b}\left(1+\frac{L_t E_b}{L_b E_t}\right)$$

$$\sqrt{D_1^2-4y^2}-\sqrt{D_1^2-N^2}+\sqrt{D_2^2-4y^2}-\sqrt{D_2^2-N^2}=\frac{2f_{bi}}{\partial y}\left(\frac{L_b}{E_b}+\frac{L_t}{E_t}\right)$$

$$f_{bi}=\frac{1}{2}\left(\frac{E_b E_t}{L_b E_t+L_t E_b}\right)\left(\sqrt{D_1^2-4y^2}-\sqrt{D_1^2-N^2}+\sqrt{D_2^2-4y^2}-\sqrt{D_2^2-N^2}\right)\partial y$$

But since it is known that the action-reaction forces are equal in magnitude for both covers, the subscript *b* can be omitted from the *f* term in this equation. Furthermore, the total resultant force across the entire nip width can be calculated by integrating with respect to y:

$$F_{res}=\int_{-\frac{N}{2}}^{\frac{N}{2}}\frac{1}{2}\left(\frac{E_b E_t}{L_b E_t+L_t E_b}\right)\left(\sqrt{D_1^2-4y^2}-\sqrt{D_1^2-N^2}+\sqrt{D_2^2-4y^2}-\sqrt{D_2^2-N^2}\right)\partial y$$

and from symmetry about the x-axis:

$$=\left(\frac{E_b E_t}{L_b E_t+L_t E_b}\right)\int_0^{\frac{N}{2}}\left(\sqrt{D_1^2-4y^2}-\sqrt{D_1^2-N^2}+\sqrt{D_2^2-4y^2}-\sqrt{D_2^2-N^2}\right)\partial y$$

$$=\left(\frac{2E_b E_t}{L_b E_t+L_t E_b}\right)\int_0^{\frac{N}{2}}\left(\sqrt{\left(\frac{D_1}{2}\right)^2-y^2}-\sqrt{\left(\frac{D_1}{2}\right)^2-\left(\frac{N}{2}\right)^2}+\sqrt{\left(\frac{D_2}{2}\right)^2-y^2}-\sqrt{\left(\frac{D_2}{2}\right)^2-\left(\frac{N}{2}\right)^2}\right)\partial y$$

$$= \left(\frac{2E_bE_t}{L_bE_t + L_tE_b} \right) \left[\begin{array}{l} \frac{y}{2}\sqrt{\left(\frac{D_1}{2}\right)^2 - y^2} + \frac{D_1^2}{8}\sin^{-1}\left(\frac{2y}{D_1}\right) - y\sqrt{\left(\frac{D_1}{2}\right)^2 - \left(\frac{N}{2}\right)^2} + \frac{y}{2}\sqrt{\left(\frac{D_2}{2}\right)^2 - y^2} + \frac{D_2^2}{8}\sin^{-1}\left(\frac{2y}{D_2}\right) \ldots . \\ \ldots . - y\sqrt{\left(\frac{D_2}{2}\right)^2 - \left(\frac{N}{2}\right)^2} \end{array} \right]_0^{\frac{N}{2}}$$

$$= \left(\frac{2E_bE_t}{L_bE_t + L_tE_b} \right) \left[\begin{array}{l} \frac{N}{4}\sqrt{\left(\frac{D_1}{2}\right)^2 - \left(\frac{N}{2}\right)^2} + \frac{D_1^2}{8}\sin^{-1}\left(\frac{N}{D_1}\right) - \frac{N}{2}\sqrt{\left(\frac{D_1}{2}\right)^2 - \left(\frac{N}{2}\right)^2} + \frac{N}{4}\sqrt{\left(\frac{D_2}{2}\right)^2 - \left(\frac{N}{2}\right)^2} \ldots \ldots . \\ \ldots \ldots + \frac{D_2^2}{8}\sin^{-1}\left(\frac{N}{D_2}\right) - \frac{N}{2}\sqrt{\left(\frac{D_2}{2}\right)^2 - \left(\frac{N}{2}\right)^2} - 0 \end{array} \right]$$

$$= \left(\frac{2E_bE_t}{L_bE_t + L_tE_b} \right) \left[-\frac{N}{4}\sqrt{\left(\frac{D_1}{2}\right)^2 - \left(\frac{N}{2}\right)^2} + \frac{D_1^2}{8}\sin^{-1}\left(\frac{N}{D_1}\right) - \frac{N}{4}\sqrt{\left(\frac{D_2}{2}\right)^2 - \left(\frac{N}{2}\right)^2} + \frac{D_2^2}{8}\sin^{-1}\left(\frac{N}{D_2}\right) \right]$$

$$F_{res} = \frac{1}{4}\left(\frac{E_bE_t}{L_bE_t + L_tE_b} \right) \left[-N\sqrt{D_1^2 - N^2} + D_1^2 \sin^{-1}\left(\frac{N}{D_1}\right) - N\sqrt{D_2^2 - N^2} + D_2^2 \sin^{-1}\left(\frac{N}{D_2}\right) \right] \quad \text{….(D-9)}$$

The first term of Eq. (D-9) can be addressed by considering the hardness-modulus relationship given in Eq. (A-1) of Appendix A. This equation is repeated below in SI units:

$$E = (6894.757)(359607)P^{-1.36208} \quad \text{(D-10)}$$

where:

E = Elastic modulus, in Pa

P = Roll cover hardness, in P&J

Applying Eq. (D-10) to the first term of Eq. (D-9):

$$= \left(\frac{E_bE_t}{L_bE_t + L_tE_b} \right)$$

$$= \left[\frac{\left[(6894.757)(359607)P_b^{-1.36208}\right]\left[(6894.757)(359607)P_t^{-1.36208}\right]}{L_b(6894.757)(359607)P_t^{-1.36208} + L_t(6894.757)(359607)P_b^{-1.36208}} \right]$$

$$= \frac{(6894.757)(359607)(P_b P_t)^{-1.36208}}{L_b P_t^{-1.36208} + L_t P_b^{-1.36208}} \qquad \text{(D-11)}$$

Which can be regarded as an equivalent stiffness term since it describes both the hardness and the thickness of both covers. As such the two factors which were used in the derivation of the model for the case of one rock-hard and one soft cover are incorporated in this term. The first factor is a proportionality factor (α) which was developed by Carvalho and Scriven [50] in a study involving the solution of the complete Navier-Stokes system coupled with Hookean spring elements. The factor is used as a pre-fix to the spring constant of Eq. (D-5). The author's determined experimentally that their model was most accurate when α was set equal to 2. The factor is adopted in this study due to the similarity in geometry and purpose with that of Carvalho and Scriven. The second factor is needed to account for the differences in the deflected volume which is less than the product of *Nd*. The volume ratio γ is derived in Appendix C from the geometry, shown in Eq. (D-12):

$$\gamma = \frac{8Nd}{D_1^2(2\varphi - \sin 2\varphi) + D_2^2(2\theta - \sin 2\theta)} \qquad \text{(D-12)}$$

where:

d = Maximum deflection at the centre of the nip, calculated from Eq. (D-3) with y=0, in m

φ = Half the nip width of the bottom roll, in rad

θ = half the nip width of the top roll, in rad

Thus Eq. (D-9) becomes:

$$F_{res} = \frac{G}{4}\left[-N\sqrt{D_1^2 - N^2} + D_1^2 \sin^{-1}\left(\frac{N}{D_1}\right) - N\sqrt{D_2^2 - N^2} + D_2^2 \sin^{-1}\left(\frac{N}{D_2}\right) \right] \qquad \text{(D-13)}$$

where:

$$G = \frac{\alpha\gamma(6894.757)(359607)(P_b P_t)^{-1.36208}}{L_b P_t^{-1.36208} + L_t P_b^{-1.36208}}$$

where:

G = Equivalent stiffness, in Pa

α = Proportionality factor, defined below

γ = Volumetric factor, defined below

L_b, L_t = Thickness of the bottom and top covers respectively, in m

P_b, P_t = Hardness of the bottom and top rolls respectively, in P&J

D. 2. Experimental verification of the model

The solutions given by Eq. (D-13) over a range of conditions were compared with the results reported by Zwinak [42]. The comparison indicated that the mathematical model was only 82% accurate. Since a higher accuracy was desired, and hopefully without complicating the model too much, the use of empirical constants was investigated to increase the accuracy of the model.

Further investigation of the mathematical results indicated that the model was very accurate for the larger-sized rolls of 72 inch diameter in Zwinak's study, but decreased with decreasing diameter to the 28 inch rolls. After reviewing the data and physical material behaviour, it was postulated that the error could be related to what is referred to hereafter as the Poisson effect. Depending on the hardness, some cover materials have a Poisson ratio which approaches 0.5, as such they tend to squeeze out on either side of the nip in addition to being compressed. This will affect the equivalent stiffness term G. As such a material factor ρ_m was coined to take this into account.

The second and more obvious effect was the size effect. The Poisson effect occurs irrespective of roll diameter, and can be regarded as a boundary effect at the ingoing and outgoing boundaries of the nip. If the Poisson effect theory is valid, then one would observe bigger discrepancies for smaller rolls, which was in fact the case. This can be explained by considering that as the roll diameters decrease, the nip widths tend to narrow, and thus the edge effects form a larger contribution to the total load. A wider nip, corresponding to bigger diameter rolls would be less sensitive to edge effects. The symbol ρ_s was used to represent the size effect, but note that it is not

independent of the Poisson effect. This fact was confirmed during the calculation of the factors ρ_m and ρ_s, because the size and Poisson effects could not be de-coupled.

The material factor ρ_m was calculated empirically, and can be read from Fig. D-3. It is interesting to note that the material factor tends to 1 as the P&J hardness tends to zero. This implies that the theoretical model is entirely accurate for hard covers, but as the covers soften they tend to squeeze out more.

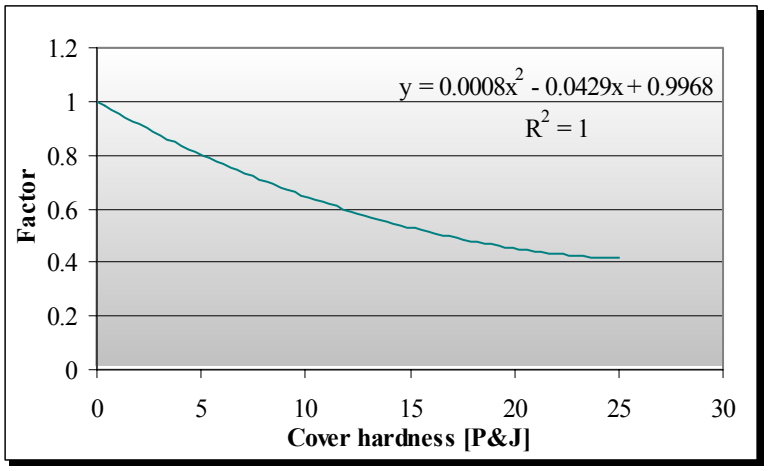

Fig. D-3 Material factor ρ_m for the correction of theoretical model

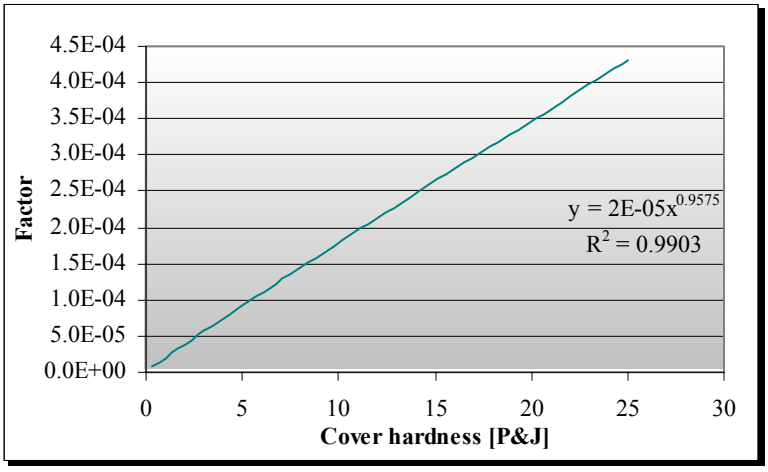

Fig. D-4 Size factor ρ_s for the correction of theoretical model

Similarly the size factor ρ_s can be read from Fig. D-4. The factors ρ_m and ρ_s can be read from Figs D-3 and D-4 or calculated from the equations which appear on each of the figures, where *x* is the

hardness of the material. Using either approach, they are combined into a single parameter known as the Poisson factor ρ_v in the equation:

$$\rho_v = \rho_m + \rho_s D_{\min} \tag{D-14}$$

where:

ρ_v = Poisson factor

ρ_m = Material factor

ρ_s = Size factor

D_{min} = Diameter of the smaller of the two rolls, in mm

The results of the theoretical model of Eq. (D-13) when combined with the Poisson factor lead to the final useable equation in the form of Eq. (D-15). The nip force F_{nip} has units of force per unit axial length of the nip, or N/m. This is in keeping with the convention of the paper industry.

$$F_{nip} = \frac{\rho_v G}{4}\left[-N\sqrt{D_1^2 - N^2} + D_1^2 \sin^{-1}\left(\frac{N}{D_1}\right) - N\sqrt{D_2^2 - N^2} + D_2^2 \sin^{-1}\left(\frac{N}{D_2}\right)\right] \tag{D-15}$$

The results of Eq. (D-15) yielded a significantly better correlation with the results of Zwinak [42]. The data considers a wide range of roll size, cover hardness and load, and the results are shown in Fig. D-5. The empirical model had a standard deviation of 11 kN/m, an average error of 3.1% and a maximum error of 7.1%. Fig. D-5 also shows results that were obtained using the Beucker model [7] and the model provided by a supplier to the industry which was discussed in Appendix B. Note that the Beucker model [7] was not expected to give an accurate result as it only accounts for one soft cover, it appears in Fig. D-5 for comparative purposes only. The agreement between the measurements by Zwinak [42] and the calculations using the present model is good, and permitted its application for the remainder of this study.

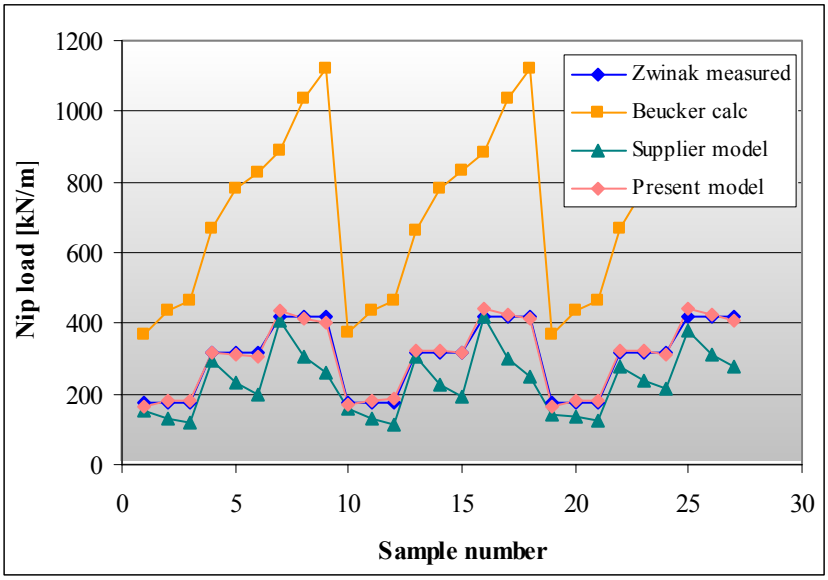

Fig. D-5 Comparison of various models with Zwinak results

Appendix E

Expansion of the cover deflection models in the third dimension

The models developed in Appendix B and Appendix D can be used to calculate the resultant vertical nip load for a nip of specified geometry and material properties. As with previous models, the loading in the nip is included in the nip width *N* term. In the present study, it was considered more practical to use the vertical interference of the roll covers as the handle on nip load. The term *d* was thus used, which represents the deflection of the roll covers in the centre of the nip. It thus also represents the point of maximum deflection. The conversion between *N* and *d* is simple, making use of an already derived Eq. (B-9). The term δ(y) is replaced by *d* and the value of y is zero. Eq. (B-9) reduces to the form shown in Eq. (E-1). The use of Eq. (E-1) is useful because it relates directly to the objectives of this study: roll wear.

$$d = \frac{1}{2}\left(D_1 - \sqrt{D_1^2 - N^2} + D_2 - \sqrt{D_2^2 - N^2}\right) \qquad \text{(E-1)}$$

For the presently derived model to be used in practical situations, the two-dimensional model was extended into the third dimension. This was required so that the nip load could be calculated at a number of points across the length of the roll. This was done by measuring the wear at a number of points along the axial length of the roll, for both press rolls. Normally press rolls are not exactly cylindrical, they are ground with a crown profile which gives a slightly larger diameter in the centre than at the edges. The purpose of the crown is to compensate for the deflection of the roll shell due to the loading along the nip and sagging due to gravity. The crown is calculated from the roll properties to give a uniform loading across the entire width of the nip. This crown profile was used as the reference when making wear measurements. A sample of these measurements is shown exaggerated in Fig. E-1. The axis for the top roll has been inverted in the figure to give an idea of the profile of the gap that exists between the rolls when they are in close proximity.

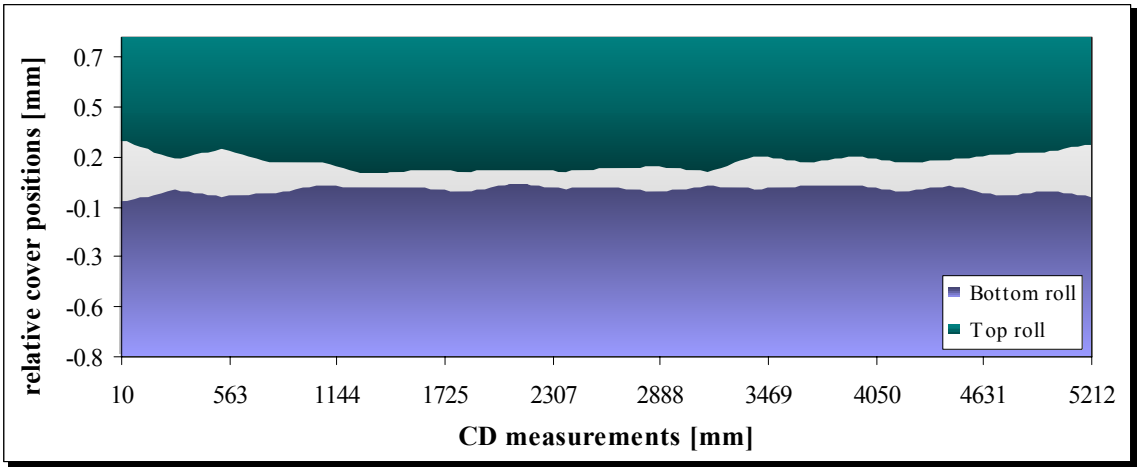

Fig. E-1 Exaggerated view of the nip area when the rolls are in close proximity

Using the measurements shown in Fig. E-1 to calculate the gap at 136 points across the roll faces, a theoretical mathematical beam was constructed with 136 individual springs. The length of each spring was shortened from the nominal value by the size of the gap. The concept is shown for five springs with arbitrary gaps in Fig. E-2. The approach is based on the work of Moore [48] in his study of crowns and cross-machine loading variations. In the present study the beam is moved closer to the straight rigid wall. The longer springs, which correspond to areas where the gap is the smallest, will make contact first. The beam is moved even further until such point that the sum of all the forces in the individual springs (calculated from Eq. (D-15)) is equal to the external load F applied to the bearing housings of the roll.

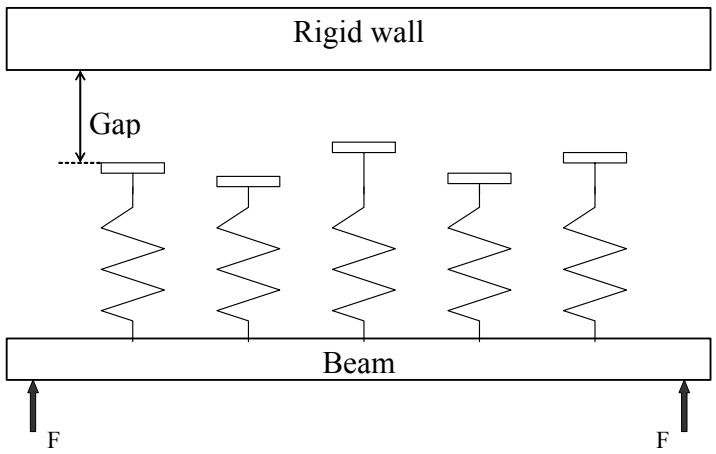

Fig. E-2 Schematic of the spring elements used in the beam model

In the particular press used in this study the external loading was via hydraulic cylinders. Furthermore, the arms which pivot to raise or lower the top roll can move independently. This implies that misalignment of the roll axes is possible. Furthermore, the spherical roller bearings which are used on this press will not act to resist this misalignment. As a result a moment equilibrium requirement was imposed in addition to the force equilibrium indicated in Fig. E-2. This was implemented in the beam model through the addition of a second degree of freedom. This degree of freedom was controlled by an angle zeta ζ, which induced an angular rotation of the beam about its centre, in addition to the linear motion. The system was solved iteratively until both force and moment equilibrium requirements were satisfied. At this point the nip load profile can be plotted from the loads in each of the individual springs. The nip load profile for the set of rolls shown in Fig. E-1 is shown in Fig. E-3. The correlation between the two figures is visually evident.

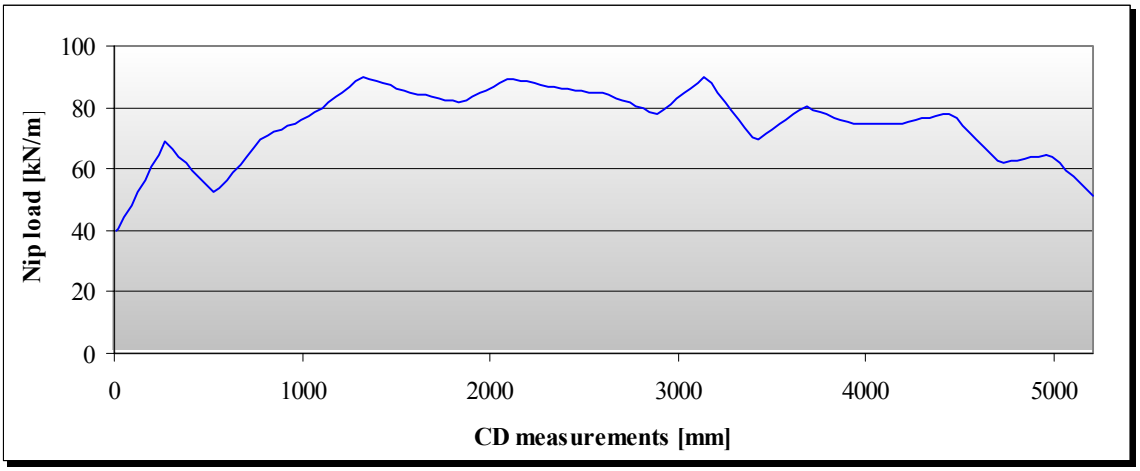

Fig. E-3 Nip load profile constructed from two degree of freedom system.

A nip load profile such as that shown in Fig. E-3 was required each time process measurements were taken over the months of this study. By taking measurements over such a long period, various permutations of nip load profiles were generated. From a reliability point of view it is important to note that while the roll wear may cause a reduction in the nip load in some areas, the load will resultantly increase in other areas of the nip in order to maintain force equilibrium. This is important since the condition based roll changes must consider the allowable stress in the felts and roll cover as well as the effect on the paper properties. Over the duration of this study the highest recorded load was 102 kN/m, which equates to 3.1 MPa. This is below the allowable limit for the roll cover materials defined by Gudehus [43] as $(^1/_{10})E$, or 7.6 MPa. The felt loading was

also below the 6-10 MPa limits. Hence for these rolls the factor limiting the amount of roll wear was the effect on paper quality.

Appendix F

Investigation of the effect of the spray dampener system

Purpose:

To determine the magnitude of the moisture profile discrepancy that can be compensated for by the spray dampener.

Summary:

The spray dampener located at the end of the drying section of Paper Machine no. 2 is intended to improve the CD moisture levels by spraying a fine mist of water in the dry areas of the sheet. In this way the moisture variations across the web will be reduced, resulting in more consistent sheet properties. The findings of this investigation are that moisture profile discrepancies of 0.7% cannot be corrected by the spray dampener. Moreover, despite good repeatability of the results, no reliable correlation between the nozzle opening actuator and the moisture increase exists. Hence the benefit of using the spray dampener system to correct even discrepancies smaller than 0.7% cannot be confirmed.

Experimental conditions:

The investigation was conducted on 19 July 2002, under the following conditions:

1. Product being manufactured: 125gsm Kraftguard.
2. Machine co-ordinated speed: 650 m/min.
3. Stock blend: 23% chemical softwood, 18% semi-chemical hardwood, 25% recycled, 35% re-processed fibre.
4. Sheet moisture measurement device: Autoline 200 manufactured by Lorentzen & Wettre.
5. Steam shower: inactive.

Method of investigation:

Under stable machine conditions, the main water supply valve to the spray dampener was opened and closed for alternating reels of production as follows:

- Reels 14,15, 17 – Spray dampener inactive (valve closed)
- Reels 9,10,11,12,13,16, 18 – Spray dampener active (valve open)

The corresponding moisture profiles were then analysed to compare the moisture profiles of the reels. Two main comparisons were made:

1. The profiles of the reels with the Spray dampener inactive were compared to each other to determine the repeatability of the process.
2. The profiles of the reels with the Spray dampener active were compared to subsequent reels where the Spray dampener was inactive. The difference between these two indicates the magnitude of the effect of the shower.

Prior to discussing the results of the two independent comparisons, it must be noted that the overall moisture values averaged across the full web width do not appear to be significantly affected by the Spray dampener system. This is shown in Fig. F-1.

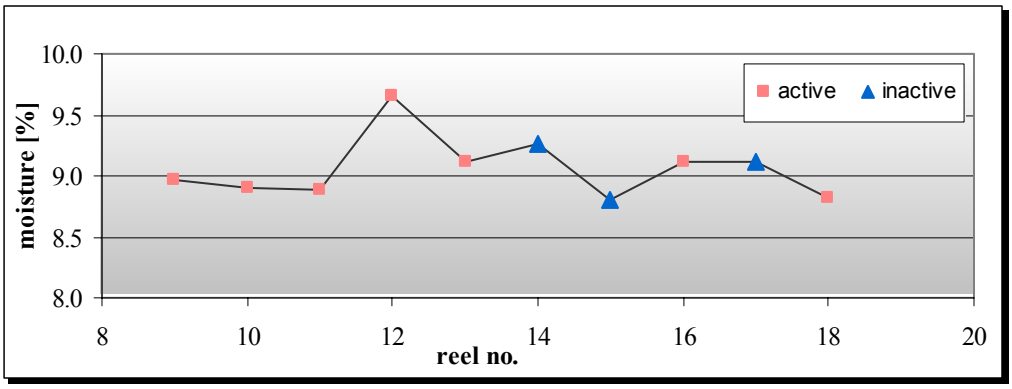

Fig. F-1 Trend of average moisture values for duration of study.

The conclusion drawn from this is that the total contribution of the shower to the overall moisture average can be regarded as small in comparison with the usual process fluctuations. This can be seen in the hours leading up to the experiment, which were considered to be stable operating conditions by the process operators, but actually include a higher variance in moisture than during the experiment itself. For the remaining analyses, the moisture profiles will be normalised to compensate for the varying moisture averages as depicted in Fig. F-1.

Results:

Repeatability of the VIB-inactive moisture profiles

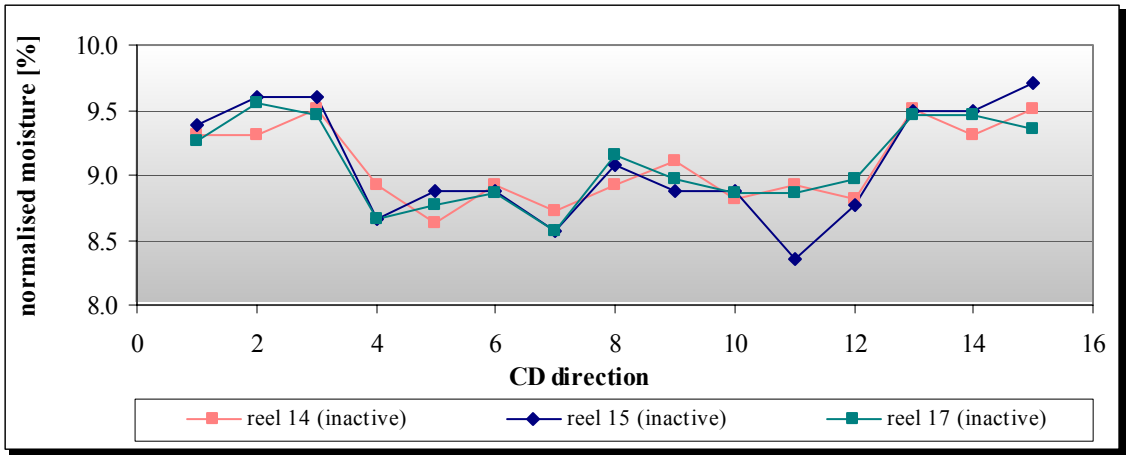

Fig. F-2 Reel moisture profiles.

With the exception of a single point measured at the 11th measurement point on reel 15, the profiles are very repeatable. The local difference between the three profiles has a range of [0.05 : 0.56] moisture percentage points.

Comparison of Spray dampener active vs. inactive profiles

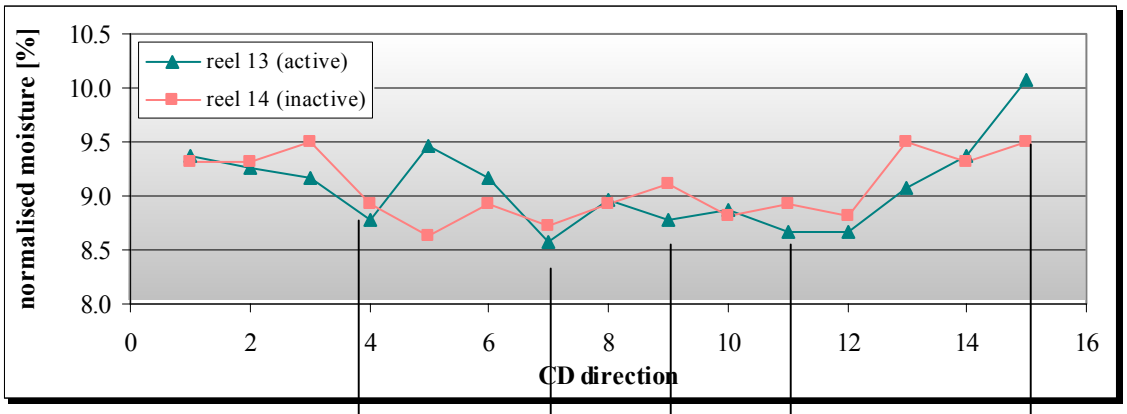

Fig. F-3 Moisture profiles of reels 13 and 14.

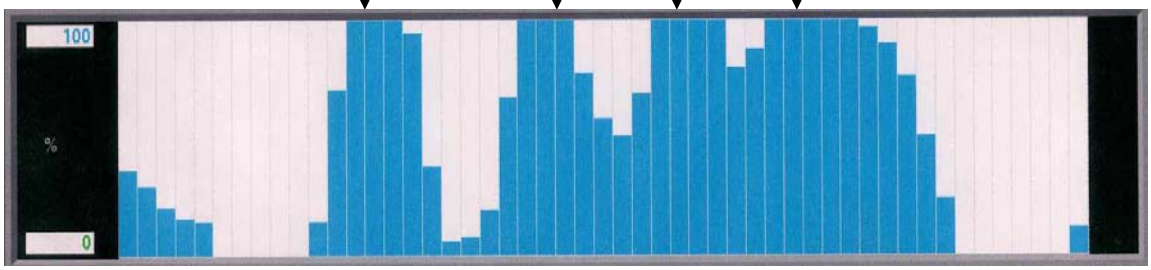

Fig. F-4 CD profile of Spray dampener nozzle actuator position.

Figs F-3 and F-4 show the sheet moisture and Spray dampener nozzle actuator settings respectively. In theory, the percentage actuator opening should provide a proportional increase of the moisture profile in that region. This would be observed as a difference between the curves of reel 13 and reel 14. Figs F-3 and F-4 show the opposite effect: some regions which showed a 100% open nozzle actually had a lower moisture content. Measurement point 15 which had its nozzle aperture closed the entire time showed an increase in moisture content, even after normalisation.

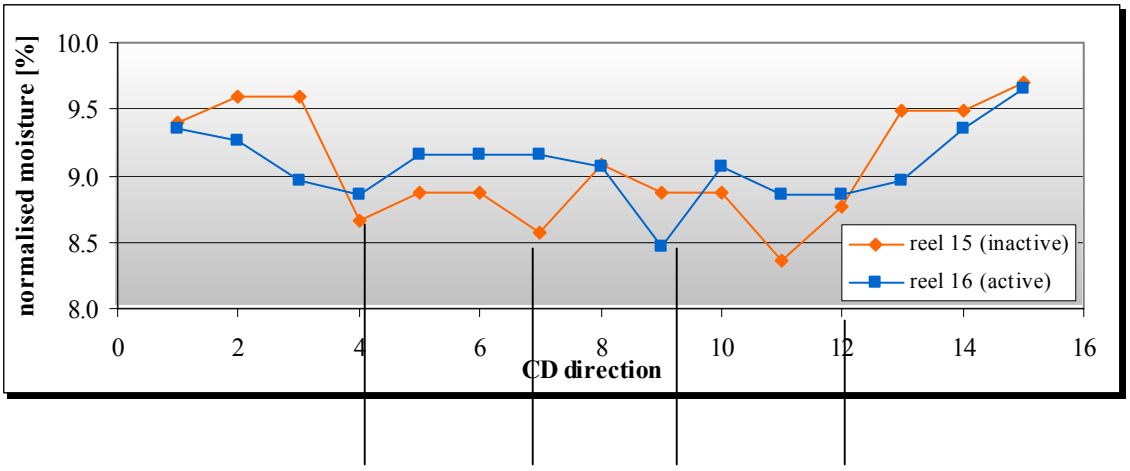

Fig. F-5 Moisture profiles of reels 15 and 16.

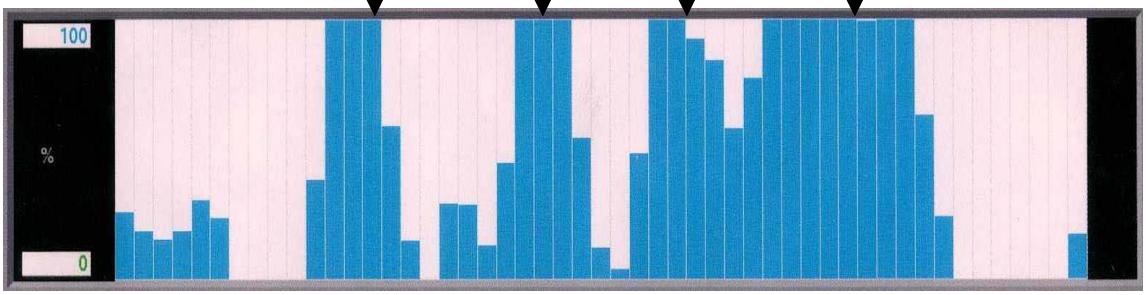

Fig. F-6 CD profile of Spray dampener nozzle actuator position.

Figs F-5 and F-6 also indicate results which do not agree with what can be regarded as normal expected behaviour. As with reels 13 vs. 14, the expected proportionality between percentage actuator opening and increase in the moisture profile was not evident. Further to this, all positions which show a 100% opening of the actuator nozzle should show a resultant increase in moisture. This was not found to be the case. In fact, the correlation was so poor that some areas showed an increase of 0.4%, while others showed a decrease of 0.6%. Thus the expected proportionality between the actuator setting and any increase in moisture can be disregarded. Fig. F-7 indicates this lack of proportionality.

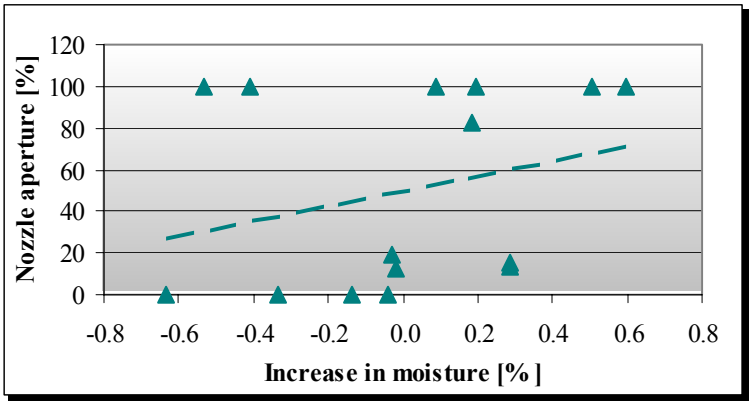

Fig. F-7 Dispersion in the data of reels 15 and 16.

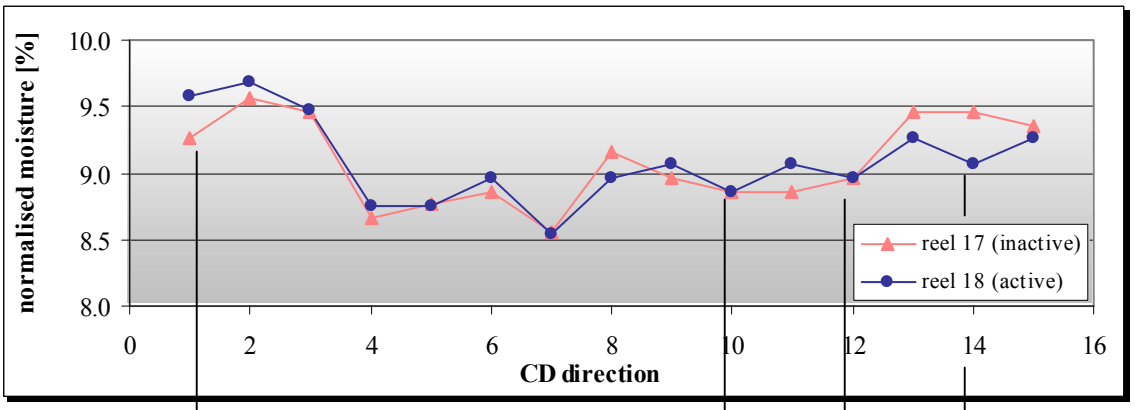

Fig. F-8 Moisture profiles of reels17 and 18.

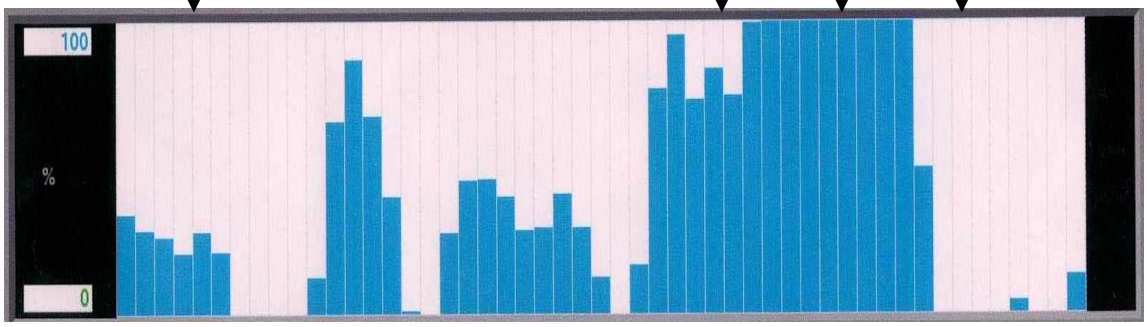

Fig. F-9 CD profile of Spray dampener nozzle actuator position.

A comparison of the profiles of reels 17 and 18 shows a closer profile correlation, the difference between the local moisture values is in the range [-0.4 : +0.3]. This close correlation indicates that the effect of the Spray dampener shower, if any, is indeed very small. Once again, any

proportionality between the Spray dampener nozzle actuator setting and the moisture increase is absent, as indicated by Fig. F-10. In fact, some of bigger increases in moisture occur in places where the Spray dampener actuators are virtually closed.

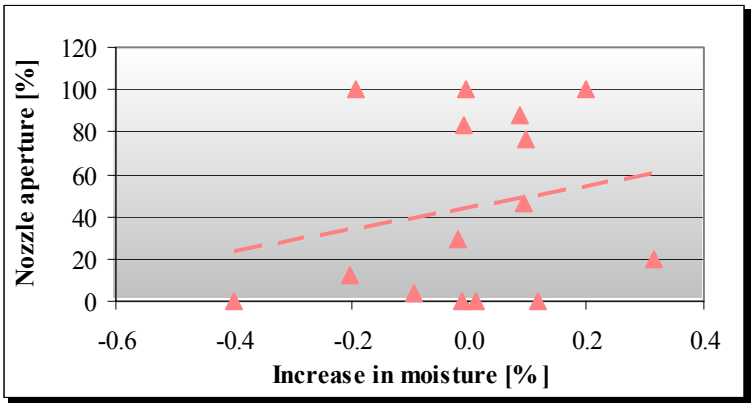

Fig. F-10 Dispersion in the data of reels 17 and 18.

Conclusions:

1. The overall moisture values, taken as the average of the moisture readings across the entire web are not affected by the Spray dampener system.
2. No consistent correlation between the nozzle aperture actuator setting and the moisture increase of the web could be found.
3. The argument that the purpose of the Spray dampener is not to increase or decrease the moisture content, but rather to reduce the number of "dry-troughs" in the moisture profile can not be supported by the results of this investigation. Even if only the absolute moisture minima for each of the profiles is considered, the conclusion is that the Spray dampener will improve the moisture content by only 0.01% for the normalised profile (reduced to -0.03% before normalisation). This improvement, when considered in relation to the natural variation in the process can be regarded as insignificant.
4. The chief purpose of this investigation was to determine if large-scale moisture profile discrepancies, such as the 0.7% drop in the centre when compared to the edges could be relieved by the Spray dampener system. Based on the fact that the dry centre was prevalent in all the measurements, the conclusion made here is that the Spray dampener system is not capable of correcting large-scale moisture discrepancies.
   - Addendum: *The findings of this report were later confirmed by a supplier of this type of equipment. The reason given for the lack of performance was that increases in production speeds and volumes on the machine had rendered this system inadequate.*